



**UNIVERSITÀ DEGLI STUDI DI SASSARI**  
**DOTTORATO IN RIPRODUZIONE, PRODUZIONE E BENESSERE ANIMALE**  
**XX CICLO 2004-2007**

**Coordinatore: Prof. Salvatore Naitana**

**THE RELATIVE EFFECTIVENESS OF 2-METHOXYESTRADIOL  
ON UNDIFFERENTIATED AND DIFFERENTIATED CELLS OF  
GLIAL AND NEURONAL ORIGIN**

**DOCENTE GUIDA:**  
**PROF. VITTORIO FARINA**

**TESI DI DOTTORATO DEL:**  
**DOTT. PAOLO MANCA**

# ***INDEX***

# INTRODUCTION

## CYTOSKELETON

General features	8
<i>Microfilaments</i>	
<i>General features</i>	9
<i>Actin</i>	9
<i>Microfilaments assembly</i>	9
<i>Microfilaments organization and functions</i>	10
<i>Intermediate filaments</i>	
<i>General features</i>	11
<i>Structure</i>	12
<i>Types of intermediate filaments</i>	12
<i>Types I and II (Acidic and Basic Keratins)</i>	12
<i>Type III</i>	13
<i>Type IV</i>	13
<i>Type V</i>	14
<i>Tubulin</i>	
<i>General features</i>	15
<i>Microtubules and tubulin structure</i>	16
<i>Microtubules assembly</i>	19
<i>Microtubules dynamics in vivo and in vitro</i>	22
<i>Microtubules-stabilizing proteins</i>	23
<i>Post-translational modifications</i>	25
<i>Tyrosination/detyrosination: the tyrosination cycle</i>	25
<i>Acetylation/deacetylation</i>	27
<i>Polyglutamination</i>	28
<i>Poliglycilation</i>	28
<i>Palmytoylation</i>	29
<i>Phosphorylation</i>	29

## STEROID HORMONES, NEUROSTEROIDS AND NEUROACTIVE STEROIDS

<i>Steroids hormones</i>	31
<i>Neurosteroids</i>	31
<i>Neuroactive steroids</i>	32
Steroid synthesis in the brain: conversion of cholesterol to pregnenolone	34
Steroid synthesis in the brain: conversion of androgens to estrogens	35

3 $\beta$ -hydroxysteroid dehydrogenase: inactivation of metabolite of steroid hormone	36
17 $\beta$ -hydroxysteroid dehydrogenase: regulation of biological activity of steroid hormones	36

## **2-METHOXYESTRADIOL: BIOCHEMICAL FEATURES AND ITS ACTIVITY *IN VITRO* AND *IN VIVO***

General features	38
Biochemical and physiological properties	38
2-Methoxyestradiol affinity for oestrogen receptors	39
2-Methoxyestradiol has an antiangiogenic activity: inhibition of HIF-1 alpha expression	40
2-Methoxyestradiol exerts an antimitotic activity: abnormal spindle, tubulin depolymerization & alteration of tubulin dynamics	41
2-Methoxyestradiol alters cell mobility, cell adhesion and trans-well migration <i>in vivo</i> and <i>in vitro</i>	43
2-Methoxyestradiol interacts with tubulin and inhibits colchicines binding site <i>in vivo</i> and <i>in vitro</i>	44
2-Methoxyestradiol induces apoptosis	44
2-Methoxyestradiol modifies tubulin expression	46

## **2-METHOXYESTRADIOL EXPOSED GLIAL AND NEURONAL CELL LINES: LITERATURE REPORTS**

2-Methoxyestradiol-exposed cells of glial origin	48
2-Methoxyestradiol-exposed cells of neuronal origin	50

## **CELL DIFFERENTIATION**

51

## **AIMS OF THE STUDY**

52

## **MATERIALS & METHODS**

Cell culture and treatments	55
Microscopic examination and proliferation assay (MTT test)	56
Indirect immunofluorescence	57
Staining with Hoechst H33342/propidium iodide (PI): viability assay	58
Western Blot	58
Statistical analysis	59

## **RESULTS**

<b>UNDIFFERENTIATED C6 &amp; C1300 CELLS</b>	
PHACO: microscopic examination	62

Hoechst 33258/propidium iodide (PI) staining: viability test	62
MTT test: cell proliferation assay	63
Western blot	
<i>Total <math>\alpha</math>-tubulin</i>	64
<i>Acetylated <math>\alpha</math>-tubulin</i>	64
<i>Tyrosinated <math>\alpha</math>-tubulin</i>	65

**TAPSIGARGIN-DIFFERENTIATED C6 & DB-CAMP-DIFFERENTIATED C1300 CELLS**

PHACO: microscopic examination	66
Hoechst 33258/propidium iodide (PI) staining: viability test	66
MTT test: cell proliferation assay	67
Western blot analysis	67
<i>Total <math>\alpha</math>-tubulin</i>	68
<i>Acetylated <math>\alpha</math>-tubulin</i>	68
<i>Tyrosinated <math>\alpha</math>-tubulin</i>	68

**FIGURES**

**UNDIFFERENTIATED C6 CELLS**

PHACO	71
Vitality test	72
MTT test	75
Western blot analysis	
<i>Total <math>\alpha</math>-tubulin</i>	76
<i>Acetylated <math>\alpha</math>-tubulin</i>	78
<i>Tyrosinated <math>\alpha</math>-tubulin</i>	82

**UNDIFFERENTIATED C1300 CELLS**

PHACO	73
Vitality test	74
MTT test	75
Western blot analysis	
<i>Total <math>\alpha</math>-tubulin</i>	77
<i>Acetylated <math>\alpha</math>-tubulin</i>	79
<i>Tyrosinated <math>\alpha</math>-tubulin</i>	81

**TAPSIGARGIN-DIFFERENTIATED C6 CELLS**

PHACO	82
Vitality test	83
MTT test	86
Western blot analysis	
<i>Total <math>\alpha</math>-tubulin</i>	87

	<i>Acetylated <math>\alpha</math>-tubulin</i>	89
	<i>Tyrosinated <math>\alpha</math>-tubulin</i>	91
<b>DB-CAMP-DIFFERENTIATED C1300 CELLS</b>		
	PHACO	84
	Vitality test	85
	MTT test	86
	Western blot analysis	
	<i>Total <math>\alpha</math>-tubulin</i>	88
	<i>Acetylated <math>\alpha</math>-tubulin</i>	90
	<i>Tyrosinated <math>\alpha</math>-tubulin</i>	92
<b>DISCUSSION</b>		94
<b>BIBLIOGRAFY</b>		102
<b>SITOGRAFY</b>		118

## ***INTRODUCTION***

# CYTOSKELETON

## General features

Cytoskeleton is considered to be the cellular *scaffolding* or *skeleton*.

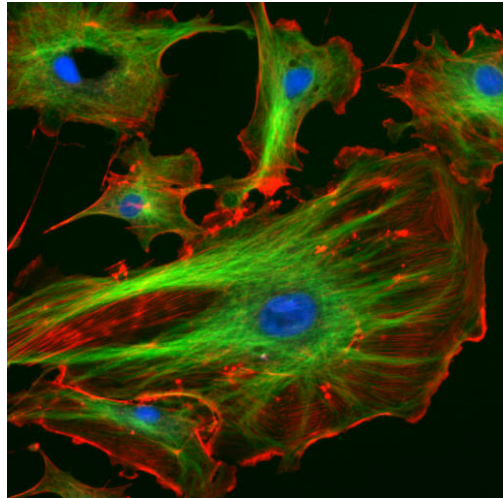


Fig. 1. The eucaryotic cytoskeleton. Bovine pulmonary artery endothelial cells: actin filaments are in red (Texas Red-Phalloidin staining), microtubules are in green (Bodipy FL goat anti-mouse staining) and nuclei in blue (DAPI dye) (From <http://rsb.info.nih.gov/ij>).

Cytoskeleton is contained, as all other organelles, within the cytoplasm of all eucaryotic cells (Fig. 1). Recent research carried out with electron microscopy on some *eubacteria* has demonstrated that cytoskeleton can be present in prokaryotic cells too (Mayer, 2006). Cytoskeleton is a dynamic fibrillary structure that is essential to keep and determine any cellular shape

changes. It is well known that cytoskeleton make possible some cell motion (by characteristic cellular structures such as *flagella* and *cilia*), and plays a crucial role both in intra-cellular transport such as in the movement of vesicles, organelles and cellular division. Cytoskeleton is a bone-like structure floating around/within the cytoplasm essentially composed by three main filaments: microfilaments or actin filaments, intermediate filaments (IFs) and microtubules. Every cytoskeletal filaments are protein structures having the capability, except intermediate filaments, to rapidly polymerize and depolymerize. Accessory proteins bound the filaments and regulate their assembly.



## MICROFILAMENTS

### General features

Microfilaments are the thinnest filamentous cytoskeletal proteins,

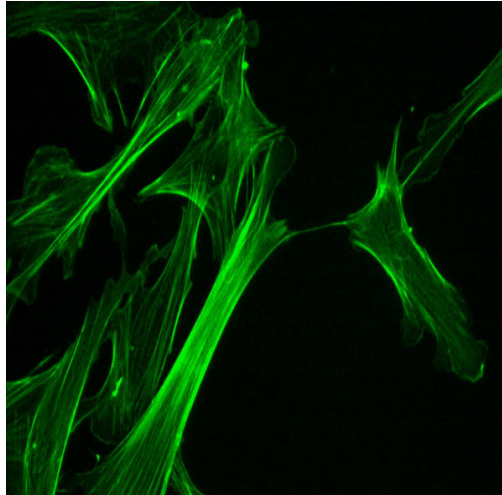


Fig. 2. Actin cytoskeleton. Mouse embryo fibroblasts: microfilaments are in green (FITC-phalloidin) (From <http://rsb.info.nih.gov/ij>).

measuring approximately 7 nm in diameter (Fig. 2).

The single subunits of actin are known as globular actin (G-actin) while the whole filamentous polymer that is constituted of G-actin subunits is called F-actin.

### Actin

G-actin is a globular structural, 42-47 kDa protein found in many eucaryotic organisms, with concentrations of over 100 $\mu$ M. It is also one of the most highly preserved proteins, differing by no more than 5% in species as diverse as *algae* and humans.

### Microfilaments assembly

Actin is the monomeric subunit of microfilaments. Microfilaments have a polar structure like the microtubules since they have a fast growing *plus* end (also known as *barbed* end) and a slow growing *minus* end (also known as *pointed* end). The terms *barbed* and *pointed* come from the arrow-like appearance of the proteic structure as it has been seen in Electron Micrographs. Filaments elongate approximately 10 times faster at the *plus* end than at the *minus* end.

When the polymerization rate at the *plus* end equals the depolymerization at the *minus* end the result is a tread-milling effect where the filaments move without changing its overall length.

Nucleation is the process of actin polymerization and it starts with the association of three G-actin monomers into a trimer. ATP-actin binds the *plus* (+) end then ATP (adenosine triphosphate) is hydrolyzed (half time 2 seconds) and the inorganic phosphate released (half time 6 minutes) (Pollard *et al.*, 2004). ADP-actin dissociates from the *minus* end so that consequent increase in ADP stimulates the exchange of bound ADP-ATP leading to more ATP-actin units. The rapid turn-over is important for cell movement. Three proteins which are regulated by cell signaling mechanisms, work for microfilaments' functionality. CapZ (known as *end capping proteins*), prevents the addition or loss of monomers at the filaments when actin turn-over is unfavorable like in the muscle apparatus. Cofilin binds to ADP-actin units and promotes their dissociation from the *minus* end preventing their reassembly as well. On the other hand, profilin reverses cofilin effect by stimulating the exchange of bound ADP for ATP. Finally, the Arp2/3 complex nucleates new actin filaments while bound to existing filaments and create the branched network.

### **Microfilaments organization and functions**

Microfilaments are an ubiquitous contractor organ not only involved in some cell-to-cell or cell-to-matrix junctions and transduction of signals but also engaged in keeping cellular shape or forming cytoplasmatic protuberances such as *pseudopodia* and *microvilli*. Moreover, microfilaments are crucial for cell movement (*cytokinesis*) and, along with myosin, muscular contraction.

Actin filaments are gathered in two types of structures: network and bundles with the characteristic features of a double-stranded helix. Networks are constituted by actin along with many actin-binding proteins (such as the Arp2/3 complex and filamin) that are characteristically concentrated at the cortical regions of the cells. Recently, it has been proved that actin network is involved in some cellular defensive mechanisms serving as barriers for molecular diffusion within the plasmatic membrane. In non-muscle actin bundles, the filaments are held together: they are kept parallel each other by actin-bundling proteins and/or cationic species. Bundles play a role in many processes such *cytokinesis* and cell movement.

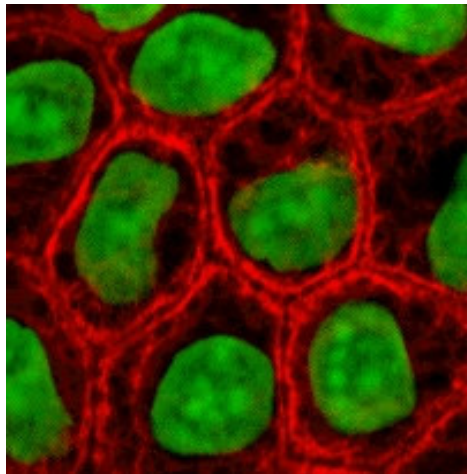


Fig. 3. Intermediate filaments in epithelial cells (MDCK). Keratin filaments which are in red (Texas Red-Phalloidin staining), are concentrated around the edge of the cells, whereas DNA is visualized in green (Methyl green staining) (From <http://en.wikipedia.org>).

## INTERMEDIATE FILAMENTS

### General features

Intermediate filaments (IFs) are heterogeneous cytoskeletal structures formed by members of a family of related proteins (Fig. 3). IFs have a diameter between that of microfilaments and microtubules (7-11nm); IFs differ from microfilaments and microtubules not only for their chemical properties but also because they are very stable structures, formed by fibrotic subunit proteins. Most types of IFs are located in the cytosol between the nuclear envelope and the cell surface membrane.

## **Structure**

The domain structure of IFs molecules is conserved. Proteins have a typical non- $\alpha$ -helical (globular) domain at the N- and C-termini which surrounds the  $\alpha$ -helical rod domain. The essential IFs building block is a parallel, in register dimer that is constituted through the interaction of the rod domain forming a coiled tail. Cytoplasmatic IFs assemble into non-polar unit-length filaments that then gather into longer structures. The characteristic anti-parallel orientation of the fibrotic subunits means that, unlike microtubules and microfilaments have a *plus* and a *minus* end, IFs lack any polarity and do not undergo tread-milling. New evidences have showed that IFs can be also dynamic and motile elements of the cytoskeleton (Helfand *et al.*, 2004).

## **Types of intermediate filaments**

There are about 70 different genes encoding for various intermediate filament proteins that are subcategorized into six types based on similarities in amino acidic sequence and protein structure.

### **Types I and II (Acidic and Basic Keratins)**

They are an heterogenous class of IFs which constitute type I (acidic) and type II (basic) IFs proteins. They are further divided in two groups:

- Epithelial keratins (about 20): typical in epithelial cells;
- Trichocytes keratins (about 13): hair keratins which make up hair, nails, horns and reptilian scales. Acidic and basic keratins bind each other forming acidic-basic heterodimers that associate to form a keratin filament.

### **Types III**

Four proteins which may form homo- or heteropolymeric proteins are classified as type III:

- Desmin: a structural component of the sarcomeres in muscle cells;
- GFAP (glial fibrillary, acidic protein): found in astrocytes and glia cells;
- Peripherin: found in peripheral nerve;
- Vimentin: the most widely diffused of all IFs proteins which can be found in fibroblasts, leukocytes, blood vessels and endothelial cells. Vimentin provides for the cellular membrane and keeps some organelles in a fixed place within the cytoplasm.

### **Type IV**

IFs that are exclusively present in the nervous system:

- Internexin: the major component of the IFs network in small interneurons and cerebellar granule cells;
- Nestin: expressed mostly in the nervous cells. They are implicated in the radial growth of the axon;
- Neurofilaments: found in high concentrations along the axon of vertebrate neurons;
- Synemin: originally found at the Z-band of avian and rodent skeletal and cardiac muscles. It occurs together with nestin and vimentin in glial progenitors during the early differentiation of the mouse central nervous system;
- Syncoilin: found at the neuromuscular junction, sarcolemma, and Z-lines.

## **Type V**

Nuclear lamins.

- Lamins have a structural function in the cell nucleus.

## TUBULIN

### General features

Microtubules are long filamentous, tube-shaped protein polymers present in all eukaryotic cells. Microtubules are crucial in some cellular activities such as morphogenesis, cell mobility, cell signaling and organelles transport. In details, microtubules rearrange during cell division to form the mitotic spindle, which is fundamental not only for the segregation and the replication of sister chromatids, but also for the orientation of the cell cleavage plane. Moreover, microtubules are the most prominent constituent of the composite and extremely organized axonemal structure of *cilia* and *flagella*. In addition, microtubules contribute in the generation of cell polarity and they work, with several motor proteins, as tracks along which organelles and/or vesicles are transported through the cell.

The great variety of microtubule functions comes from the amazing structural flexibility of microtubule organization depending, in a large extent, on their remarkable biochemical and functional properties. Microtubular arrays in eukaryotic cells are dynamic, able to assembly (polymerize), disassembly (depolymerize) and rearrange within few seconds or minutes. This typical property is called *microtubular dynamics*. It is well known that *microtubular dynamics* are based on intrinsic dynamic properties of the tubulin polymers themselves which are regulated by the biochemical features of the main microtubule building block, the tubulin  $\alpha$ - $\beta$  heterodimer.

Among tubulin biochemical attitudes, there is the tubulin intrinsic capability to interact *in vivo* and *in vitro* with a great number of other proteins such as small molecules, nucleotides or drugs that can modify the physiological characteristic of the whole polymer. Finally, it is of interest considering that tubulin is a GTPase as well. The phenomenon of GTP hydrolysis occurs during tubulin polymerization and is essential for the microtubular functional properties.



Fig. 4. Three-dimensional model of tubulin. The protein is a dimer consisting of two monomers that are almost identical in structure. Each monomer is formed by a core of two beta sheets (blue and green) surrounded by helices, and each binds to a guanine nucleotide (pink) (From <http://www.lbl.gov>).

### **Microtubules and tubulin structure**

Microtubules are composed of  $\alpha$ -tubulin and  $\beta$ -tubulin heterodimers.  $\alpha$  and  $\beta$  tubulin monomers are proteins of about 450 amino acids and each monomers

have a molecular mass of about 50,000Da (Fig. 4).

Tubulins are ubiquitous and, in eukaryotic organisms, several genes are known encoding for six  $\alpha$ -tubulin

and seven  $\beta$ -tubulin isotypes. Three  $\alpha$ -tubulin isotypes (1, 2 and 4) and five  $\beta$ -tubulins (I, II, III, IVa and IVb) are expressed in the brain (Luduena *et al.*, 1998; Lee *et al.*, 1990; Redeker *et al.*, 1998) (Table 1).



Tubulins $\alpha$ and $\beta$ isotypes	Comments	References
$\alpha 1/\beta 2$	<ul style="list-style-type: none"> <li>• Highly expressed during brain development</li> <li>• Associated with neurite outgrowth</li> </ul>	Luduena <i>et al.</i> , 1998
$\alpha 4$	<ul style="list-style-type: none"> <li>• Without a C-terminal tyrosine residue</li> <li>• Glutamylated at two residues</li> </ul>	Redeker <i>et al.</i> , 1998
$\beta I/\beta II$	<ul style="list-style-type: none"> <li>• Highly expressed during brain development</li> </ul>	Luduena <i>et al.</i> , 1998
$\beta III$	<ul style="list-style-type: none"> <li>• Neuronal specific</li> </ul>	Lee <i>et al.</i> , 1990
$\beta IVa, b$	<ul style="list-style-type: none"> <li>• Highly expressed during brain development</li> </ul>	Luduena <i>et al.</i> , 1998

Table 1. Overview of the various tubulin isoforms (from Bianchi *et al.*, 2005).

$\alpha$ -tubulin and  $\beta$ -tubulin heterodimers arrange linearly into protofilaments that associate laterally forming microtubular structures with an outer diameter of 25 nm (Fig. 5).

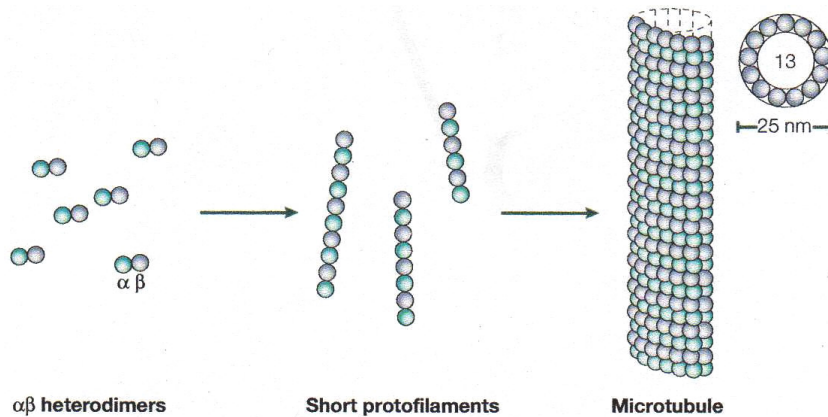


Fig. 5.  $\alpha$ - $\beta$  tubulin heterodimers arrange linearly into protofilaments (From Westermann and Weber, 2003).

Different experimental conditions *in vitro* may vary the number of protofilaments of microtubules between 10 and 15, whereas they are 13 in physiological conditions *in vivo*. The organization of  $\alpha$ - and  $\beta$ -tubulin heterodimers in the microtubular structure is polarized, and this feature determines important structural and kinetic differences at the microtubule ends.  $\alpha$  and  $\beta$ -tubulin heterodimers are arranged in a typical head-tail configuration in which they are polarized with a faster elongating end, named *plus*, exposing  $\beta$  subunits, and a slower elongating *minus* which show the alpha subunit *in vivo*. The *minus* end of the microtubules is associated with the centrosome and is localized close to the center of the cell, while the *plus* end is peripheral (Valiron *et al.*, 2002) (Fig. 6).

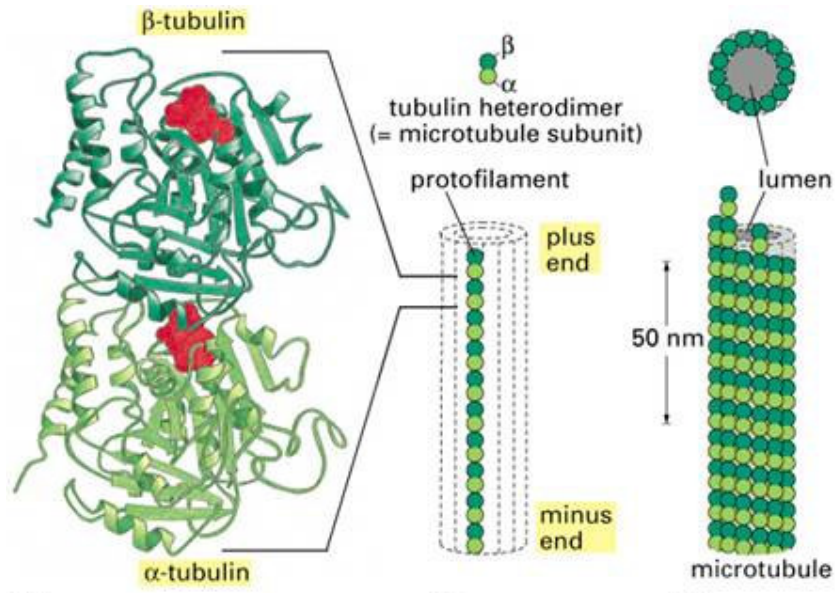


Fig. 6.  $\alpha$  and  $\beta$ -tubulin are arranged in a head-tail configuration in which they are polarized with a faster elongating end, named *plus*, exposing  $\beta$  subunits, and a slower elongating *minus* end showing the alpha subunit (From Alberts *et al.*, 2002).

### Microtubules assembly

Microtubule assembly proceeds in three phases: nucleation, elongation and steady-state.

Nucleation, also known as microtubules aggregation, is the phase of microtubular assembly in which a small cluster of  $\alpha$  and  $\beta$  tubulin monomers aggregate to form a short microtubule nucleus arranged to initiate polymerization properly. The nucleation may give in a variety of conditions. Temperature is a fundamental factor; indeed, tubulin aggregation generally occurs at 30°-37°C, whereas lower temperature do not arise microtubules aggregation anymore. Another fundamental condition is microtubule incorporation as a complex with GTP whose energy input from hydrolysis works for tubulin dynamics. Nucleation is followed by the so-called elongation phase during which  $\alpha$ - $\beta$  dimers are added to the end of each microtubular structure just formed.

Steady state is the last phase of tubulin assembly. *In vitro* studies have probed that a determined proportion of tubulin is in the polymerized

form, whereas another tubulin pool stands soluble (free proportion). Fascinatingly, the amount of soluble tubulin, which is in form of dimers during the steady state, varies with buffer conditions and this amount constitutes the critical concentration for microtubule assembly. Steady state is characterized by a constant GTP hydrolysis. Consumption of energy is necessary for maintenance of the steady state of microtubules since microtubules use energy to continuously provide molecular exchanges between  $\alpha$ - $\beta$  constitutive subunits and the tubulin molecules of the soluble pool (Margolis and Wilson, 1981). Several studies have clarified the mechanisms that are involved in such a continuous exchange. The first is known as *tread-milling*. *Tread-milling* depends on a typical property of microtubular ends at the steady state (or pause): the *plus* end continuously incorporates new tubulin dimers, while at the same time the *minus* end loses them. The energy required for such a dynamic process comes from GTP hydrolysis but the precise mechanism that joins the functional asymmetry of the tubulin ends is still unknown. When tubulin ends are in a fixed position, *tread-milling* results in a sort of microtubular migration that reproduces the propagation of a wave of tubulin assembly and disassembly. By contrast, when microtubular ends are kept in a stationary position, tread-milling generates an apparent flux that travels from the *minus* to the *plus* end (Margolis and Wilson, 1981) (Fig. 7).

The second mechanism is known as dynamic instability. Some models of study showed that, while a population of microtubules exhibits a steady state, an individual microtubule persists in a slow phase of assembly and rapid phase of disassembly so that it never reaches an

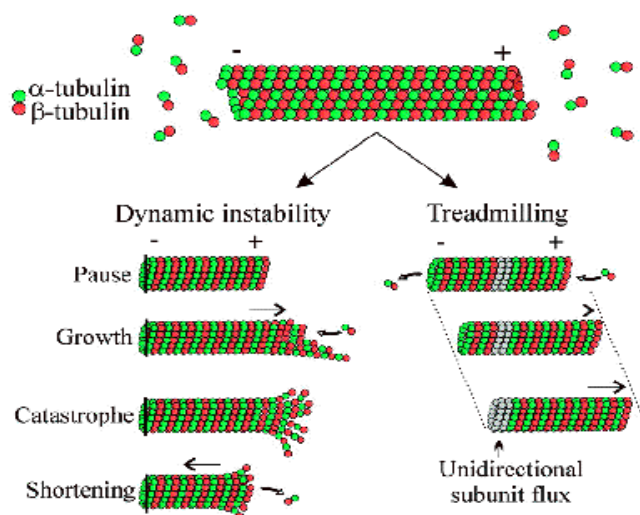


Fig. 7. Tread-milling & dynamic instability (From <http://www.ijpb.versailles.inra>).

equilibrium length. In details, the phase between slow assembly and fast disassembly is called *catastrophe* and the phase between disassembly and assembly is referred to as *rescue* (Fig. 7).

Taking into account these notions, microtubular dynamics are, by definitions, the intrinsic capability of microtubular polymers to rapidly change its biochemical and functional properties as consequence of overall environmental conditions. Polymerized microtubules are intrinsically labile but at the steady state, the whole microtubular system remains out of equilibrium. Events like temperature fall below 10°-15°C readily depolymerize microtubules. Moreover, other events such as removal of GTP, dilution of microtubule suspension with consequent decrease in soluble tubulin concentration, can induce tubulin disassembly. In addition, specific drug as colchicine, vinblastine or nocodazole can easily trigger tubulin depolymerization with different mechanisms of action. In details, colchicine and vinblastine perturb tubulin assembly into microtubules consequently inducing tubulin depolymerization. Naconazole sequesters tubulin dimers in inactive form that, decreasing the soluble pool of tubulin below the critical concentration,

induces microtubules depolymerization (Fig. 8).

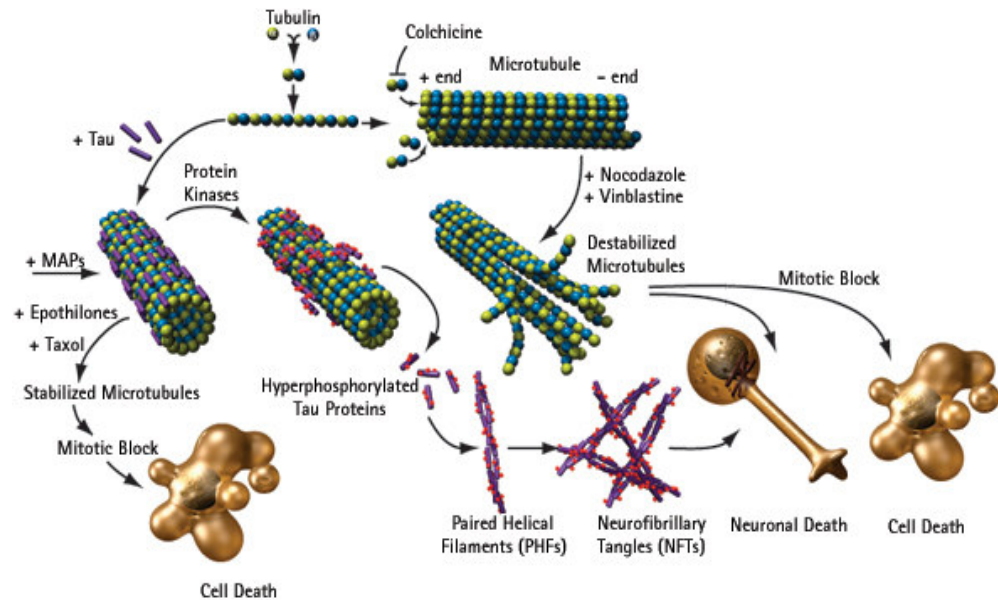


Fig. 8. Tubulin pathways: perturbation of tubulin dynamics via specific MAPs such as Tau or traditional anticancer agents may lead to mitosis block and, by consequence, cell death (From <http://merckbiosciences.com>).

### Microtubules dynamics *in vivo* and *in vitro*

*In vivo* studies on microtubule dynamics have revealed some extensive similarities with microtubule dynamics *in vitro*. Microtubule dynamics and dynamic instability (the main mechanism of microtubules turnover) has been clearly demonstrated in eukaryotic cells. However, differences in the rate of microtubular assembly (10-15% higher than *in vitro* microtubules formed by pure tubulin) and the control of the microtubular polymer by cell effectors has been found (Cassimeris, 1993). It is well known that cell regulation influences both microtubule nucleation and assembly. Nucleation *in vivo* is only provided by the centrosome (also called microtubule-organizing center) and in most cells, the *minus* ends of microtubules are linked to the centrosome. Moreover, microtubule dynamics *in vivo* are regulated by many microtubule-associated proteins (MAPs) that

are usually classified in two main groups: proteins that stabilize and proteins that destabilize microtubules. Recent studies have also highlighted other function of MAPs depending on cellular context, especially with regard to regulation of the mitotic spindle, assembly, and overall microtubular organization and dynamicity *in vivo*. MAPs have been also discovered to interact with actin, intermediate filaments and to modulate microtubule dynamics as motor proteins.

### **Microtubules-stabilizing proteins**

Microtubule-stabilizing proteins promote tubulin assembly and stabilize microtubules. Members of this family include the proteins tau, MAP2 (present in the axon and dendrites, respectively), and MAP4.

A new group of MAPs inducing much higher microtubular stability has been recently identified. This group includes Lis1 (Lissencephaly Isolated Type 1), doublecortin, BPAG1 (Bullous Pemphigoid Antigen 1) and STOP (Stable Tubulin Only Peptide) proteins. Lis1 is distributed along microtubules, not only in neuronal cells but also in several cell phenotypes. Lis1 interacts with the microtubule motor dynein. In details, production of dynein increases retrograde movement of cytoplasmic dynein and leads to peripheral accumulation of microtubules. These findings suggest that the amount of Lis1 may stimulate specific dynein functions in neuronal migration and axon growth (Smith *et al.*, 2000). Doublecortin is expressed in migrating and differentiating neurons and it can be associated *in vitro* and *in vivo* with microtubules acting as microtubular stabilizer. BPGA1 has the property to physically link actin, intermediate filaments and microtubular networks. BPGA1 can bind and stabilize microtubules *in vitro* so that microtubules become sensitive to various

depolymerizing agents, including cold. Cold stability can also be due to microtubules association with different variants of STOP that are typical calmodulin-regulated proteins. In spite of STOP come from a single gene, variants have different start genes of transcription and are expressed in many tissues at diverse stages of development. In neuronal cells, STOP proteins seem to be associated with microtubules: they are the major factors responsible for the slow turnover of neuronal microtubules and apparently required for neuronal differentiation. In addition, STOP proteins can be associated with microtubules in the mitotic spindle and such association appears to be fundamental for the progress of the mitotic process.

Though several proteins have been identified as microtubule-stabilizing proteins, their mechanisms of action are not well known yet. Op18/stathmin is a small ubiquitous protein which has been shown to destabilize microtubules by increasing the catastrophe frequency and regulating microtubules levels both *in vivo* and *in vitro* (Belmont and Mitchison, 1996). Two mechanisms involved in the Op18/stathmin mechanism of action have been postulated. Op18/stathmin has been hypothesized to sequester tubulins, lowering the total soluble amount of tubulin available for polymerization. Furthermore, Op18/stathmin may act directly on microtubules like a catastrophe-promoting factor. Another class of microtubule-stabilizing proteins is formed by the members belonging to the superfamily of kinesin-related microtubules motor proteins. XKCM (Xenopus Kinesin-Related Protein) is a kinesin-related motor protein with the capability to inhibit mitotic spindle *in vitro* and to determine microtubule catastrophe *in vivo*. Heat-shock proteins (HSP27, HSP70 and HSP9) have been seen inhibiting microtubule formation *in vitro* at high concentrations as well. Finally, a small acidic polypeptide,



MINUS (Microtubule Nucleation Suppressor), biochemically purified from cultured cell lines and bovine brain, was ascertained to block microtubule nucleation *in vitro* in centrosome presence or absence.

### **Post-translational modifications**

Microtubules heterogeneity is determined by several post-translational modifications such as tyrosination/detyrosination, acetylation, polyglycylation, polyglutamylolation, phosphorylation and palmitoylation (Westermann and Weber, 2003). These modifications usually occur at the carboxy-terminal domain of the  $\alpha$ - $\beta$  heterodimer, in correspondence of the outer surface of the microtubule where it can interact with other proteins (Westermann and Weber, 2003).

#### ***Tyrosination/detyrosination: the tyrosination cycle***

Tyrosination is a post-translational modification consisting in the addition of a carboxy-terminal tyrosine to most  $\alpha$ -tubulins (Fig. 9).

The first step of this modification is the removal of the carboxy-terminal tyrosine (detyrosination) by a tubulin tyrosine carboxipeptidase (TTCP). This post-translational modification occurs after microtubule assembly since the TTCP prefers polymers. (Argarana *et al.*, 1978). The tyrosinated tubulin displays a carboxy-terminal glutamic acid that is usually referred as Glu-tubulin. In addition, losing Glu-tubulin the penultimate glutamate residue through the enzymatic action of a still unknown peptidase,  $\Delta 2$  tubulin can be generated as well (Paturle-Lafanechère *et al.*, 1991). Interestingly,  $\Delta 2$  cannot be a substrate for the tubulin tyrosine ligase (TTL) and does not take part to the tyrosinated cycle (Paturle-Lafanechère *et al.*, 1991).  $\Delta 2$  represents the final stage of  $\alpha$ -tubulin

maturation, it constitutes a considerable proportion of brain tubulin and it is known as a marker of very long-lived, stable microtubules (Paturle-Lafanechère *et al.*, 1994).

An ATP-dependent reaction catalyzed by the activity of TTL can restore the carboxy-terminal tyrosine (Tyr-tub). TTL, in contrast with TTCP, prefers tubulin dimers as substrate so occurs exclusively before tubulin assembly (Argarana *et al.*, 1977).

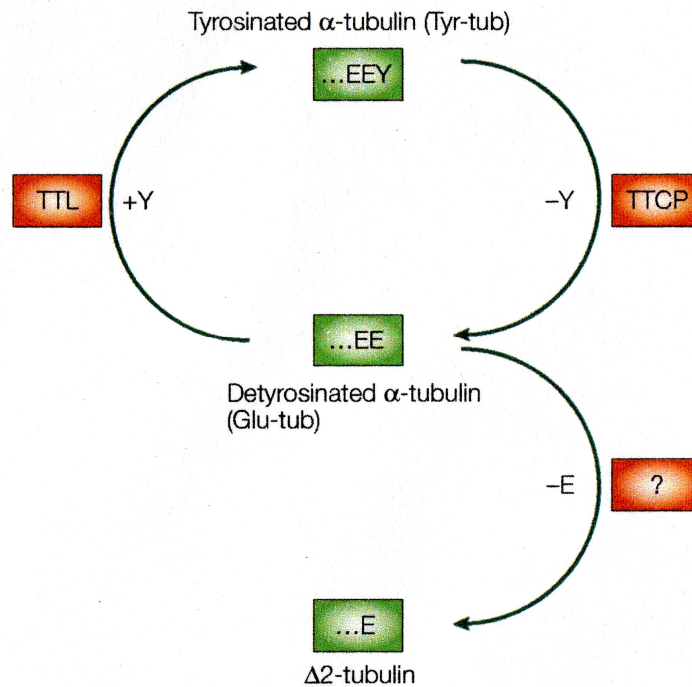


Fig. 9. The tyrosination cycle of  $\alpha$ -tubulin. The carboxy-terminal tyrosine of  $\alpha$ -tubulin can be removed by the tubulin tyrosine carboxypeptidase (TTCP) to generate Glu-tubulin (Glu-tub). In an ATP dependent reaction, the carboxy-terminal tyrosine (Tyr-tub) can be restored through the enzymatic activity of tubulin tyrosine ligase (TTL). Glu-tubulin can lose the penultimate glutamate residue through the activity of an unknown peptidase to generate  $\Delta 2$  tubulin, which cannot function as substrate for TTL and is therefore removed from the cycle (From Westermann and Weber, 2003).

Although detyrosination itself does not stabilize microtubules, it is considered marker of dynamic microtubule. Moreover, detyrosination is thought to be crucial for the cross-talk of microtubule and intermediate filaments as well (Gurland *et al.*, 1995) (Table 2). It has been shown that  $\alpha$ -tubulin can incorporate 3-nitrotyrosine, a modified amino acid generated by the reaction of nitric oxide species with tyrosine. Interestingly, nitrotyrosination is catalyzed both *in vivo* and *in vitro* by the same enzyme, TTL, involved in tyrosination. It has been proposed that this incorporation is irreversible and that the accumulation of 3-nitrotyrosine leads to microtubule dysfunction and cellular injury (Zedda *et al.*, 2004).

### ***Acetylation/deacetylation***

Acetylation is a well known post-translational modification that takes place at lysine-40 in the amino terminus of  $\alpha$ -tubulin located in the lumen of microtubules (Nogales, 2001).

Even if the tubulin acetyltransferase enzyme has not been identified, recently the two enzymes catalyzing the reaction of deacetylation has been found. The enzymes are two histones deacetylase: HDAC6 (Histone Deacetylase 6) and SIRT2 (Sirtuins 2). HDAC6 belongs to the deacetylase family and it is mostly located in the cytoplasm in association with microtubules (Hubbert *et al.*, 2002). SIRT2 is the namesake of a family of closely related enzymes, the sirtuins, that are hypothesized to play a key role in the organism response to stresses such as heat or starvation (Frye *et al.*, 2005).

Acetylation takes place after microtubule assembly. It is marker of stable microtubules being associated with stable microtubular structures such as axonemes (Sasse *et al.*, 1988). Furthermore, has been proposed a role for tubulin acetylation in cell mobility on the basis of the fact that HADC6 over-expression increased the chemiotactic movements in cultured cell, whereas inhibition of the same enzyme blocks cell migration.

### ***Polyglutamylation***

Polyglutamilation is a not very usual form of reversible post-translational modification of glutamate residues occurring in  $\alpha$ - $\beta$  dimers and in two nucleosome assembly proteins (NAP1 and NAP2). For this reason, it seems that chromatin structural proteins are regulated by this post-translational modification.

In polyglutamylation, a polyglutamate side chain of variable length is attached, through an isopeptide bond, to the  $\gamma$  carboxy-group of a glutamate in the carboxy-terminal tail of tubulin (Boucher *et al.*, 1994). Polyglutamylase and polydeglutamylase are the enzymes involved in glutamylation/deglutamylation processes.

Recent findings have revealed a prominent role of polyglutamylation in the interaction between microtubules and their associated proteins (i.e. MAPs 55) in centriole maturation/stability (Gagnon *et al.*, 1996) and in ciliar/flagellar mobility as well (Million *et al.*, 1999) (Table 2).

### ***Polyglycylation***

It is the most important post-translational modification of axonemal microtubule. Polyglycylation is the covalent attachment of a polyglycine side chain through an isopeptide bond to the carboxyl

group of conserved glutamate residues at the carboxyl-terminus of  $\alpha$ - $\beta$  tubulin. This modification was originally discovered in *Paramecium* (Redeker *et al.*, 1994) and later shown in mammalian neurons as well (Banerjee *et al.*, 2002).

Presently, the enzymes catalyzing polyglycylation are not known. Genetic studies carried out on *Tetrahymena thermophila* have provided some information about the possible functions of polyglycylation. In *Tetrahymena* polyglycylation is essential for cellular activities related to axonemal organization, ciliary motility and cytokinesis (Xia *et al.*, 2000) (Table 2).

### ***Palmitoylation***

Palmitoylation consists in the incorporation of the palmitic acid on the  $\alpha$ -subunit at cysteine 376 (Caron *et al.*, 1997). Studies carried out on the budding yeast *Saccharomyces cerevisiae* revealed that palmitoylation of  $\alpha$ -tubulin is necessary for the correct positioning of astral microtubules and for the right microtubule interactions with the cell cortex (Caron *et al.*, 2001) (Table 2).

### ***Phosphorylation***

Phosphorylation is not a common post-translational modification. It consists in the phosphorylation of a serine residue within the carboxy-terminal tail of  $\beta$ -tubulin. Phosphorylation plays a crucial role in the regulation of some MAPs and may be involved in neuronal differentiation since it regulates the axon outgrowth of class III  $\Delta 2$ -tubulin. (Eipper *et al.*, 1974) (Table 2).

<b>Tubulin isotypes</b>	<b>Post translational modifications</b>	<b>Comments</b>	<b>Proposed functions</b>	<b>References</b>
$\alpha$ - $\beta$ tubulins	Tyrosination detyrosination	Marker of dynamic microtubules	<ul style="list-style-type: none"> <li>• Cross-talk to intermediate filaments</li> <li>• Cell differentiation</li> </ul>	Cumming <i>et al.</i> , 1984 Erck <i>et al.</i> , 2005
$\alpha$ -tubulins	Generation of $\Delta 2$ tubulin	Marker for stable very-longed microtubule	<ul style="list-style-type: none"> <li>• Removing tubulin from tyrosination cycle</li> </ul>	Paturle-Lafanechère <i>et al.</i> , 1994
$\alpha$ -tubulin	Acetylation deacetylation	Marker for stable microtubule	<ul style="list-style-type: none"> <li>• Regulation of cell mobility</li> <li>• Bindings of the MAPs</li> </ul>	Sasse and Gull, 1988
$\alpha$ - $\beta$ tubulin	Polyglutamylaton	Multiple glutamylaton sites possible	<ul style="list-style-type: none"> <li>• Centriole maturation, flagellar motility</li> <li>• Regulation of interaction with MAPs</li> </ul>	Boucher <i>et al.</i> , 1994
$\alpha$ - $\beta$ tubulin	Polyglycylation	Multiple glycylation sites possible	In <i>Tetrahymena</i> : <ul style="list-style-type: none"> <li>• Ciliary motility</li> <li>• Cytokinesis</li> </ul>	Xia <i>et al.</i> , 2000
$\alpha$ -tubulin	Palmitoylation	Present in budding yeast	<ul style="list-style-type: none"> <li>• Positioning of astral microtubules</li> </ul>	Caron <i>et al.</i> , 2001
$\alpha$ - $\beta$ tubulins	Phosphorylation	Mainly in $\beta$ -tubulin	<ul style="list-style-type: none"> <li>• Neuronal differentiation</li> </ul>	Eipper 1974

Table 2. Overview of the various tubulins modifications and their proposed functions (From Westermann and Weber, 2003).

## **STEROID HORMONES, NEUROSTEROIDS AND NEUROACTIVE STEROIDS**

### **Steroid hormones**

Steroid hormones are mainly synthesized in the adrenal glands, the gonads and the feto-placental organ. They can easily cross the blood-brain barrier because of their high lipid solubility. The central and peripheral nervous systems are crucial target organs of steroid hormones. Moreover, an extensive steroid metabolism occurs in the brain, several brain regions and peripheral nervous system. Indeed, each of these areas are equipped with the enzymes necessary for the synthesis of steroid as well. The synthesis of steroids may take place particularly, but not exclusively, in myelinating glial cells, from cholesterol or steroidal precursors deriving from peripheral sources. Steroids have been found to play a pivotal role in the development, growth, maturation and differentiation of human brain. Indeed, the activity of steroidogenic enzymes have been identified in specific areas of human fetal brain.

### **Neurosteroids**

The term neurosteroids was firstly defined by Baulieu and co-workers (Baulieu *et al.*, 1990). They discovered that a number of steroid hormones existed in higher concentrations in the nervous system than in the plasma and that these steroids were synthesized in the brain. Nowadays it is known that neurosteroids can be metabolized in the brain from precursor compounds originating from endocrine sources, and can be synthesized *de novo* in the brain from cholesterol.

### **Neuroactive steroids**

Neuroactive steroids are steroids that produce a rapid, non-genomic action in the brain, generally through the action on ligand - or voltage-gated channels (Stoffel-Wagner, 2001). For this reason neuroactive steroids differ significantly from classic steroid hormones since they mainly act upon intracellular receptors resulting in a long lasting, genomic effect (Truss *et al.*, 1988). Neuroactive steroids can either positively or negatively modulate the activity of several ligand-gated ion channel-associated receptors including  $\gamma$ -aminobutyric acid type A ( $GABA_A$ ), serotonin type 3 ( $5-HT_3$ ), glycine and glutamate N-methyl-D-aspartate ( $NMDA_A$ ),  $\alpha$ -amino-3-hydroxy-5-methyl-4-isoxazolepropionic acid (AMPA) and kainite receptors.

Examples of neuroactive steroids are: a) the pregnane steroids 4-pregnene-3,20-dione (progesterone, P),  $3\beta$ -OH-5-pregnen-20-one (pregnenolone, Preg), pregnenolone sulphate (PregS),  $3\alpha$ -OH-5 $\beta$ -pregnan-20-one (pregnanolone),  $3\alpha$ -hydroxy-5 $\alpha$ -pregnan-20-one (allopregnanolone, ALLO),  $3\alpha,21$ -dihydroxy-5 $\alpha$ -pregnan-20-one (allotetrahydrodeoxycorticosterone, THDOC), dihydrodeoxycorticosterone (DHDOC) b) androstane steroids OH-androst-5-en-20-one (dehydroepiandrosterone, DHEA) and DHEA-sulphate (DHEAS).

As mentioned above, neuroactive steroids can exert a bimodal activity since some are agonist, they are known as GABA-agonist (i.e. THDOC), and other neurosteroids are antagonists, the so called GABA antagonists (i.e. P, DHEA, DHEAS). Moreover, the binding of specific neuroactive steroids (i.e.  $3\alpha$ -reduced neurosteroids) to  $GABA_A$  receptors can lead to either inhibition or enhancement of GABA inhibitory effects (Majewska, 1992). For this reason it is clear that neuroactive steroids play a crucial role in mediating many



brain functions and activities. For instance, pregnenolone sulfate and DHEAS-induced (GABA-antagonist) inhibition of GABA<sub>A</sub> receptors may determine effects ranging from anxiety and excitability to seizure susceptibility. Moreover, DHEA and DHEAS, the most abundant circulating neuroactive steroids hormones in humans, can exert a neuroprotective action (Baulieu *et al.*, 1998). Interestingly, a correlation between the decrease in DHEA and DHEAS concentrations, that are strictly related to age and stress conditions, and neuronal vulnerability to degeneration has been established. For instance, marked decrease of DHEA and DHEAS concentrations have been reported in patients affected by neurodegenerative diseases such as Alzheimer's disease and multi-infarct dementia (Näsman *et al.*, 1991; Magri *et al.*, 2000). Neuroprotection by DHEA and DHEAS was also observed *in vivo*, whereas the mechanisms by they act are still unknown (Baulieu *et al.*, 1998).

In addition, great deal of investigations have ascertained a correlation between effects of sex hormones and human cognitive functions. The most prominent examples are the effects of oestrogens and androgens on verbal fluency, the performance of spatial tasks, verbal memory tests and fine-motor skills (Hampson *et al.*, 1990; Phillips and Sherwin, 1992a; Phillips and Sherwin, 1992b).

There is a considerable documentation about oestrogenic influences on brain morphology and neurochemistry including the enhancement of the cholinergic system that is involved in learning and memory (McEwen *et al.*, 1995; McEwen and Alves, 1999). All brain activities induced by neuroactive steroids are subjected to sex-

specific differences. Thus, oestrogen effects differ quantitatively or qualitatively between sexes.

Finally, oestrogens may exert neurotrophic and neuroprotective effects such as induction of neuritis outgrowth, dendritic spines, and synaptogenesis. They also influence the neuronal excitability, improve gene expression and exhibit intrinsic antioxidant activity (McEwen and Alves, 1999).

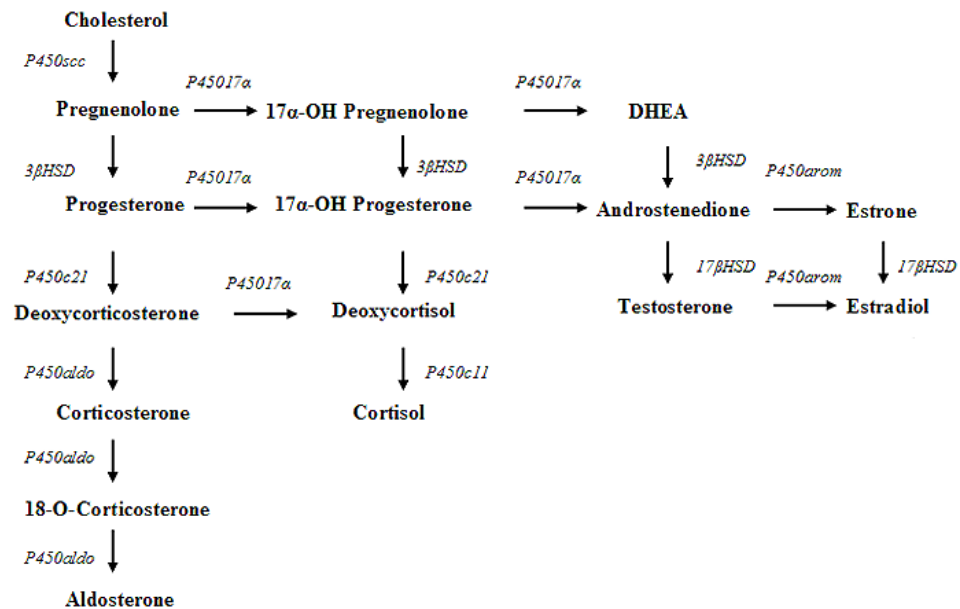


Fig. 10. Steroids hormones pathways.

### **Steroid synthesis in the brain: conversion of cholesterol to pregnenolone**

The first step in the synthesis of all steroid hormones is the conversion of cholesterol to pregnenolone, catalyzed by the enzyme cytochrome P450 cholesterol side-chain cleavage enzyme (P450<sub>scc</sub>) (Fig. 10). In addition to adrenal glands and gonads that are the main sources of steroid production, P450<sub>scc</sub> is also present in the placenta, primitive gut and brain (Mellon *et al.*, 1993).

Recently, it has been identified the localization of P450<sub>scc</sub> mRNA in specific areas of human brain. High amounts of P450<sub>scc</sub> mRNA were found in temporal and frontal neocortex, subcortical white matter from the temporal lobe and in the hippocampus of children and adults. Interestingly, concentrations in the temporal lobe increase markedly during childhood and reach adult levels at puberty. Moreover, P450<sub>scc</sub> mRNA levels were significantly higher in the temporal and frontal neocortex as well as in the hippocampus of women in comparison with men (Beyenburg *et al.*, 1999). These data establish a crucial age- and sex-dependent expression of P450<sub>scc</sub> mRNA in the human brain and provide clear evidence that pregnenolone can be synthesized in the central nervous system.

### **Steroid synthesis in the brain: conversion of androgens to estrogens**

Cytochrome P450 aromatase catalyzes the conversion of androgens to estrogens in specific temporal and frontal brain areas (Fig. 10). Androgens may be metabolized in the brain following two different pathways. The aromatase pathway consists in the transformation of testosterone into estradiol and androstenedione into estrone; this is similar to 5 $\alpha$ -reductase pathway which converts testosterone into dihydrotestosterone and occurs in the majority of the peripheral androgen dependent structures (e.g. prostate).

Aromatase activity has been found higher in the placenta than in the human brain. Moreover, aromatase activity both in temporal and in frontal brain areas has been demonstrated. Interestingly, frontal aromatase activity was always higher than temporal aromatase activity regardless of sex and/or disease state. By contrast, in temporal lobe and hippocampus, the brain areas in which 5 $\alpha$ -

reductase was ascertained, the expression levels of  $5\alpha$ -reductase are very similar (Wozniak *et al.*, 1998).

### **3 $\beta$ -hydroxysteroid dehydrogenase: inactivation of metabolite of steroid hormones**

In liver metabolism, 3 $\beta$ -hydroxysteroid dehydrogenase (3 $\beta$ -HSD) plays an essential role leading to physiologically inactive metabolites of steroid hormones (Fig. 10). However, three functional 3 $\beta$ -HSD isozymes (type 1, 2 and 3) have been characterized on the basis of their affinity for  $5\alpha$ -dihydrotestosterone. The isozyme 1 is expressed exclusively in the liver, whereas the isozyme 2 is present both in the human hippocampus and liver (Khanna *et al.*, 1995).

### **17 $\beta$ -hydroxysteroid dehydrogenase: regulation of the biological activity of steroid hormones**

There are seven human isozymes of 17 $\beta$ -hydroxysteroid dehydrogenase (17 $\beta$ -HSD) (Fig. 10). 17 $\beta$ -HSD plays a crucial role in the regulation of the biological activity of sex hormones. 17 $\beta$ -HSD is essential for the biosynthesis of the strong androgens and oestrogens, (testosterone and estradiol) from their weaker precursors androstenedione and estrone (Peltoketo *et al.*, 1999). These conversions are reversible and thus can lead to a deactivation of the respective sex hormones. The different isozymes show an individual cell-specific expression as well as a typical substrate specificity. The importance of the 17 $\beta$ -HSD activity in the maintenance of physiological levels of estradiol and testosterone is reflected by its ubiquitous distribution in peripheral tissues. As it regards the central nervous system, 17 $\beta$ -HSD expression has been ascertained not only in specific areas of the adult brain such as human temporal lobe and

hippocampus but also in human fetal brain. The expression levels of  $17\beta$ -HSD are significantly higher in the subcortical white matter than in the cerebral neocortex. The main expression of  $17\beta$ -HSD in the subcortical white matter suggests that glial cells could play a role in the biosynthesis and deactivation of sex steroids in the brain. Finally, there is no sexual dimorphism in the expression or activity of  $17\beta$ -HSDs (Martel *et al.*, 1994).

## 2-METHOXYESTRADIOL: BIOCHEMICAL FEATURES AND ITS ACTIVITY IN *VITRO* AND IN *VIVO*

### General features

2-Methoxyestradiol (2ME) (Fig. 11) is an endogenous steroid metabolite of 17 $\beta$ -estradiol. It has been developed as a novel antitumor agent for its extreme effectiveness in several cancer lines *in vitro* and *in vivo*. 2ME may also be active in cells of central and peripheral nervous system. Peculiar mechanisms of 2ME action make this molecule extremely attractive for the study of the pathogenesis and the treatment of several diseases occurring in the nervous system.

### Biochemical and physiological properties

2ME is one of the most biologically active endogenous metabolite of 17 $\beta$ -estradiol (E2). E2 is metabolized to 2-hydroxyestradiol

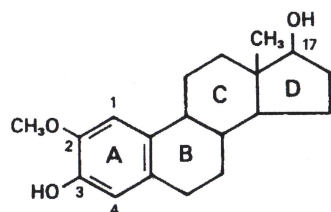


Fig. 11. 2-Methoxyestradiol.

(2OH) through cytochrome P450<sub>scc</sub> by a NADPH-dependent cytochrome P450-linked monooxygenase system. Then, 2OH is rapidly O-methylated at the 2-position by ubiquitously present catechol-O-methyltransferase to 2ME (Brueggemeier *et al.*, 1989). 2ME binds the sex hormone-binding globulin (SHBG) in the blood and represents a fundamental step in the elimination of the potentially toxic catechol oestrogens produced by proliferating cells (Gelbke *et al.*, 1976; Dawling *et al.*, 2001). 2ME plasma levels of women are higher than those found in men and they can be even more elevated during pregnancy (Berg *et al.*, 1992).

## **2-Methoxyestradiol affinity for oestrogen receptors**

In spite of the fact that 2ME has a biochemical similarity with  $17\beta$ -estradiol, other oestrogens and several their metabolites, 2ME estrogenic activity and its affinity for oestrogen receptors (ERs: ER $\alpha$ , ER $\beta$ , ER $\alpha\beta$  subtypes) are still matter of debate.

Firstly, Martucci and Fishman have showed that 2ME has a low binding affinity for uterine cytosolic ERs and a very low biological activity as a conventional oestrogen. Indeed, these Authors have seen that continuous administrations of 2ME in ovariectomized rats did not exert any uterotrophic activity and did not modify LH plasma level (Martucci and Fishman, 1979). By contrast, in HUVEC (Umbilical Vein Endothelial Cells), MDA-MB-435 and MDA-MB-231 (Human Breast Carcinomas Cells) cell lines, 2ME has been probed exerting a significant binding affinity for ER $\alpha$  even if its biological activity was independent from ERs activation (LaVallee *et al.*, 2002).

The above mentioned results disagree with findings provided by Banerjee and co-workers. Exposing GH3 (Rat Pituitary Tumor Cells), MCF-7 (Epithelial Tumour Cells) and MIA-Pa-Ca-2 (Pancreatic Adenocarcinoma Cells) cell lines to 2ME micromolar concentration, these Authors have demonstrated that, not only has 2ME a high binding affinity for ERs- $\alpha$  but also it can modulate ERs- $\alpha$  activation. Interestingly, 2ME seemed to exert a biphasic effect in cellular function being a stimulus for cell growth at low doses and having a reversed action at higher concentrations (Banerjee *et al.*, 2003).

Finally, a study carried out on 2ME-exposed MCF-7 (Epithelial Tumoral Cells) cell line has supplied further data that make stronger Banerjee's hypothesis. Indeed, a direct link between 2ME

effects and 2ME affinity for ERs has been clearly established. Taking into account Authors' conclusions, the common notion about 2ME low affinity for ERs should have come from mere methodological misunderstandings. Indeed, a new methodological approach has let them to find a direct link between 2ME high affinity to ERs as a real oestrogen agonist and 2ME biological activity even inducing, in this case, tumour growth (Sutherland *et al.*, 2005).

### **2-Methoxyestradiol has an antiangiogenic activity: inhibition of HIF-1 alpha expression**

2ME was initially considered as a direct inhibitor of angiogenesis since it strongly inhibits endothelial cell proliferation and cell migration *in vitro*. Moreover, oral 2ME-administration in mice has been seen reducing the neovascularization and suppressing growth of solid tumours (Fotsis *et al.*, 1994). The mechanisms involved in such a 2ME-antiangiogenic activity have been partially clarified. Studies carried out on MDA-MB-231 (Human Breast Cancer Cells), PC-3 (Human Prostatic Cancer Cells) cell lines and endothelial cells have revealed that 2ME-antiangiogenic activity is mediated through inhibition of HIF-1 $\alpha$  expression. HIF-1 $\alpha$ , a heterodimer of  $\alpha$  and  $\beta$  subunits, is a proangiogenic transcription factor that interacts with some hypoxia response elements (HREs) and enhances the transcription of multiple proangiogenic proteins including VEGF-A (Vascular Endothelial Growth Factor). In normoxic conditions, HIF-1 $\alpha$  is degraded by the proteasome system, whereas it can be stabilized by hypoxia conditions (Mabjeesh *et al.*, 2003). A recent study has presented new evidences on the role of 2ME as inhibitor of angiogenesis. It has



been highlighted that 2ME can determine a marked depolymerization of the microtubules in EC (Endothelial Human Pulmonary Cells) cell line inducing evident lung vascular barrier dysfunctions (Bogatcheva *et al.*, 2007).

### **2-Methoxyestradiol exerts an antimitotic activity: abnormal spindle, tubulin depolymerization & alteration of tubulin dynamics**

Antimitotic activity was the first mechanism that has been discovered being cause of 2ME cytotoxic effect *in vitro*. Since almost 20 years ago, Seegers and co-workers have probed that 2ME determined anomalies during cellular mitosis at high concentrations (between 10 and 25 $\mu$ M). In MCF-7 (Human Breast Adenocarcinoma Cells) and HeLa (Human Cervical Adenocarcinoma Cells) 2ME exposed-cell lines, 2ME was discovered to determine an abnormal and fragmented spindle formation (also known as bipolar) with disoriented microtubular arrangement in the metaphase of dividing cells (Seegers *et al.*, 1989).

Abnormal polymerization of mitotic spindle was observed in SK-OV-3 (Human Ovarian Carcinoma Cells), HeLa (Human Cervical Carcinoma Cells), PC3 and DU 145 (Human Prostate Carcinomas Cells) cell lines as well. Low 2ME micromolar concentrations have been seen interfering with the normal polymerization of the mitotic spindle microtubules. Indeed, anomalous spindles appeared to be short and not properly organized so that the consequent dysfunctional alignment of DNA determined the mitotic arrest. Moreover, high 2ME micromolar concentrations exposure could trigger a marked tubulin depolymerization. In details, from 5 to

10 $\mu$ M 2ME micromolar exposure, 50% of microtubules were lost, whereas a complete inhibition of tubulin polymerization was observed between 16.6 and 19.9 $\mu$ M 2ME exposure (Tinley *et al.*, 2003).

By contrast, some studies have hypothesized that 2ME exerts its antimitotic activity more intensively altering tubulin dynamics rather than determining microtubular depolymerization. In a study carried out on MCF-7 (Human Mammary Carcinoma Cells) cell line, Attalla and co-workers have reported that, the mitosis block following 2ME micromolar concentration (between 5 and 20  $\mu$ M) exposure was not exclusively accompanied by depolymerization of tubulin and resultant inhibition of mitotic spindle assembly. The mere defect in mitosis was confirmed by the arrest of chromosomes in the metaphasal plate since cells whose mitosis was blocked by a tubulin depolymerizing drug (i.e. colcemide) showed their chromosomes dispersed in the cytoplasm. According to this study, 2ME mitosis-block is similarly induced by several anti-calmodulin agents or some compounds that affect microtubules dynamics (i.e. taxol and vinblastine). Thus, given the fact that metaphase to anaphase transition is a calmodulin-dependent step and 2ME inhibits calmodulin activity *in vitro*, 2ME metaphasal arrest has been proposed to occur *via* inhibition of calmodulin (Attalla *et al.*, 1996).

Brueggemeier and co-workers., agree with the hypothesis that 2ME antimitotic effect is due to 2ME-induced alteration of microtubular dynamics rather than the solely microtubule depolymerization. These Authors have ascertained that bipolar spindle formation, block of mitosis and disruption of microtubules in MCF-7/ER+, MDA-MBA-231/ER (Breast Cancer Cells) cell lines were induced

starting from 8.7 $\mu$ M exposure (Brueggemeier *et al.*, 2001). Recently, Kamath and co-workers have provided new evidences about such 2ME property. In details, they ascertained that in MCF7 (Human Mammary Carcinoma Cell) cell line 2ME-induced mitotic arrest was not accompanied by detectable microtubular depolymerization. The Authors found that tubulin depolymerisation 2ME-induced needed 2ME concentrations higher than those necessary to affect microtubular dynamics. These findings support the assumption that, at its lowest effective concentrations, 2ME may cause mitotic arrest and suppress microtubular dynamics by stopping microtubule growth parameters, increasing the time of steady-state and interfering with chromosome progression or cell division. This hypothesis could be also reinforced by the fact that the mitosis block 2ME-induced on actively dividing cells is more effective if they have a high proliferation rate (Kamath *et al.*, 2006).

### **2-Methoxyestradiol alters cell mobility, cell adhesion and trans-well migration**

2ME cytotoxic activity could be related to the alteration of other cytoskeletal functions such as cell motility, cell adhesion and trans-well migration. 2ME was established to arrest spontaneous BCR-ABL transformed Ba/F3 cells (Mouse Peripheral Blood, pro B) mobility by changing their morphology and volume. Cells exposed to micromolar 2ME concentrations (from 1 to 5 $\mu$ M) showed a reduction in number of *pseudopodia* and were detached from fibronectin-coated surfaces in which they have grown. In addition, 2ME markedly inhibited the spontaneous cell migration trough a trans-well membrane. Functional modifications were accompanied

by depolymerization of tubulin, appearance of disorganized microtubules and nuclear morphological features typical of defective mitosis. Taken together, these data suggest that 2ME regulates multiple cellular functions related to the main physiological cytoskeletal activities (Sattler *et al.*, 2003).

### **2-Methoxyestradiol interacts with tubulin and inhibits colchicine-binding site *in vitro* and *in vivo***

Depending on the *in vitro* reaction conditions, 2ME can bind to the colchicine site of tubulin, be incorporated in a polymer resulting in altered stability properties or block tubulin polymerization. In presence of 1.0M glutamate/1.0mM and MgCl<sub>2</sub> at 37°C, 2ME arrests the nucleation and propagation phase of tubulin assembly, whereas do not interfere with the reaction extent. Interestingly, the polymer formed in presence of 2ME is cold-stable and has little morphological abnormalities. Under sub-optimal conditions (0.8M glutamate/absence of MgCl<sub>2</sub> at 25-30°C) 2ME could totally inhibit tubulin polymerization (D'Amato *et al.*, 1994).

2ME can bind to the colchicine binding-site of tubulin in unpolymerized  $\alpha$ - $\beta$  tubulin dimers as well. In glutamate-induced tubulin assembly and in preformed tubulin, significant amounts of 2ME interact with tubulin forming abnormal polymers with altered properties (Hamel *et al.*, 1996). The complete block of tubulin polymerization in MDA-MB-435 cells (Human Breast Cancer Cells) has confirmed the 2ME capability to bind the colchicine binding-site (Cushman *et al.*, 1995).

### **2-Methoxyestradiol induces apoptosis**

2ME can induce apoptosis in cancer cell lines through several pathways. 2ME may determine inhibition of the transcription of superoxide dismutase (SOD) which protects cellular from damage and cell death determined by superoxide radicals. Tumour cells are more dependent on SOD than normal cells, since they have a higher superoxide production but a lower level of SOD than normal cells (Huang *et al.*, 2003). This is one of the mechanisms by which 2ME is extremely effective in fast-growing cells (i.e. cancer cells), whereas it does not affect slow-growing cells (i.e. normal cells). When exposed to 2ME micromolar concentrations (from 1 to 2 $\mu$ M), normal skin fibroblast strain HSF43 (Human Fibroblast Cells) is not susceptible to 2ME.

In SV40 (Simian Vacuolating Virus 40) T antigen-transformed, HSF43 cell line, 2ME determines G<sub>2</sub>/M block, nuclear fragmentation, micronucleation and increase in p53 peculiar of apoptosis. The Authors argued that 2ME, being a microtubule poison, it may act as enhancer of 2ME apoptotic effect. Similar results were obtained from TK6 and WTK (Lymphoblast Cells) cell lines (Seegers *et al.*, 1997).

In addition, it has been ascertained that 2ME can start various mitogen-activated protein (MAP) kinases such as MAPKs/ERK, JNK or p38 MAPKs involved in the regulation of some cellular activities. MAPKs/ERK is a signal pathway coupling growth factors of intracellular responses to cell receptors. MAPKs/ERK is activated by mitogenic stimuli and plays a crucial role in regulation of cell proliferation and differentiation. Moreover, JNK and p38 MAPK control gene expression, mitosis and cell differentiation or survival. JNK/p38 MAPK are triggered by pro-inflammatory cytokines and environmental stresses such as osmotic shock, UV

light, heat shock or growth factor withdrawal. Finally, Bcl-2, a family of genes and proteins that govern mitochondrial outer membrane permeabilisation (MOMP) and may be either pro-apoptotic or anti-apoptotic factors, can be phosphorylated by MAPK kinases activation. Bcl-2 phosphorylation is a crucial biochemical event related to the triggering of cellular apoptosis. 2ME through MAPK indirect or direct activation may induce Bcl-2 phosphorylation and consequent cellular apoptosis. Several studies have highlighted this assumption. In K5628 (Human Erythromyeloid Leukemia) cell line, 2ME-induced microtubular damages may determine phosphorylation of Bcl-2 uncoupling from JNK/SAPK activation. However, the Authors hypothesized that JNK/SAPK is indirectly involved in the pathway that leads to Bcl-2 activation (Attalla *et al.*, 1998). By contrast, in OVCAR-3 (Human Ovarian Carcinoma Cell) cell lines it was found that Bcl-2 phosphorylation is solely related to p38 MAPK activation, whereas JNK or ERK are not necessary to Bcl-2 phosphorylation (Bu *et al.*, 2006). These findings disagree with a study carried out on LNCaP (Human Prostate Cancer Cells) cell line where JNK activation was discovered to be the crucial pathway implicating in Bcl-2 phosphorylation. The data obtained let the Authors to form the hypothesis that, different mechanisms leading to Bcl-2 phosphorylation may be due to MAPKs exhibition of cell-type specific responses (Shimada *et al.*, 2003).

## **2-Methoxyestradiol modifies tubulin expression**

Gokmen-Polar and co-workers has compared the effects of 2ME on stable 2ME-resistant cells with a  $\beta$ -tubulin mutation in MDA-MB-435 (Human Breast Cancer Cells), W435 (Human Carcinoma

Cells) and P435 (Parental Cells) cell lines. A dose-dependent depolymerization of microtubules was observed when P435 cells were exposed to 2ME micromolar concentrations, whereas 2ME-resistant cells remained unaffected. Indeed,  $IC_{50}$  were 0.38 $\mu$ M for P435, 12.29 $\mu$ M for W435 and 15.23 $\mu$ M for 2ME-resistant cells. Interestingly, levels of acetylated and detyrosinated  $\alpha$ -tubulin decreased in P435 cells in a clear dose-dependent manner, while they were unchanged in 2ME-resistant cells. Taken together this data suggest that 2ME induces microtubules alteration only in cells with tubulin isoforms that have affinity for 2ME (Gokmen-Polar *et al.*, 2005).

## **2-METHOXYESTRADIOL-EXPOSED GLIAL AND NEURONAL CELL LINES: LITERATURE REPORTS**

### **2-Methoxyestradiol-exposed cells of glial origin**

In a study carried out on DAOY, D341, D283 (Human Medulloblastoma Cells) cell lines and U87 and T98 (Human Astrocytoma/glioblastoma Cells) high-grade anaplastic cell lines, it has been shown that 2ME acts as inhibitor of cell growth more efficiently in tumour than in non-tumour cells. At 0.5, 1, 2 and 3 $\mu$ M concentrations, 2ME causes 38%, 80% decrease in growth of astrocytoma/glioblastoma and medulloblastoma cells respectively, by blocking cycle progression mainly in G2/M phase. This study also proved that 2ME-mediated growth inhibition occurs with induction of apoptosis. Interestingly, 2ME-induced apoptosis was not accompanied by modification of the expression of p53 and Bax (Kumar *et al.*, 2003).

Moreover, another work carried out on U87, T98, U138 (Human Astrocytoma/glioblastoma Cells) cell lines and cultured rat astrocytes 2ME-exposed (from 0.001 to 10 $\mu$ M for 2 days) determined a marked growth inhibition (between 60% and 90%) only in glioblastoma cells. 2ME antiproliferative effect was accompanied by an increase in apoptotic cells with abnormal nuclear morphology. Treatment of U87, T98 and U138 cells with 3.3 $\mu$ M 2ME resulted in 39%, 20% and 82% growth inhibition in comparison with control and cells were blocked at G2/M phase. In addition, elevated levels of the tumour suppressor protein p53 were only detectable in U87 and in rat astrocytes. According to the Authors' conclusions, given the fact that rat astrocytes have a much slower proliferation rate than glioblastoma cells and that 2ME did



not induce nuclear alterations in astrocytes, 2ME appears to be less effective in astrocytes than in glioblastoma cells (Lis *et al.*, 2004). Chamaon and co-workers observed that 2ME-exposure (0.2, 2 and 20 $\mu$ M for 6 days) of U87, U138, LN405 (Human Glioblastoma Cells) cell lines and RG2 (Rat glioma Cell) cell line caused a significant reduction of the viable cell number. When compared with control, the drug-specific cell reduction was in the range between 10% and 40% for lower 2ME concentrations and between 75% and 100% for higher 2ME concentrations. Caspase-3 activity increase, nuclear fragmentation and micronucleation in all 2ME-treated cells, revealed the apoptotic nature of cell death. Interestingly, the Authors observed that during interphase, 2ME-induced morphological alterations were not accompanied by complete distraction of microtubular network. These findings were suggestive that 2ME had no effect on interphase microtubules since it needed a much higher concentration to generate aberrant mitotic spindles resulting in mitotic block an induction of apoptosis (Chamaon *et al.*, 2005).

A recent study carried out on the cell lines above mentioned (U87, U138, LN405 and RG-2) confirmed that 2ME-exposure (2 and 20 $\mu$ M for 24 and 78 h) determined a significant reduction of the viable cells number. Moreover, the death-inducing apoptotic mechanism was further probed by micronucleation and nuclear fragmentation, whereas the role of the death receptor 5 remained controversial. Indeed, short incubation with 2ME (20 $\mu$ M for 24 h) determined death-cell independently of death receptor 5 up-regulation (Braeuninger *et al.*, 2005).

## **2-Methoxyestradiol-exposed cells of neuronal origin**

Retinoic acid (RA)-differentiated human neuroblastoma (SH-SY5Y) cell line was sensitive to 2ME in a concentration-dependent manner from 0.3 to 10 $\mu$ M. 2ME micromolar exposure induced cell death and internucleosomal DNA fragmentation peculiar of defective mitosis. Interestingly, it has been found that 2ME may induce the protein synthesis inhibitors cycloheximide and apopain (Asp-Glu-Val-Asp-H, aldehyde) in inhibitor-sensitive neuronal cell death (Nakagawa-Yagi *et al.*, 1996).

## CELL DIFFERENTIATION

Previously published works have ascertained that neuronal differentiation occurs when neuronal cells show at least one cytoplasmic process longer than the main diameter of the cell body (Chang *et al.*, 2006). Moreover, inhibition of cell proliferation, hypertrophy of cell bodies and nuclei, elongation of cytoplasmic processes, as well as the tendency to flatness and multipolarity of cells, are typical of differentiated neurons (Miyake *et al.*, 1975).

Axonal extension is accompanied by an increase in the number and length of microtubules, which in the axon are typically arranged parallel to the axis. Both intrinsic capability to elongate axons, and extrinsic signals, such as serum deprivation, dimethyl sulfoxide, retinoic acid, N<sup>6</sup>,2'-O-dibutyryl-adenosine-3',5'-cyclic-monophosphate (db-cAMP) regulating the outgrowth at the axonal tip, play a role in cellular differentiation (Seyedin *et al.*, 1981).

Exposure to taspigargin (TG) micromolar concentrations may also induce differentiation in rat glioma cells (C6). C6 cell differentiation results in a marked cell proliferation decrease and modification of cell morphology since cells from a round, flat shape acquire a typical spindle shape extending long cytoplasmic processes (Kuo *et al.*, 2004).

## AIMS OF THE STUDY

2ME is a novel antiangiogenic, cytotoxic and antimitotic drug candidate in phase I and II clinical trials for the treatment of a broad range of tumour types.

As we reported, 2ME mainly acts inducing defective mitosis and alteration of tubulin dynamics. Indeed, 2ME directly interacts with tubulin, inhibits tubulin colchicine binding-site and induces abnormalities in polymerization of mitotic spindle resulting in a perturbation of tubulin expression. Interestingly, 2ME seems to be more effective in fast-growing cells (i.e. tumour cells) than in slow-growing cells (i.e. normal cells). Cell line sensitivity may be due to not only to the specific sensitiveness of cell phenotypes but also to the 2ME capability to interact more efficiently with cells having a high microtubular dynamic.

Taking into account these assumptions, we provided an *in vitro* model of study in order to find new evidences about some 2ME mechanisms of action in the central nervous system (SNC). For this reason we chose two continuous cell lines of glial (rat glioma, clone C6) and neuronal origin (mouse neuroblastoma, clone C1300) representative of the main SNC cellular phenotypes. Moreover, since C6 and C1300 are fast-growing and highly proliferating cell lines, they may represent a useful model for the comprehension of mechanisms by which 2ME exerts its antimitotic and cytotoxic action. In addition, we studied 2ME action on differentiated C6, C1300 cell lines with the aim to systematically compare the relative effectiveness of 2ME toxicity on undifferentiated fast-growing cell lines and differentiated slow-growing cell lines of glial and neuronal origin.

To summarize, purposes of this work are:

- find possible differences in the relative effectiveness of 2ME toxicity on cells of glial and neuronal origin;
- systematically compare possible differences in the relative effectiveness of 2ME toxicity on undifferentiated fast-growing cell lines and differentiated slow-growing cell lines of glial and neuronal origin.

In order to evaluate the relative effectiveness of 2ME we provided a study on morphological features, cell vitality, cell proliferation and tubulin dynamics in C6/C1300 undifferentiated/differentiated cells undergone experimental protocols.

In conclusion, this study would like to contribute to 2ME activities knowledge on cells of glial and neuronal origin *in vitro* and it is aimed at setting a model for successive therapeutic or clinical *in vivo* applications.

## ***MATERIALS & METHODS***

## Cell culture and treatments

In the present work were used two continuous cell lines: rat glioma (C6) and murine neuroblastoma (C1300) cells. Indirect immunofluorescence assessed the specific cellular phenotype: antibodies to glial fibrillary acidic protein (GFAP), an intermediate-filament (IF) protein that is highly specific for astroglial lineage cells, and anti- $\beta$ -tubulin class III, marker of neuronal cells, were applied for C6 and C1300 cell lines respectively (Fig. 12).

Cells came from the *Istituto Zooprofilattico Sperimentale della Lombardia e dell'Emilia* (American Type Culture Collection, Rockville, MD, USA).

C6 and C1300 cell lines at passage 60 were cultured in basal phenol-red-free RPMI-1640 medium supplemented with 10% heat inactivated dextran-coated charcoal-stripped newborn calf serum, 2 $\mu$ M L-glutamine, 100 units/ml penicillin G and 100  $\mu$ g/ml streptomycin sulphate. Cells were seeded in 75 cm<sup>2</sup> flasks with basal medium at the concentration of 5.6X10<sup>5</sup> per ml and they grown at 37°C in a 5% CO<sub>2</sub> humidified atmosphere. Only basal medium was used for control cells; the amounts of 2ME (*Sigma*) were added to the basal medium. Final 2ME micromolar concentrations (0.01, 0.1, 1, 5, 10 $\mu$ M) were chosen taking into account data from literature (Lis *et al.*, 2003, Chamaon *et al.*, 2005). Moreover, 2ME micromolar concentrations were serially diluted from a stock solution containing 20 mg of 2ME dissolved in 1 ml DMSO (0.00001% v/v). Since DMSO could have a toxic effect on cells, a further control was set by incubating cells in basal medium containing DMSO at the same concentration applied to dissolve 2ME (DMSO control cells). Cells were treated with the

toxic for 5 days, after 3 days the culture medium was replaced by fresh medium.

C6 and C1300 cells were differentiated adding 4 $\mu$ M of taspigargin and 10 $\mu$ M of db-cAMP respectively to the basal medium. Cells were treated for 5 days, after 3 days the medium was replaced by fresh medium.

Finally, differentiated monolayers were exposed to 2ME micromolar concentrations (0.1, 1 and 5 $\mu$ M) and cultured following the above mentioned experimental conditions.

### **Microscopic examination and cell proliferation assay (MTT test)**

In order to estimate morphological features, undifferentiated and differentiated C6, C1300 monolayers were daily observed in the living state under phase-contrast optics (PHACO) at 20X magnification with an inverted microscope (*Leitz*, DMIL) and photographed by a digital camera. Pictures were captured in bitmap format.

Evaluation of cell growth rate on undifferentiated C6 and C1300 cells (MTT test) was performed. Cells were plated in 96-well plates containing 50x10<sup>3</sup> cells in 200 $\mu$ l of basal medium and then exposed to the different 2ME micromolar concentration (0.01, 0.1, 1, 5, 10 $\mu$ M) following the above indicated experimental protocols. After 5 days of treatment, cells were incubated in 3-(4,5-dimethylthiazolyl-2)-2,5-diphenyltetrazolium bromide assay (MTT Cell Titer96<sup>®</sup>, *Promega*, Madison, WI, USA) for 1h. MTT was bio-reduced by living cells into a colored formazan product that is soluble in culture medium. Absorption values were read setting the automatic microtiter reader at 492nm (*Uniskan II*, *Labsystem*,



Helsinki, Finland). This method correlates absorbance reading to the number of living cells.

MTT test was also carried out on differentiated cells. Undifferentiated C6 and C1300 cells were seeded in 96-well plates containing  $50 \times 10^3$  cells in 200  $\mu$ l and treated with 4  $\mu$ M of tapsigargin and 10  $\mu$ M of db-cAMP for 5 days. After differentiation cells were exposed to 2ME micromolar concentrations (0.1, 1, 5  $\mu$ M) taking into account the above-mentioned protocols.

### **Indirect immunofluorescence**

In order to determine markers of specific cellular phenotype, indirect immunofluorescence was performed.

Cells were seeded and cultured for 48 h on chamber slides, then fixed in methanol at  $-20^\circ\text{C}$  for 10 minutes, rinsed 3 x 10 min in PBS and finally blocked in 10% normal goat serum (NGS).

With the aim at identifying the astroglial lineage, monoclonal antibody against glial fibrillary acidic protein (GFAP) (clone G-A-5; *Sigma*, St. Louis, MO, USA) at dilution of 1:400 for 1 hour at  $37^\circ\text{C}$  was used. GFAP was detected by fluorescein isothiocyanate (FITC) conjugated anti-mouse (*Sigma*) secondary antibody (1:128 dilution).

To label neuronal phenotypes, monoclonal antibody against  $\beta$ -tubulin class III (clone SDL-3D10, *Sigma*) was applied at the dilution of 1:800 for 1 h followed by fluorescein isothiocyanate (FITC) conjugated anti-mouse (*Sigma*) secondary antibody (1:128 dilution).

After the immunocytochemistry the slides were mounted, observed at 20X magnification with UV fluorescent inverted microscope (*Leitz*,

DMIL) and photographed by a digital camera. Pictures were captured in a bitmap format.

### **Staining with Hoechst H33342/propidium iodide (PI): viability assay**

Hoechst H33342/propidium iodide (PI) staining was performed to get cell viability estimation. Differentiated and undifferentiated C6, C1300 cells were cultured on chambers slides and underwent all protocols above indicating. The vital cells were stained with Hoechst 33342 (*Sigma*), while death cells were stained with propidium iodide (*Sigma*).

After 5 min the cells were observed using a UV fluorescent inverted microscope (*Leitz*, DMIL) using the UV filter to visualize both dyes simultaneously. The nuclei of the viable cells were blue (Hoechst +ve) and morphologically normal. Death cells were bright orange/red stained. This direct staining method allowed all dead cells to be counted. The cell death rate was estimated as  $\text{dead cell} / \text{total cell number} \times 100$  and intra-observer and inter-observer variability were each  $<2\%$ .

### **Western blot**

Cells were suspended in microtubule-stabilizing solution (5 $\mu\text{M}$  TRIS HCl pH 8.0, 2 $\mu\text{M}$  EGTA, 0.1 $\mu\text{M}$  phenylmethylsulfonyl fluoride), supplemented with protease inhibitors (Complete-mini, *Roche*, Basel, Switzerland). Cells were homogenized mechanically and then sonicated. Protein content was determined (DC Protein Assay, *BioRad*, Hercules, CA, USA) and aliquots of 15 $\mu\text{g}$  proteins each were fractionated in SDS-PAGE 12% gel and after that

transferred onto nitrocellulose membranes. Non-specific protein binding was blocked incubating membranes with 0.1% Tween 20 and 5% skim milk in PBS. Nitrocellulose membranes were incubated with primary monoclonal antibodies against total  $\alpha$ -tubulin (clone DM1A, *Sigma*), acetylated- $\alpha$ -tubulin (clone 6-11B-1, *Sigma*), tyrosinated  $\alpha$ -tubulin (clone TUB-1A2, *Sigma*), overnight at 4°C at 1:500, 1:500, 1:1.000 dilution respectively. An anti-mouse IgG-alkaline phosphatase-conjugated antibody (Anti-mouse Ig-AP, Fab fragment, *Roche*) was used at 1:1.000 dilution for 1h at room temperature. The immunoreactive bands were visualized by incubating the membrane with nitro blue tetrazolium/5-bromo-4-chloro-3-indolyl phosphate (NBT/BCIP) (*Roche*) and heat fixed. Signals were quantified using Scion Image software. The anti  $\alpha$ -tubulin antibody visualized the  $\alpha$ -tubulin subunits as a single band located approximately 55kDa.

### **Statistical analysis**

All data were expressed as % of control (mean  $\pm$ SEM) of 4-6 single experiments. Data were analyzed using Student's *t*-test. Statistical significance was set at  $P < 0.05$ .

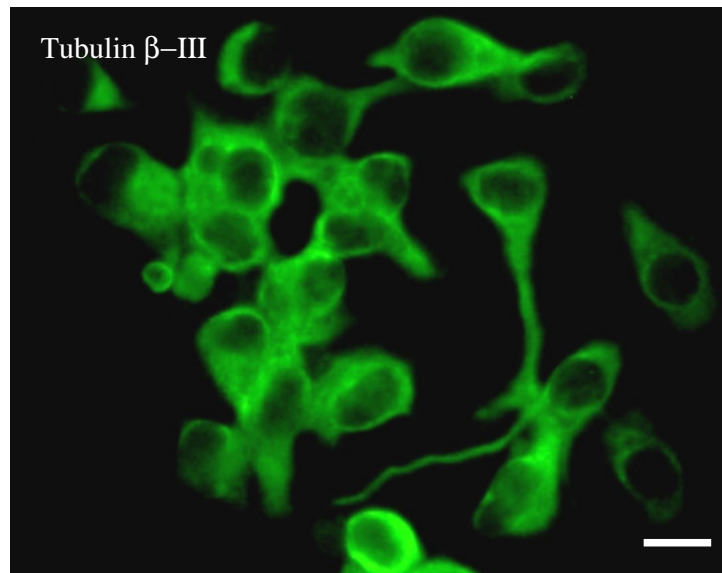
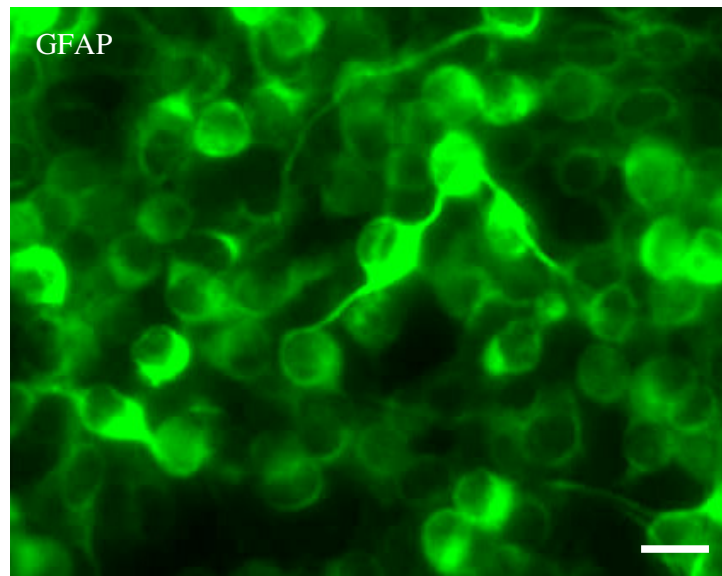


Fig. 12. Indirect immunofluorescence assessed the specific cellular phenotype: glial fibrillary acidic protein (GFAP), an intermediate-filament (IF) protein that is highly specific for cells of astroglial lineage and anti- $\beta$ -tubulin class III as marker of neuronal cells were applied for undifferentiated C6 and C1300 cell lines respectively. Cells were viewed using a fluorescence microscope at 40X. Bar = 100 $\mu$ m.

## ***RESULTS***

## **UNDIFFERENTIATED C6 & C1300 CELLS**

In the initial experiments we found that both cell lines were sensitive to the toxic effects of 2ME at micromolar concentrations (0.01, 0.1, 1, 5 and 10 $\mu$ M for 5 days) but undifferentiated C1300 cells were more sensitive than undifferentiated C6 cells.

### **PHACO: microscopic examination**

Undifferentiated C6 control cells, 0.01 and 0.1 $\mu$ M 2ME-exposed cells were confluent and uniform in size. If compared with control cells, 1 $\mu$ M 2ME-treated cells were reduced in number (about 30%), whereas 5 and 10 $\mu$ M 2ME-exposed cells displayed morphological alterations, such as flatness, globular shape and presence of cytoplasmic vacuoles. In addition, most cells were detached from the dishes and retraction or absence of their cytoplasmic processes were observed (Fig. 13).

Undifferentiated C1300 control cells were confluent at 90% and uniform in size; starting from 0.01 $\mu$ M cells were flat and shrunk and reduction in number (10% approximately) was ascertained. Reduction in number was more remarkable in 0.1 $\mu$ M (30% approx.) and mainly in 1 $\mu$ M (50% approx.) 2ME-treated-cells. At 5 and 10 $\mu$ M a significant proportion of cells appeared detached from the dishes, exhibited numerous cytoplasmic vacuoles and lost their cytoplasmic processes (Fig. 15).

### **Hoechst 33258/propidium iodide (PI) staining: viability test**

Hoechst 33258/propidium iodide (PI) staining revealed that 2ME-induced nuclear damages and cell death were greater in

undifferentiated C1300 cells than in undifferentiated C6 cells at the same micromolar concentrations.

Undifferentiated C6 control cells, 0.01 and 0.1 $\mu$ M 2ME-treated cells had single nuclei which were stained in blue by Hoechst dye, i.e. were viable. In 1, 5 $\mu$ M and mostly in 10 $\mu$ M 2ME-exposed monolayers, dead cells (about 30% at 1, 60% at 5 and 100% at 10 $\mu$ M), nuclear fragmentation and micronucleation peculiar of defective mitosis were detectable (Fig. 14).

Undifferentiated C1300 control cells had oval, homogeneous nuclei and did not display nuclear changes. About 20-40% of 0.01, 0.1 and 1 $\mu$ M 2ME-exposed cells showed the PI red staining and morphological features characteristic of cell death. The percentage of dead cells was greater in 5 and 10 $\mu$ M exposed-cells where it was 90-100% approximately (Fig. 16).

#### **MTT test: cell proliferation assay**

We examined the effect of 2ME on cell proliferation rate of undifferentiated C6 and C1300 cells using the MTT test (CellTiter96®). Cells underwent all protocols described in Materials & Methods and after 5 days of 2ME exposure cells proliferation rate was measured. Quantitative analysis of this phenomenon is shown in Fig. 17.

Undifferentiated C6 cells showed from 1  $\mu$ M concentration a gradual dose-dependent decrease (from -15 to -70%) in growth rate, when growth rate was fixed at 100% in control cells. Interestingly, 0.01 and 0.1 $\mu$ M exposure increased growth rate which was approximately +10, +5%. When compared to control cells, undifferentiated C1300 cells were sensitive to 2ME in a

marked dose-dependent manner: starting from 0.01 $\mu$ M a dramatic growth rate decline (from -30 to -90%) was ascertained.

### **Western blot analysis**

2ME down-regulated the expression of tubulin both in undifferentiated C6 and C1300 cell lines in a dose-dependent manner. However,  $\alpha$ -acetylated tubulin and mostly  $\alpha$ -tyrosinated tubulin down-regulation is more intense in undifferentiated C1300 than in undifferentiated C6 cells.

### ***Total $\alpha$ -tubulin***

Undifferentiated C6 cells:  $\alpha$ -tubulin levels were %C= 78  $\pm$ 2.5 in 0.01 $\mu$ M 2ME-treated cells; protein expression similarly decreased in 0.1 $\mu$ M 2ME-exposed cells (%C= 62  $\pm$ 1.3), 1 $\mu$ M-exposed (%C= 55 $\pm$ 3.6) and 5  $\mu$ M (%C= 62  $\pm$ 2.0) mono-layers and in 10 $\mu$ M-treated cells (%C= 65  $\pm$ 1.5) (Fig. 18).

Undifferentiated C1300 cells: 2ME treatment slightly decreased  $\alpha$ -tubulin levels in 0.01 $\mu$ M and 0.1 $\mu$ M 2ME-treated cells (%C= 91 $\pm$ 2.1 and 81  $\pm$ 1.8). Down-regulation was more marked in 1, 5 and 10 $\mu$ M 2ME-exposed cells in which protein levels were %C= 41  $\pm$ 1.9, %C= 46  $\pm$ 2.7, %C= 40  $\pm$ 2.3 respectively (Fig. 19).

### ***Acetylated $\alpha$ -tubulin***

Undifferentiated C6 cells: levels of acetylated  $\alpha$ -tubulin were %C= 85  $\pm$ 1.2 in 0.01 $\mu$ M 2ME-exposed cells decreasing in a dose dependent manner in 0.1 $\mu$ M (%C= 78  $\pm$ 0.9), 1 $\mu$ M (%C = 68  $\pm$ 1.7), 5 $\mu$ M (%C= 68  $\pm$ 1.5) and mostly in 10 $\mu$ M 2ME-treated cells (%C= 55  $\pm$ 0.4) (Fig. 20).



Undifferentiated C1300 cells: 2ME exposure did not modify the expression of acetylated  $\alpha$ -tubulin at 0.01 $\mu$ M (%C= 100  $\pm$ 2.2) and determined a slight down-regulation of its levels at 0.1 $\mu$ M (%C= 89  $\pm$ 1.5) and 1 $\mu$ M (%C= 87  $\pm$ 1.3). Levels of acetylated  $\alpha$ -tubulin declined from %C= 51  $\pm$ 0.5 to %C= 33  $\pm$ 1.4 in 5 and 10 $\mu$ M respectively (Fig. 21).

### ***Tyrosinated $\alpha$ -tubulin***

Undifferentiated C6 cells: 2ME determined a slight down-regulation of tyrosinated  $\alpha$ -tubulin at 0.01 $\mu$ M (%C= 94  $\pm$ 1.3). Protein levels dropped at 0.1 $\mu$ M (%C= 80  $\pm$ 2.1), 1 $\mu$ M (%C = 76  $\pm$ 2.4), 5 $\mu$ M (%C= 77  $\pm$ 1.9) and mostly at 10 $\mu$ M (%C= 45  $\pm$ 1.5) (Fig. 22).

Undifferentiated C1300 cells: No significant modifications of tyrosinated  $\alpha$ -tubulin expression were ascertained at 0.01 and 0.1 $\mu$ M (%C= 95  $\pm$ 2.5 and %C= 95  $\pm$ 2.1 respectively). A constant dose-dependent decline was observed in 1 and 5 $\mu$ M (%C= 49  $\pm$ 1.4 and %C= 47  $\pm$ 1.2), whereas in 10  $\mu$ M 2ME-exposed cells levels of the protein dropped as far as %C= 30  $\pm$ 0.3 (Fig. 23).

## **TAPSIGARGIN-DIFFERENTIATED C6 & db-cAMP-DIFFERENTIATED C1300 CELLS**

In the last experiments we found that both tapsigargin-differentiated C6 and db-cAMP-differentiated C1300 cell lines were less sensitive than undifferentiated cells to the toxic effects of 2ME at 0.1, 1 and 5 $\mu$ M for 5 days. Moreover, we ascertained that, between db-cAMP-differentiated C1300 and tapsigargin-differentiated C6 cells, C1300 cells were still more sensitive than C6 cells.

### **PHACO: microscopic examination**

Tapsigargin-differentiated C6 and db-cAMP-differentiated C1300 cells were confluent at 50% approximately. Cells were polygonal, uniform in size with hypertrophic cell body and displayed cytoplasmic processes up to  $\pm 70$   $\mu$ m long (Figg. 24, 26).

After 2ME-treatment tapsigargin-differentiated C6 and db-cAMP-differentiated C1300 cells kept a polygonal shape and long cytoplasmic processes but a reduction in number was evident in 1 and 5 $\mu$ M 2ME-exposed monolayers. 5 $\mu$ M 2ME-exposed cells retracted most of their cytoplasmic processes and appeared shrunk with cytoplasmic vacuoles. Morphological alterations were more marked in db-cAMP-differentiated C1300 than in tapsigargin-differentiated C6 cell lines (Figg. 24, 26).

### **Hoechst 33258/propidium iodide (PI) staining: viability test**

Hoechst 33258/propidium iodide (PI) staining revealed that 2ME-exposure determined nuclear damages and cell death in tapsigargin-differentiated C6 and db-cAMP-differentiated C1300 cells. However, significant nuclear damages and cell death started to be

evident from 2ME micromolar concentrations which were higher than those detected in undifferentiated C6 and C1300 cells.

Control cells and 0.1  $\mu\text{M}$  2ME-treated cells single nuclei which were stained in blue by Hoechst dye both in tapsigargin-differentiated C6 and db-cAMP-differentiated C1300 cells. In 1 and 5 $\mu\text{M}$  exposed-cells, nuclear fragmentation and micronucleation peculiar of defective mitosis were detected. The percentage in average of death cells was higher in db-cAMP C1300 differentiated cells (65% approximately) than tapsigargin-differentiated C6 cells (about 40%) at the same concentrations (Figg. 25, 27).

#### **MTT test: cell proliferation assay**

We examined the effects of 2ME on cell viability of tapsigargin-differentiated C6 and db-cAMP-differentiated C1300 cell lines using the MTT test (CellTiter96®). Cells underwent all protocols described in Materials & Methods and after 5 days of 2ME exposure the cells proliferation rate was measured. Quantitative analysis of this phenomenon is shown in Fig. 28.

Tapsigargin-differentiated C6 cells showed a decrease in the number of viable cells (-20%) in 0.1 $\mu\text{M}$  2ME exposed cells, when growth rate was fixed at 100% in control cells. At 1 and 5 $\mu\text{M}$  the drop of the growth rate was more remarkable (-80%).

db-cAMP-differentiated C1300 cells appeared to be more sensitive than tapsigargin-differentiated C6 cells since the growth rate at 0.1 $\mu\text{M}$  was - 60% and at 1 $\mu\text{M}$ , at 5 $\mu\text{M}$  between -85, -90%.

#### **Western blot analysis**

2ME determines a slight down-regulation of total  $\alpha$ -tubulin, tyrosinated  $\alpha$ -tubulin and up-regulated acetylated  $\alpha$ -tubulin

expression both in taspigargin-differentiated C6 and db-cAMP-differentiated C1300 cells. Down-regulation is higher in db-cAMP-differentiated C1300 than taspigargin-differentiated C6, whereas up-regulation is more marked in taspigargin-differentiated C6 than in db-cAMP-differentiated C1300.

### ***Total $\alpha$ -tubulin***

Taspigargin-differentiated C6 cells: 2ME determined a slight down-regulation of total  $\alpha$ -tubulin expression in 0.1 $\mu$ M (%C= 94 $\pm$ 2.7). At 1 and 5 $\mu$ M levels of protein were %C= 87 $\pm$ 0.5 and %C= 80 $\pm$ 3.1 % respectively (Fig. 29).

db-cAMP-differentiated C1300 cells: 2ME exposure determined a similar decreased in  $\alpha$ -tubulin expression in 0.1 and 1 $\mu$ M 2ME-exposed cells (%C= 85  $\pm$ 0.5 and %C= 82 $\pm$ 0.7). Down-regulation of protein levels was more evident in 5 $\mu$ M 2ME-treated cells where values fell up to %C= 61  $\pm$ 2.3 (Fig. 30).

### ***Acetylated $\alpha$ -tubulin***

Taspigargin-differentiated C6 cells: when compared with control, acetylated  $\alpha$ -tubulin levels were up-regulated in 0.1 $\mu$ M (%C= 90  $\pm$ 0.8), 5 $\mu$ M (%C= 95 $\pm$ 2.5) and mainly 1 $\mu$ M (%C= 100 $\pm$ 1.5) 2ME-exposed cells (Fig. 31).

db-cAMP-differentiated C1300 cells: 2ME treatment upregulated acetylated  $\alpha$ -tubulin expression since protein levels increased in 0.1  $\mu$ M (%C= 87 $\pm$ 1.2), 5 $\mu$ M (%C= 96 $\pm$ 3.2) and mainly in 1 $\mu$ M (%C= 100  $\pm$ 2.7) 2ME-treated cells in comparison with control (Fig. 32).

### ***Tyrosinated $\alpha$ -tubulin***

Tapsigargin-differentiated C6 cells: 2ME slightly downregulated protein expression in 0.1 and 1 $\mu$ M 2ME treated cells (%C= 95  $\pm$ 2.2 and %C= 90 $\pm$ 2.7). Levels of protein declined as far as %C =74 $\pm$ 0.9 in 5 $\mu$ M 2ME-exposed cells (Fig. 33).

db-cAMP-differentiated C1300 cells: a slight decrease in tyrosinated  $\alpha$ -tubulin expression was ascertained in 0.1 $\mu$ M exposed cells (%C= 93 $\pm$ 2.7). Down-regulation was more marked in 1 $\mu$ M and mostly in 5 $\mu$ M exposed cells in which values were %C= 80 $\pm$ 1.2 and %C= 68 $\pm$ 0.5 respectively (Fig. 34).

## ***FIGURES***

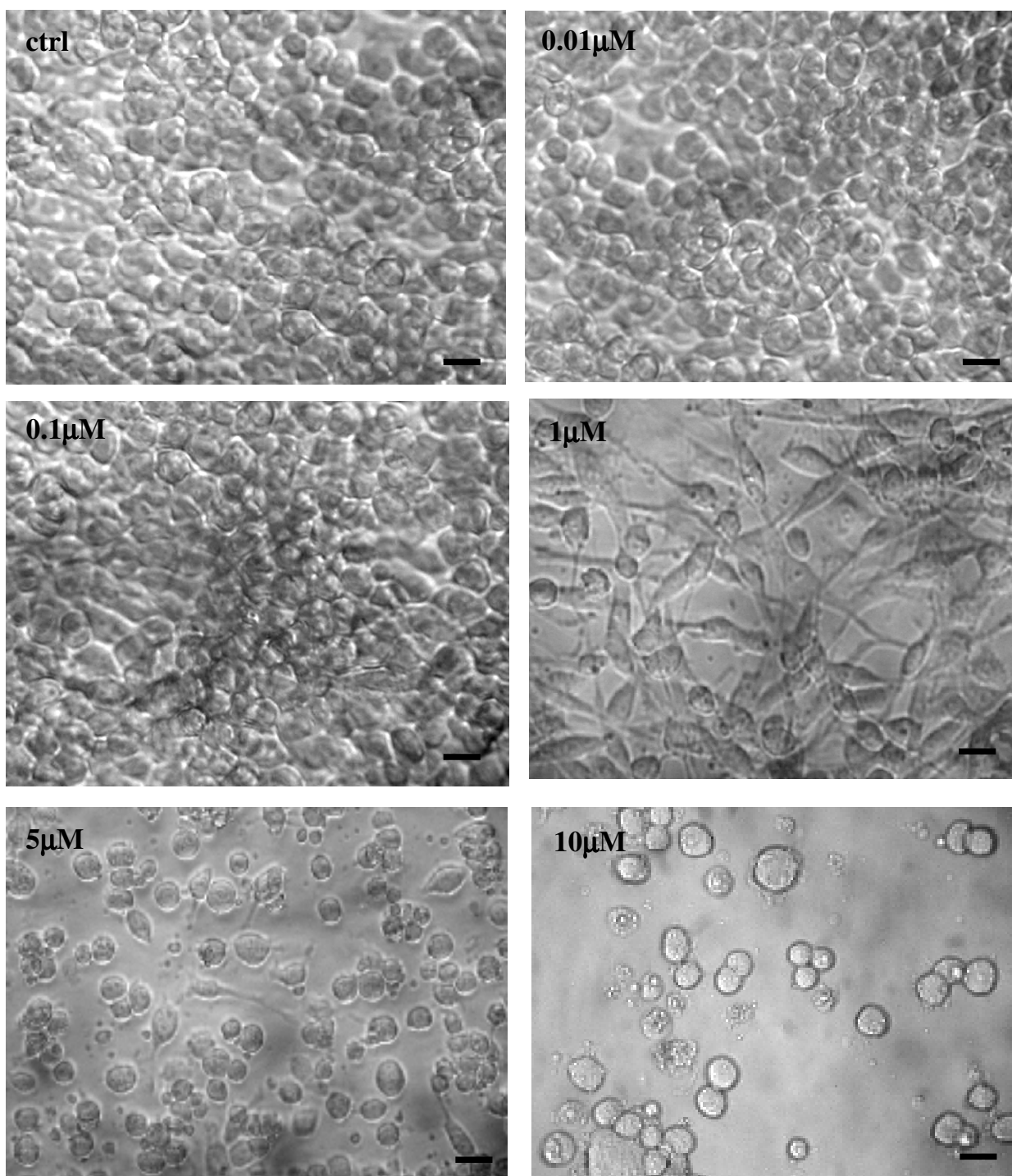


Fig. 13. Morphology of undifferentiated C6 cells after 2ME-exposure. Cells were cultured with RPMI-1640 medium containing 10% DCC-stripped serum. Cells were exposed to different 2ME micromolar concentrations (0.01, 0.1, 1, 5 and 10µM for 5 days) and viewed by contrast phase microscope at 20X. Control cells (ctrl), 0.01 and 0.1µM 2ME-exposed cells were confluent and uniform in size. If compared with control cells, 1µM 2ME-treated cells were reduced in number (about 30%), whereas 5 and 10µM 2ME-exposed cells displayed morphological alterations, such as flatness, globular shape and presence of cytoplasmic vacuoles. In addition, most cells were detached from the dishes and retraction or absence of their cytoplasmic processes were observed. Bar= 30µm.

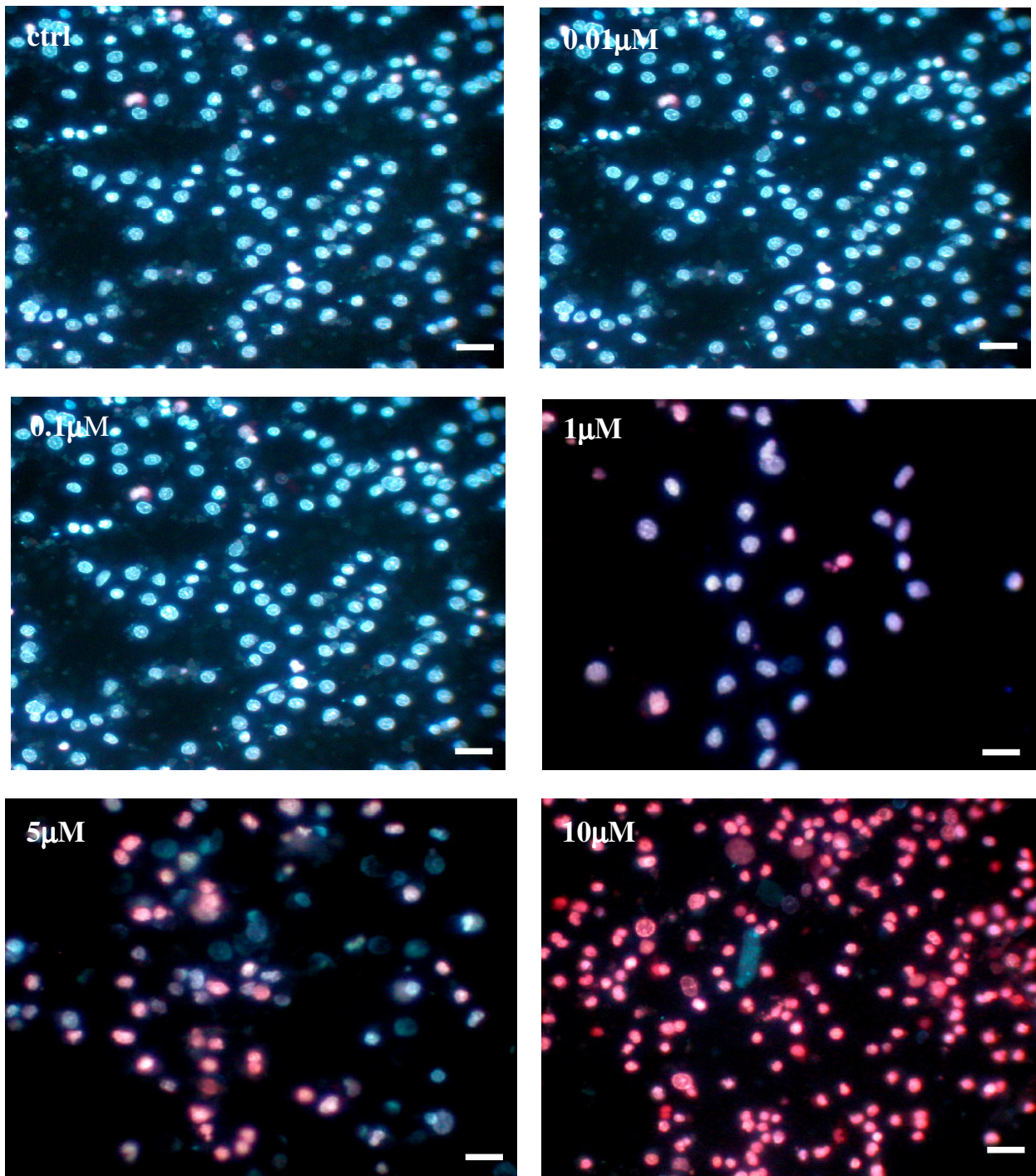


Fig. 14. Alterations in nuclear morphology of undifferentiated C6 cells induced by 2ME. Cells were cultured in RPMI-1640 medium containing 10% DCC-stripped serum. Cells were exposed to different 2ME micromolar concentrations (0.01, 0.1, 1, 5 and 10 $\mu$ M for 5 days), stained with Hoechst 33258/propidium iodide and finally viewed using a fluorescence microscope with a broad band filter (excitation wave length 365 nm) at 20X. Control cells (ctrl), 0.01 and 0.1 $\mu$ M 2ME-treated cells had single nuclei and were stained in blue by Hoechst dye, i.e. were viable. In 1, 5 $\mu$ M and mostly in 10 $\mu$ M 2ME-exposed monolayers, dead cells (about 30% at 1 $\mu$ M, 60% at 5 $\mu$ M and 100% at 10 $\mu$ M), nuclear fragmentation and micronucleation peculiar of defective mitosis were detectable. Bar= 15 $\mu$ m.



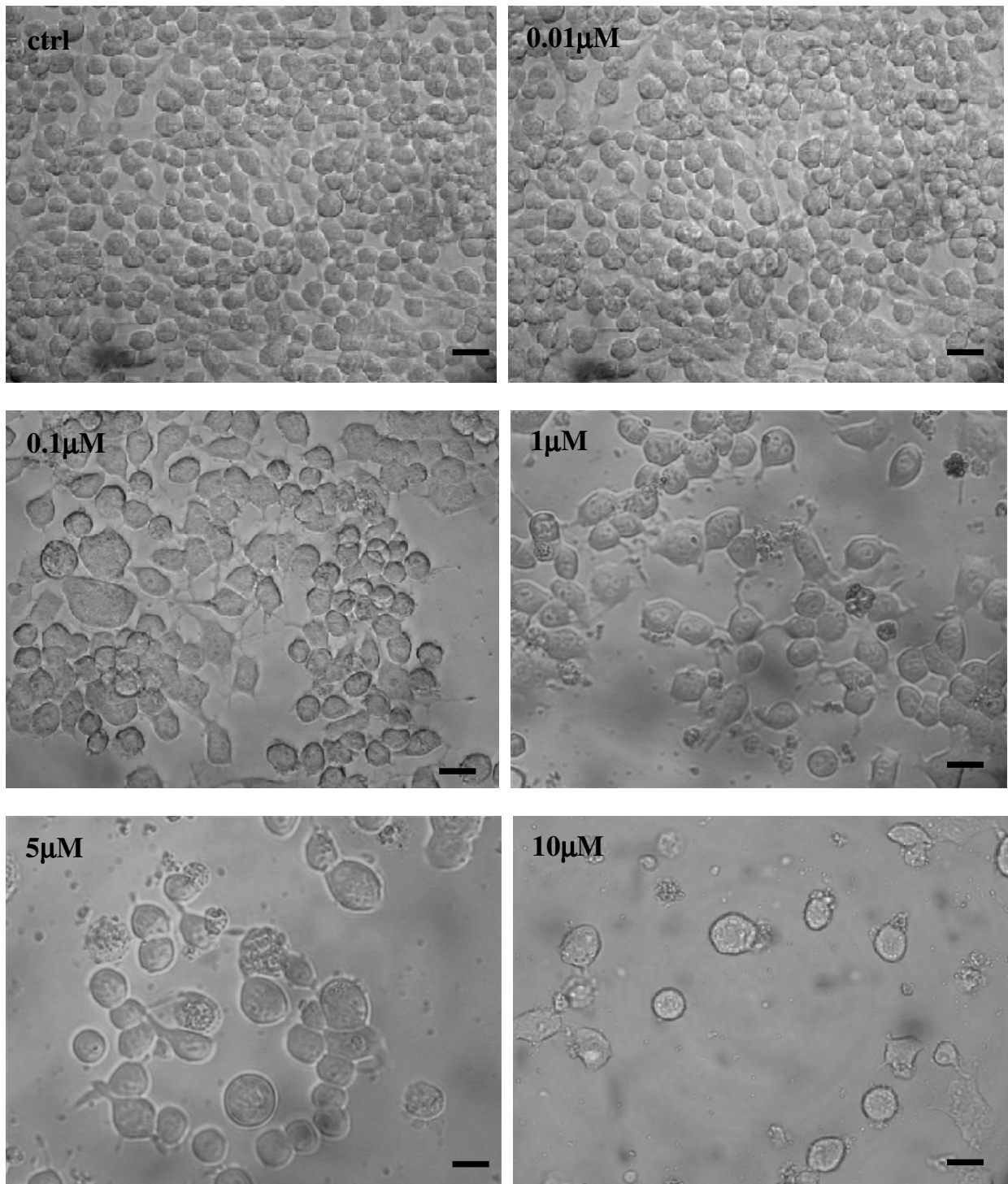


Fig. 15. Morphology of undifferentiated C1300 cell line after 2ME-exposure. Cells were cultured with RPMI-1640 medium containing 10% DCC-stripped serum. Cells were exposed to different 2ME micromolar concentrations (0.01, 0.1, 1, 5 and 10 $\mu$ M for 5 days) and viewed by contrast phase microscope at 20X. Control (ctrl) cells were confluent at 90% and uniform in size; starting from 0.01  $\mu$ M, cells were flat and shrunk and reduction in number (10% approximately) was ascertained. Reduction in number was more remarkable at 0.1 $\mu$ M (30% approximately) and mainly in 1 $\mu$ M 2ME-treated cells. 5 and 10 $\mu$ M a significant proportion of cells appeared detached from the dishes, exhibited numerous cytoplasmic vacuoles and lost their cytoplasmic processes. Bar= 30 $\mu$ m.

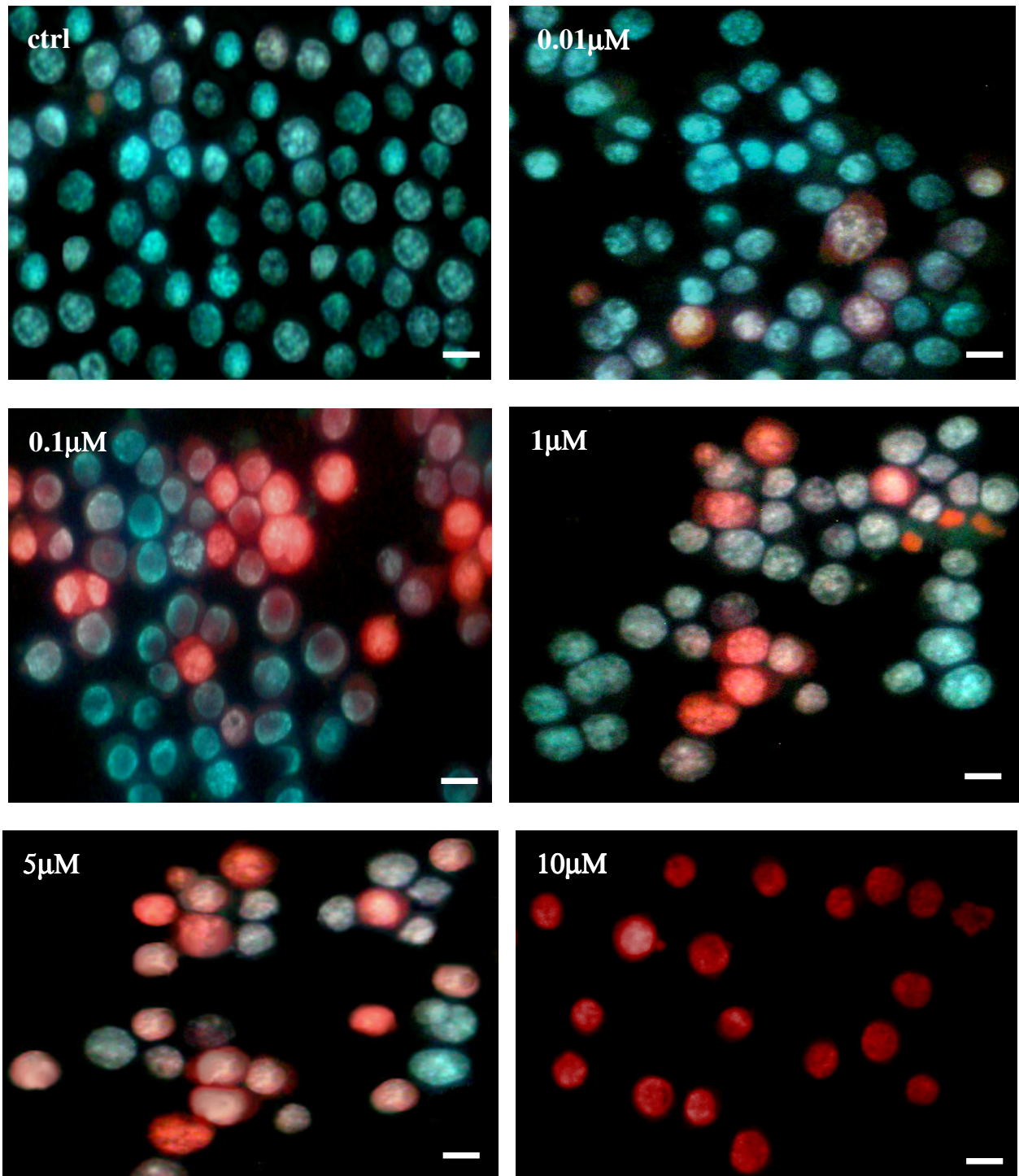


Fig. 16. Alterations in nuclear morphology of undifferentiated C1300 cells induced by 2ME. Cells were cultured in RPMI-1640 medium containing 10% DCC-stripped serum. Cells were exposed to different 2ME micromolar concentrations (0.01, 0.1, 1, 5 and 10 μM for 5 days), stained with Hoechst 33258/propidium iodide and finally viewed using a fluorescence microscope with a broad band filter (excitation wave length 365 nm) at 20X. Control cells (ctrl) had oval, homogeneous nuclei and did not display nuclear changes. About 20-40% of 0.01, 0.1 and 1 μM 2ME-exposed cells showed the PI red staining and morphological features characteristic of cell death. The percentage of dead cells was greater in 5 and 10 μM 2ME exposed-cells where it was 90-100% approximately. Bar= 15 μm.

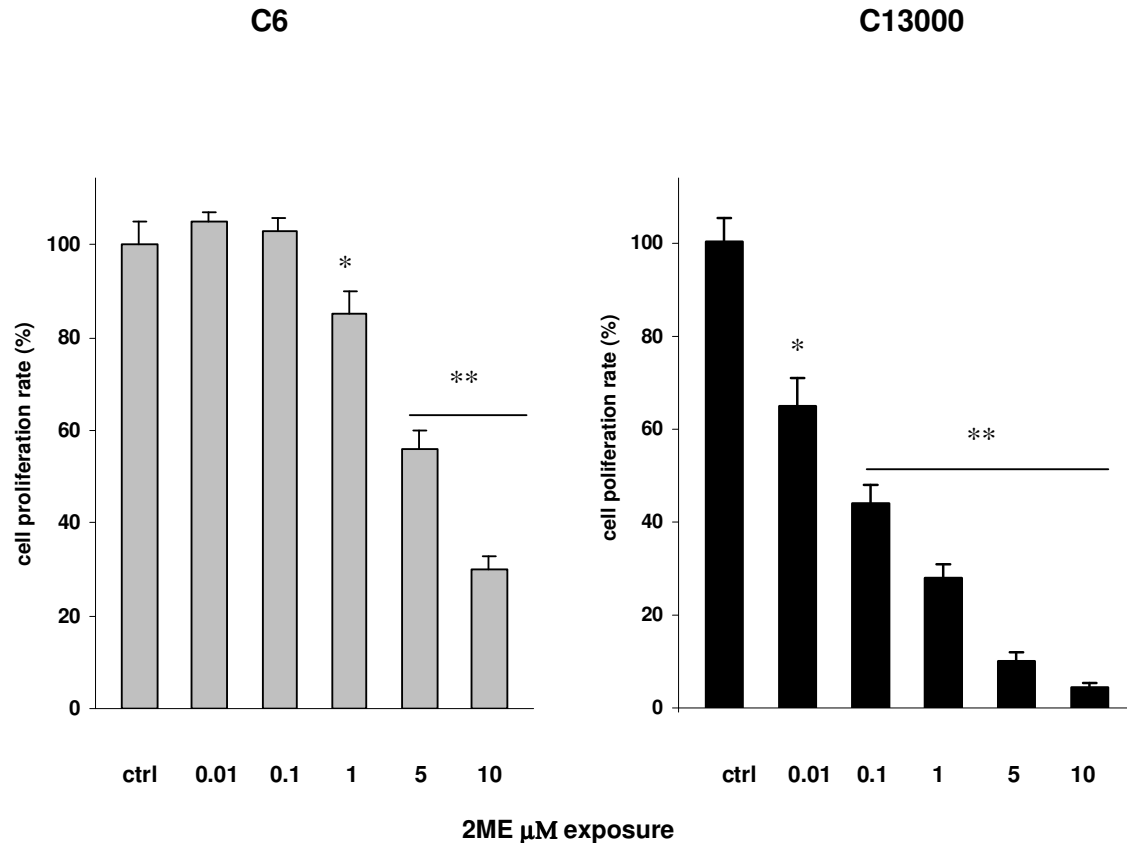


Fig.17. Evaluation of number of viable cells (MTT test) in undifferentiated C6 and C1300 cell lines. Cells were plated in 96-well plates containing  $50 \times 10^3$  cells in  $200 \mu\text{l}$  RPMI-1640 containing 10% DCC-stripped serum and then exposed to different 2ME micromolar concentration (0.01, 0.1, 1, 5 and  $10 \mu\text{M}$  for 5 days). Then, cells were incubated in 3-(4,5-dimethylthiazolyl-2)-2,5-diphenyltetrazolium bromide assay (MTT, Cell Titer® 96) for 1h. MTT was bioreduced by living cells into a coloured formazan product that is soluble in tissue culture medium. Absorption values were read setting the automatic microtiter reader at 492nm (Uniskan II). This method correlates absorbance reading to the number of living cells. Undifferentiated C6 cells (left) showed since  $1 \mu\text{M}$  concentration a gradual dose-dependent decrease (from -15% to -70%) in growth rate, when growth rate was fixed at 100% in control cells. Interestingly,  $0.01 \mu\text{M}$  and  $0.1 \mu\text{M}$  2ME-exposure increased growth rate which was approximately +5% , +10%. When compared to control cells, undifferentiated C1300 cells (right) were sensitive to 2ME in a marked dose-dependent manner: starting from  $0.01 \mu\text{M}$  a dramatic growth rate decline (from -30 to -90%) was ascertained. \* $P < 0.05$ , \*\* $P < 0.001$  (Student's *t* test) vs control cells (ctrl).

## C6 cells: total $\alpha$ -tubulin - 1:500

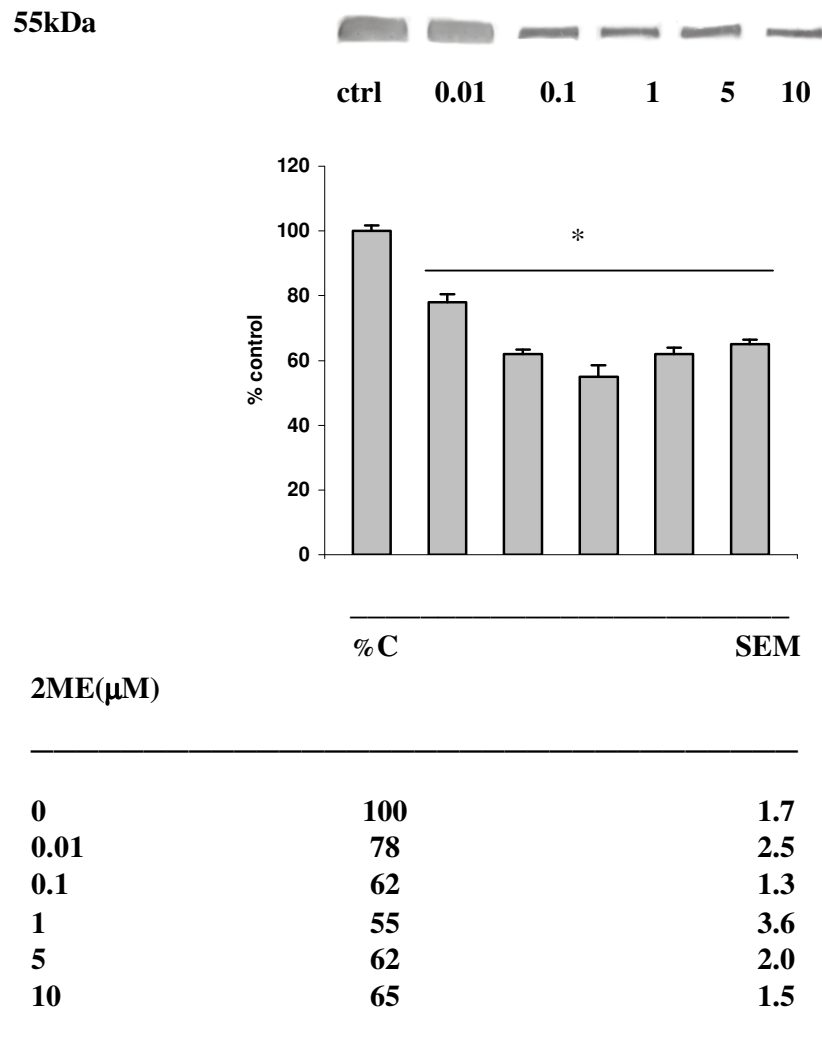


Fig. 18. Effect of 2ME on total  $\alpha$ -tubulin expression in undifferentiated C1300 cells. Representative Western blot band, histogram and values of densitometric analysis of the bands. The blot is representative from four experiments and %C values (SEM) represent the mean values of four different experiments. Data are expressed as mean  $\pm$ SEM (n=4), \* $P=0.05$  (Student's  $t$  test) vs control cells (ctrl).

## C1300 cells: total $\alpha$ -tubulin - 1:500

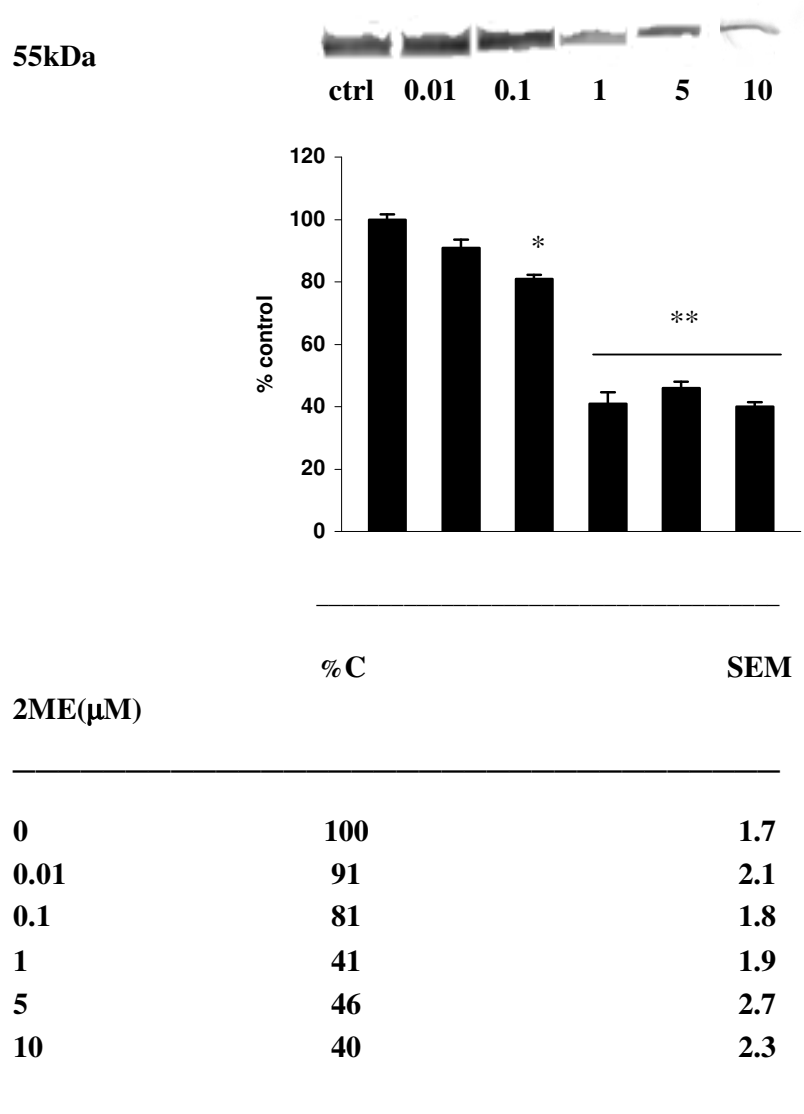
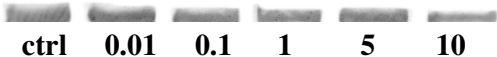


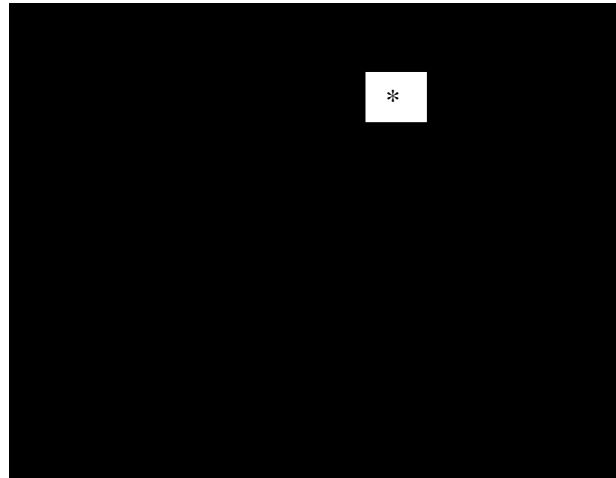
Fig. 19. Effect of 2ME on total  $\alpha$ -tubulin expression in undifferentiated C6 cells. Representative Western blot band, histogram and values of densitometric analysis of the bands. The blot is representative from four experiments and %C values (SEM) represent the mean values of four different experiments. Data are expressed as mean  $\pm$ SEM (n=4), \* $P$ =0.05, \*\* $P$ =0.01 (Student's  $t$  test) vs control cells (ctrl).

## C6 cells: acetylated $\alpha$ -tubulin - 1:500

55kDa



ctrl 0.01 0.1 1 5 10



2ME ( $\mu$ M)	% C	SEM
0	100	1.9
0.01	85	1.2
0.1	78	0.9
1	68	1.7
5	68	1.5
10	55	0.4

Fig. 20. Effect of 2ME on acetylated  $\alpha$ -tubulin expression in undifferentiated C6 cells. Representative Western blot band, histogram and values of densitometric analysis of the bands. The blot is representative from four experiments and %C values (SEM) represent the mean values of four different experiments. Data are expressed as mean  $\pm$ SEM (n=4), \* $P=0.05$ , (Student's  $t$  test) vs control cells (ctrl).

## C1300 cells: acetylated $\alpha$ -tubulin - 1:500

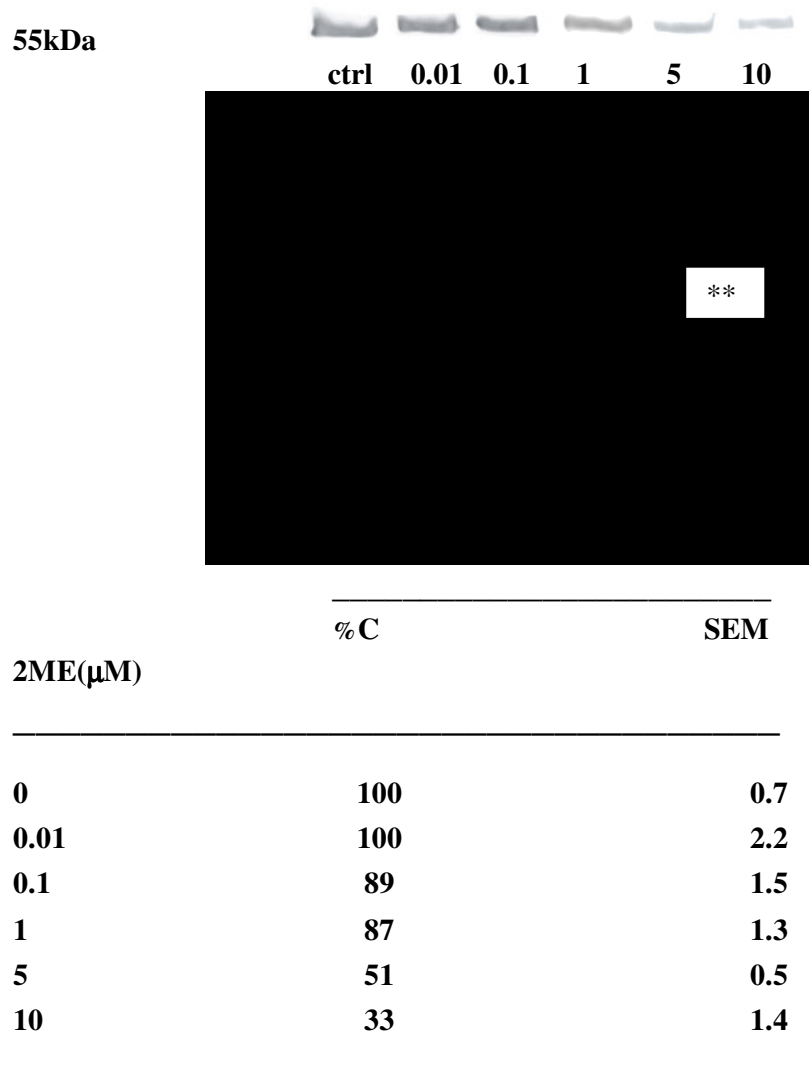


Fig. 21. Effect of 2ME on acetylated  $\alpha$ -tubulin expression in undifferentiated C1300 cells. Representative Western blot band, histogram and values of densitometric analysis of the bands. The blot is representative from four experiments and %C values (SEM) represent the mean values of four different experiments. Data are expressed as mean  $\pm$ SEM (n=4), \*\* $P=0.01$ , (Student's  $t$  test) vs control cells (ctrl).

## C6 cells: tyrosinated $\alpha$ -tubulin - 1:1.000

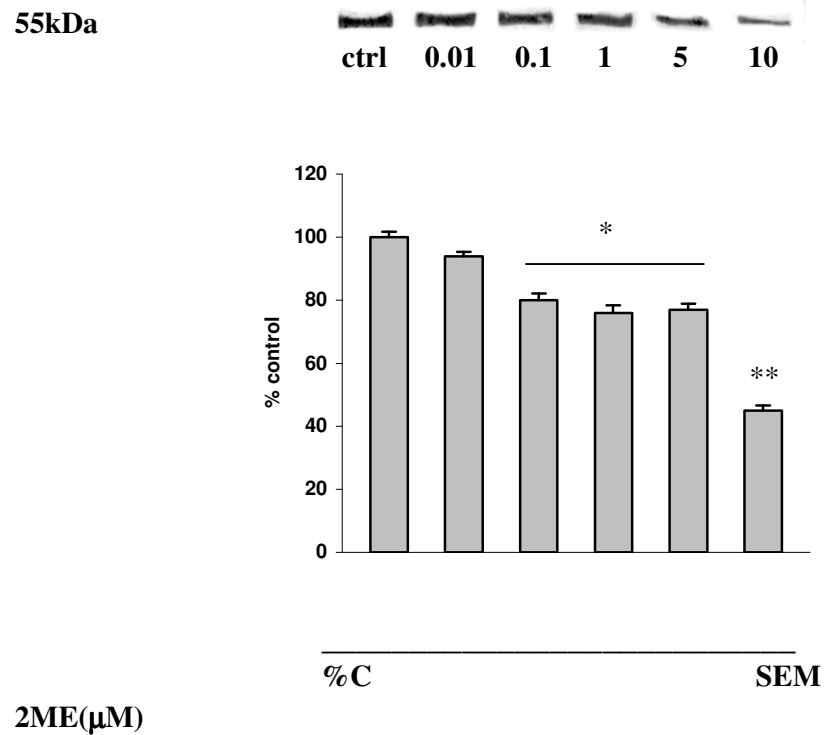
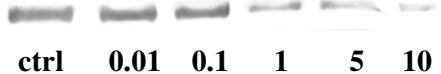


Fig. 22. Effect of 2ME on tyrosinated  $\alpha$ -tubulin expression in undifferentiated C6 cells. Representative Western blot band, histogram and values of densitometric analysis of the bands. The blot is representative from four experiments and %C values (SEM) represent the mean values of four different experiments. Data are expressed as mean  $\pm$ SEM (n=4), \* $P$ =0.05, \*\* $P$ =0.01, (Student's  $t$  test) vs control cells (ctrl).

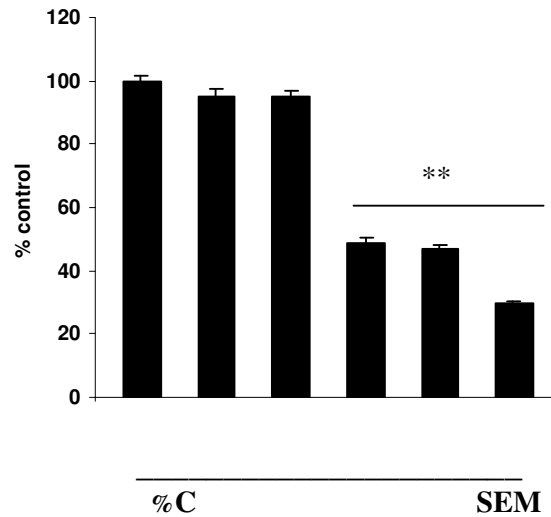


## C1300 cells: tyrosinated $\alpha$ -tubulin - 1:1.000

55kDa



ctrl 0.01 0.1 1 5 10



2ME( $\mu$ M)

2ME ( $\mu$ M)	% C	SEM
0	100	1.7
0.01	95	2.5
0.1	95	2.1
1	49	1.4
5	47	1.2
10	30	0.3

Fig. 23. Effect of 2ME on tyrosinated  $\alpha$ -tubulin expression in undifferentiated C1300 cells. Representative Western blot band, histogram and values of densitometric analysis of the bands. The blot is representative from four experiments and %C values (SEM) represent the mean values of four different experiments. Data are expressed as mean  $\pm$ SEM (n=4), \*\* $P=0.01$ , (Student's  $t$  test) vs control cells (ctrl).

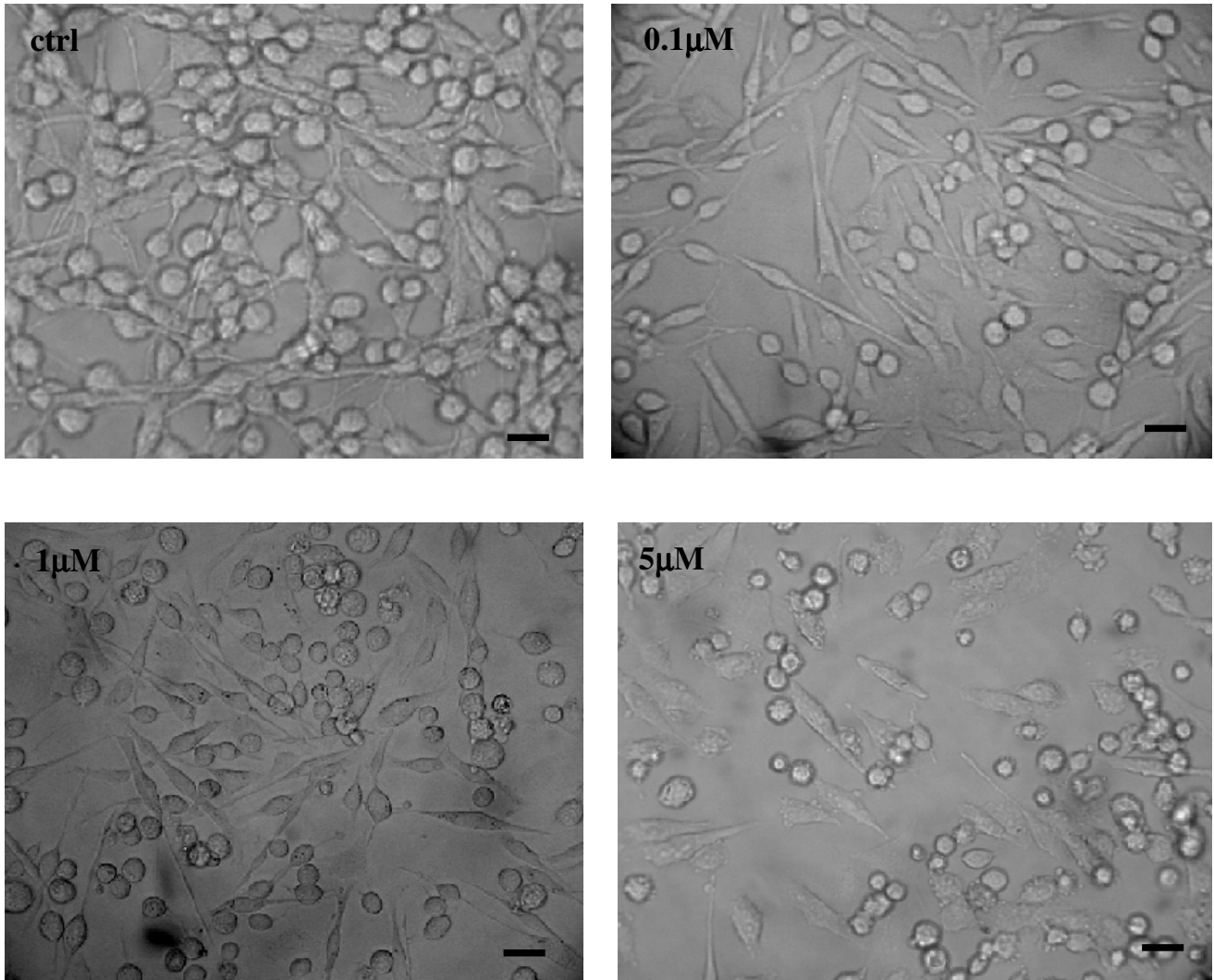


Fig. 24. Morphology of taspigargin-differentiated C6 cells after 2ME-treatment. Undifferentiated C6 cells were exposed to 4 $\mu$ M taspigargin diluted in RPMI-1640 medium containing 10% DCC-stripped serum for five days, then cells were treated with different 2ME micromolar concentrations (0.1, 1, 5 $\mu$ M for 5 days) and viewed by contrast phase microscope at 20X. Control cells (ctrl) were confluent at 50% approximately with hypertrophic cell bodies and cytoplasmic processes up to  $\pm 70\mu$ m long. After 2ME treatment a reduction in number was ascertained. At 1 $\mu$ M some cells appeared shrunk and rounded, whereas 5 $\mu$ M 2ME-treated cells retracted most of their cytoplasmic processes and showed numerous cytoplasmic vacuoles. Bar= 30 $\mu$ m.

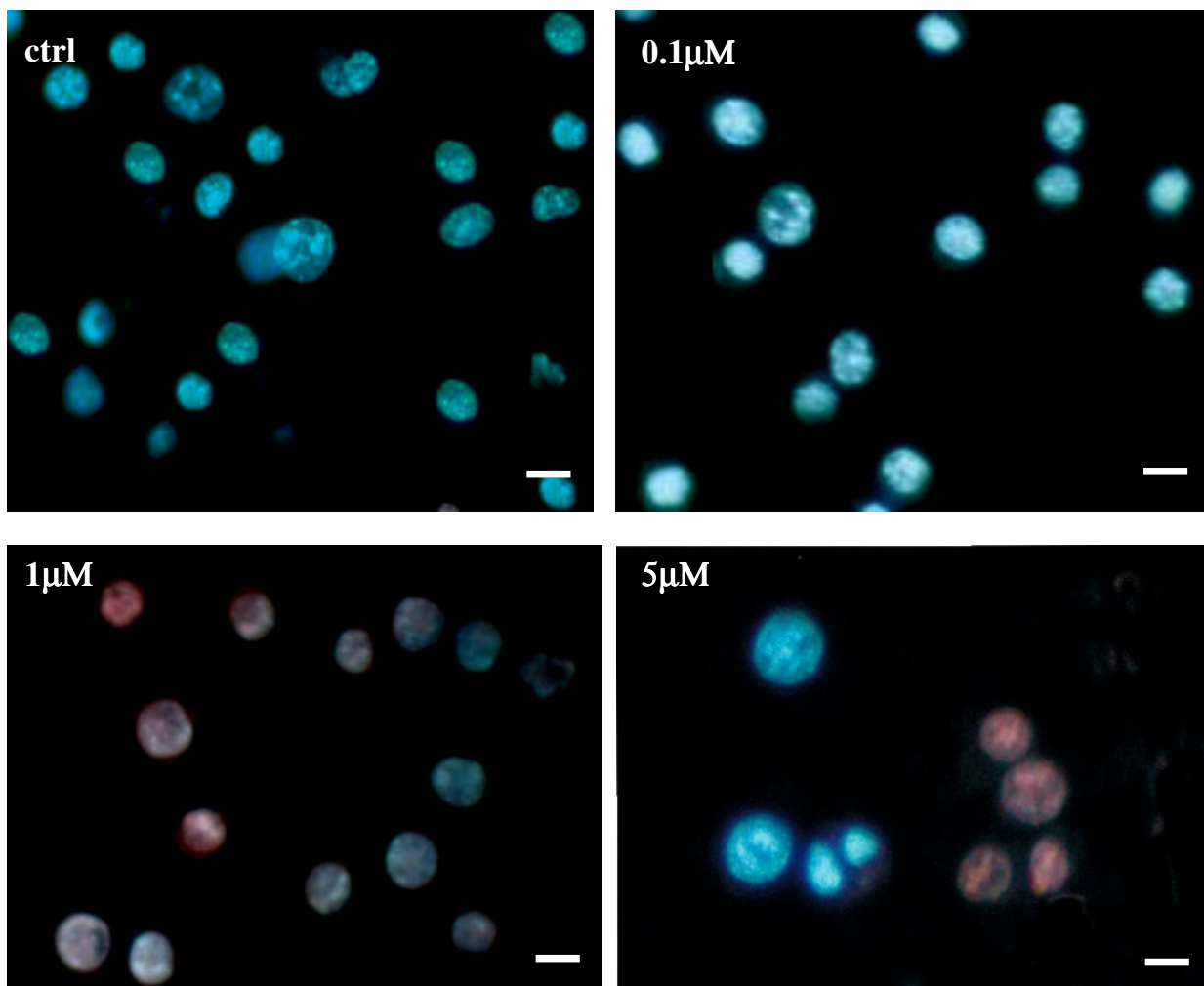


Fig. 25. Morphology of taspigargin-differentiated C6 cell line after 2ME-treatment. Undifferentiated C6 cells were exposed to 4 $\mu$ M taspigargin with RPMI-1640 medium containing DCC 10% serum, then treated for 5 days with 2ME micromolar concentrations (0.1, 1, 5 $\mu$ M for 5 days), stained with Hoechst 33258/propidium iodide and finally viewed using a fluorescence microscope with a broad band filter (excitation wave length 365nm). Control cells (ctrl) and 0.1 $\mu$ M 2ME-treated cells had single nuclei and they did not display nuclear alterations. In 1 and 5 $\mu$ M exposed-monolayers dead cells (red nuclei) were 28% and 57% respectively. Bar= 15 $\mu$ m.

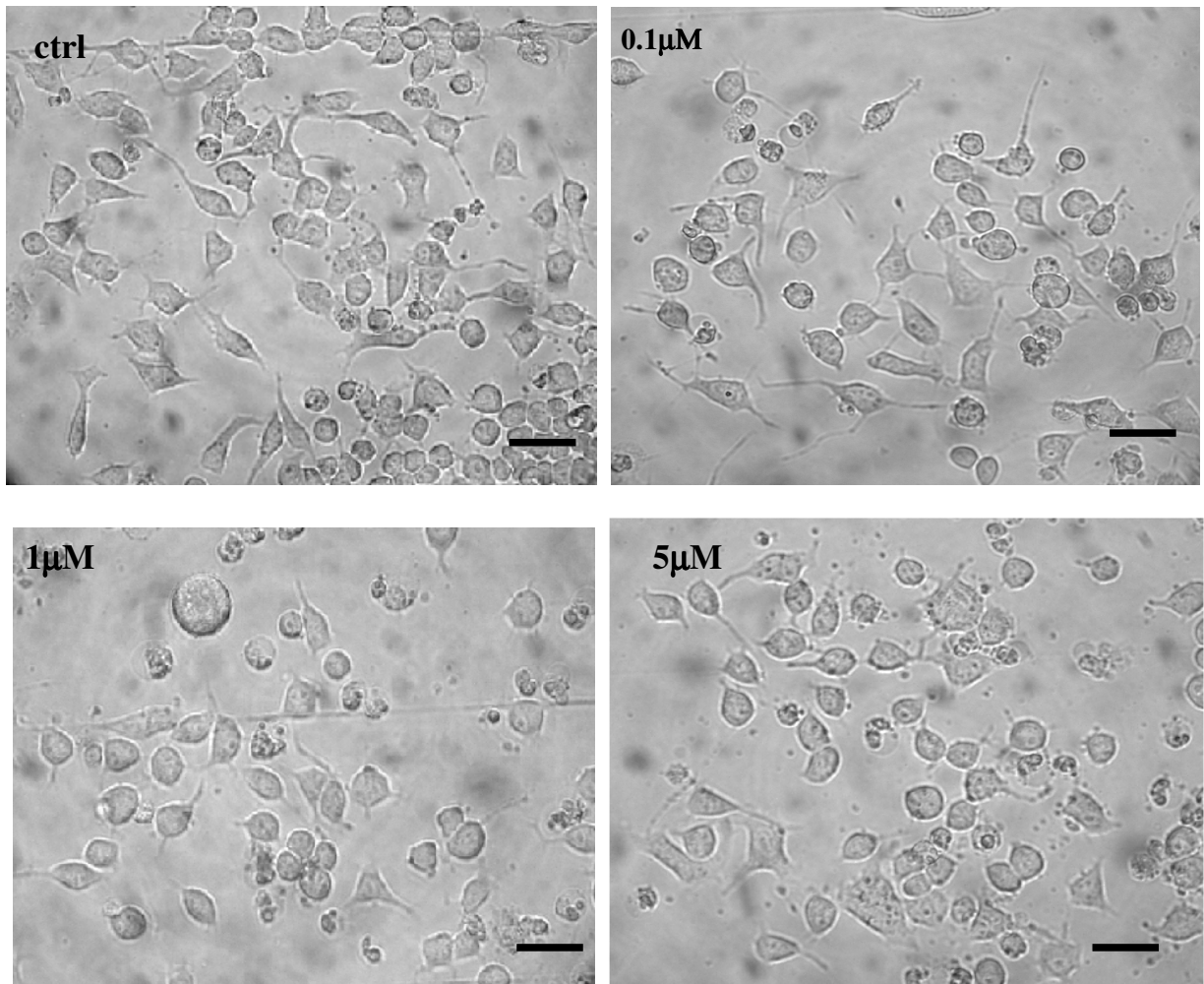


Fig. 26. Morphology of db-cAMP-differentiated C1300 cell line after 2ME-treatment. Undifferentiated C1300 cells were exposed to 10  $\mu\text{M}$  db-cAMP with RPMI-1640 medium containing 10% DCC-stripped serum for five days, then cells were treated with different 2ME micromolar concentrations (0.1, 1, 5  $\mu\text{M}$  for 5 days) and viewed by contrast phase microscope at 20X. Control cells (ctrl) were uniform in size with a polygonal shape and long cytoplasmic processes. 2ME-treatment determined a reduction in cell number; at 1  $\mu\text{M}$  and in a greater extent at 5  $\mu\text{M}$  some cells were rounded, flat and they retracted most of their cytoplasmic processes. Bar= 30  $\mu\text{m}$ .

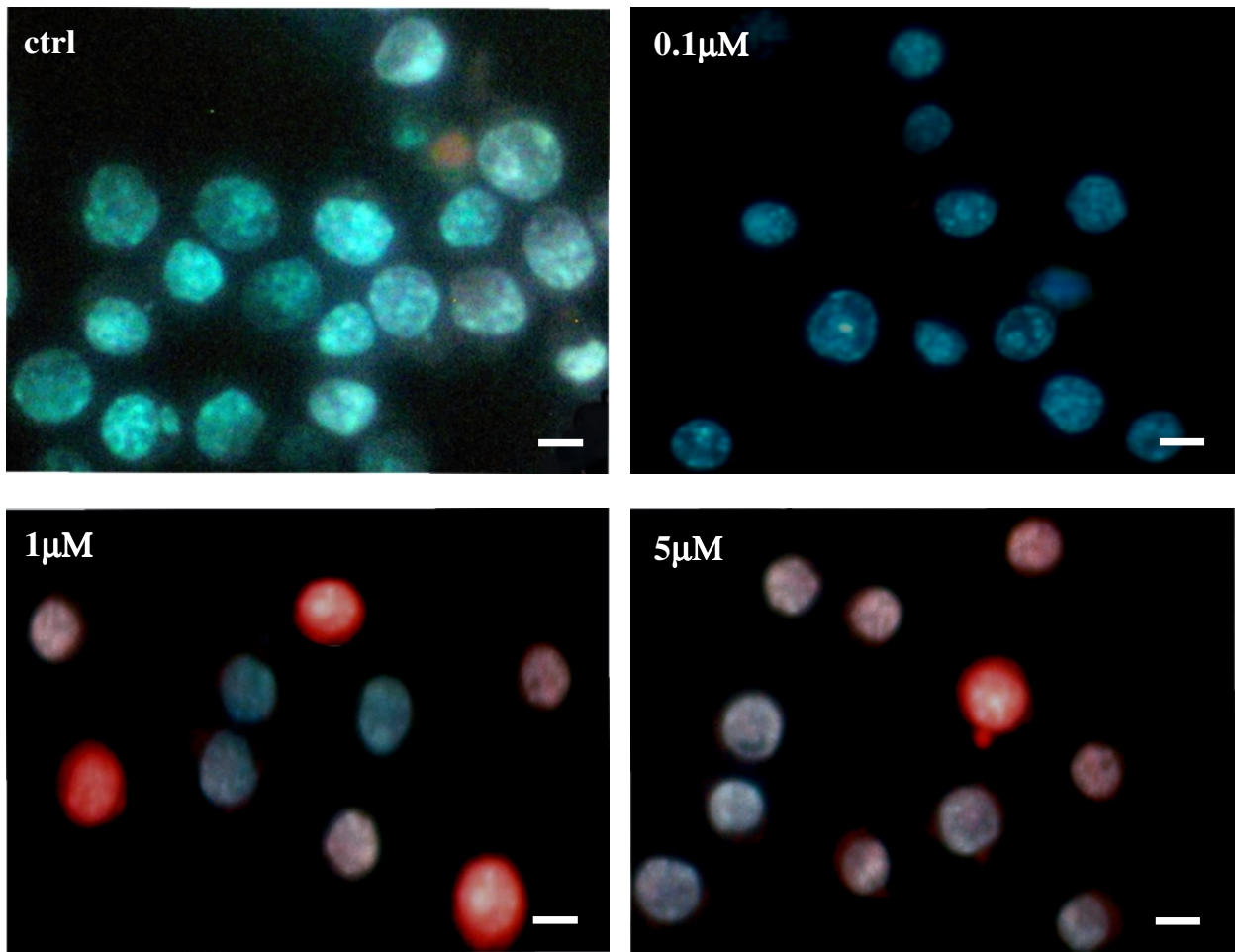


Fig. 27. Morphology of db-cAMP-differentiated C1300 after 2ME-treatment. Undifferentiated C1300 were exposed to 10  $\mu\text{M}$  db-cAMP with RPMI medium containing DCC 10% serum, then exposed to different 2ME micromolar concentrations (0.1, 1 and 5  $\mu\text{M}$  for 5 days), stained with Hoechst 33258/propidium iodide and finally viewed using a fluorescence microscope with a broad band filter (excitation wave length 365nm). The nuclei of control cells and 0.1  $\mu\text{M}$  2ME-treated cells were stained in blue by Hoechst dye, i.e. viable. In 1 and 5  $\mu\text{M}$  2ME exposed-monolayers, a great deal of cells (red nuclei) were dead (about 60-66%). Bar= 15 $\mu\text{m}$ .

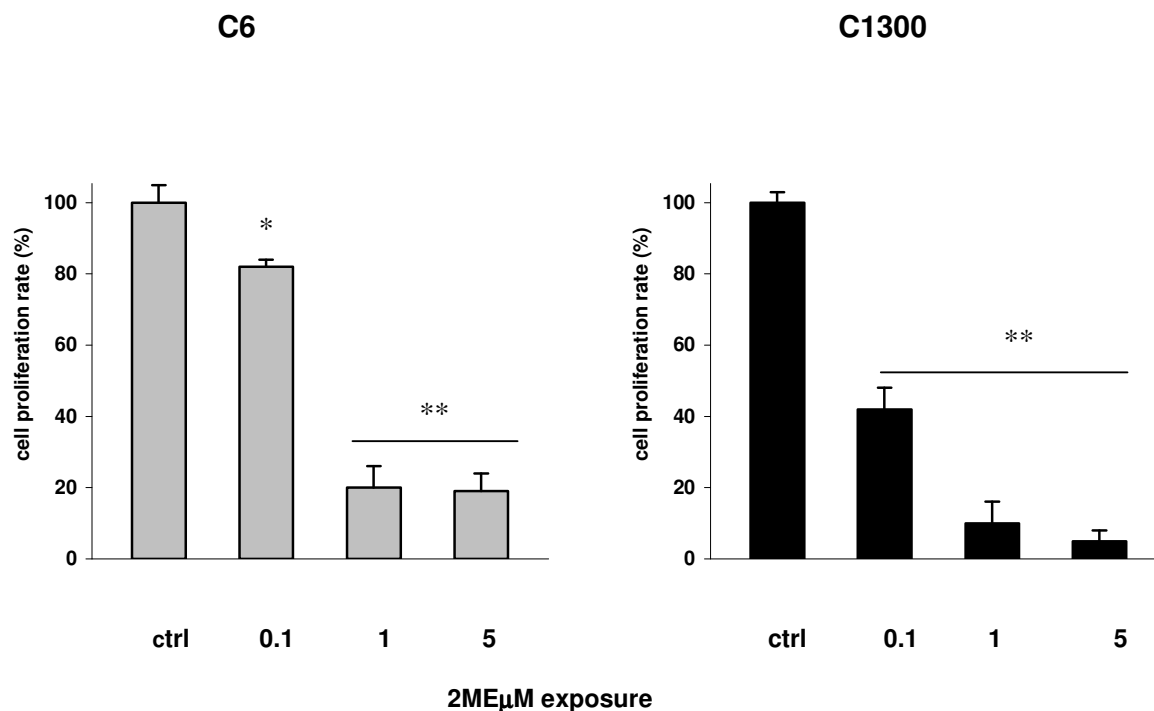


Fig. 28. Evaluation of number of viable cells (MTT test) in tapsigargin-differentiated C6 and db-cAMP-differentiated cell lines. Undifferentiated C6 and C1300 cells were plated in 96-well plates containing  $50 \times 10^3$  cells in 200 $\mu$ l RPMI-1640 medium with 10% DCC serum. C6 and C1300 cells were exposed for 5 days to 4 $\mu$ M tapsigargin and 10 $\mu$ M db-cAMP respectively. Then, cells were treated with different 2ME micromolar concentration (0.1, 1 and 5 $\mu$ M for 5 days). Finally cells were incubated in 3-(4,5-dimethylthiazolyl-2)-2,5-diphenyltetrazolium bromide assay (MTT, Cell Titer® 96) for 1h. MTT was bioreduced by living cells into a colored formazan product that is soluble in tissue culture medium. Absorption values were read setting the automatic microtiter reader at 492nm (*Uniskan II*). This method correlates absorbance reading to the number of living cells. Tapsigargin-differentiated C6 cells (left) showed a decrease in the number of viable cells (-20%) in 0.1 $\mu$ M 2ME exposed cells, when growth rate was fixed at 100% in control cells. At 1 and 5 $\mu$ M the drop of the growth rate was more remarkable (-80%). db-cAMP-differentiated C1300 cells (right) appeared more sensitive than tapsigargin-differentiated C6 cells since the growth rate at 0.1 $\mu$ M was -60% and at 1, 5 $\mu$ M between -85, -90%. \* $P < 0.05$ , \*\* $P < 0.01$  (Student's *t* test) vs control cells.

## Tapsigargin-differentiated C6 cells: total $\alpha$ -tubulin - 1:500

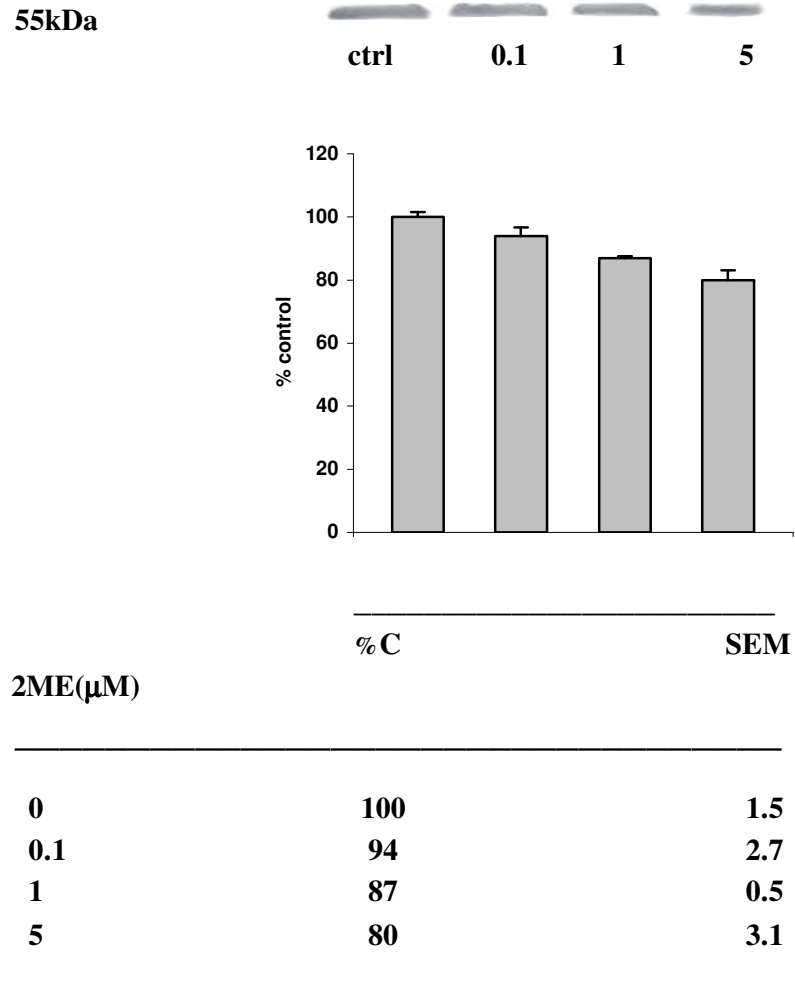
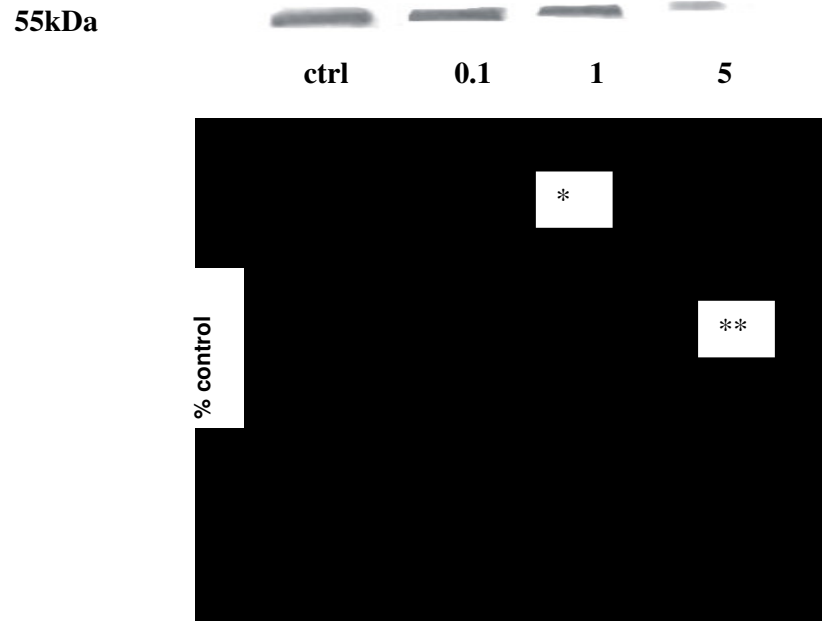


Fig. 29. Effect of 2ME on total  $\alpha$ -tubulin expression in tapsigargin-differentiated C6 cells. Representative Western blot band, histogram and values of densitometric analysis of the bands. The blot is representative from four experiments. The %C values (SEM) represent the mean values of four different experiments. Data are expressed as mean  $\pm$ SEM (n=4).

**db-cAMP-differentiated-C1300 cells:  
total  $\alpha$ -tubulin - 1:500**



2ME( $\mu$ M)	% C	SEM
0	100	1.6
0.1	85	0.5
1	82	0.7
5	61	2.3

Fig. 30. Effect of 2ME on total  $\alpha$ -tubulin expression in db-cAMP differentiated C1300 cells. Representative Western blot band, histogram and values of densitometric analysis of the band. The blot is representative from four experiments. The %C values (SEM) represent the mean values of four different experiments. Data are expressed as mean  $\pm$ SEM (n=4), \* $P=0.05$ , \*\* $P=0.01$ , (Student's  $t$  test) vs control cells.



## Tapsigargin-differentiated C6 cells: acetylated $\alpha$ -tubulin - 1:500

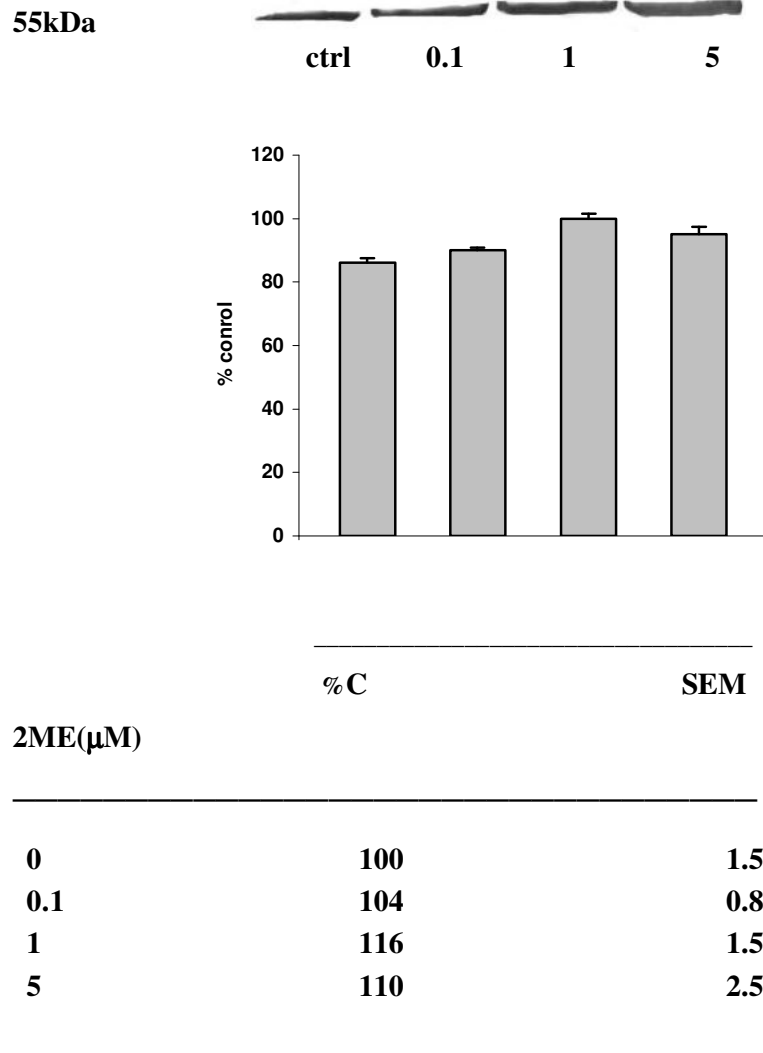
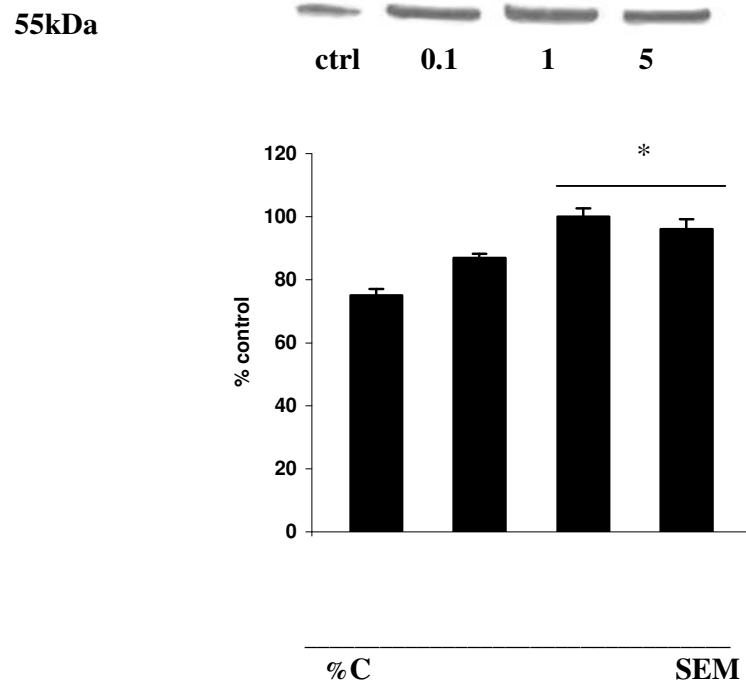


Fig. 31. Effect of 2-ME on acetylated  $\alpha$ -tubulin expression in tapsigargin-differentiated C6 cells. Representative Western blot band, histogram and values of densitometric analysis of the bands. The blot is representative from four experiments. The %C values represent the mean values of four different experiments.

**db-cAMP-differentiated-C1300:  
acetylated  $\alpha$ -tubulin - 1:500**

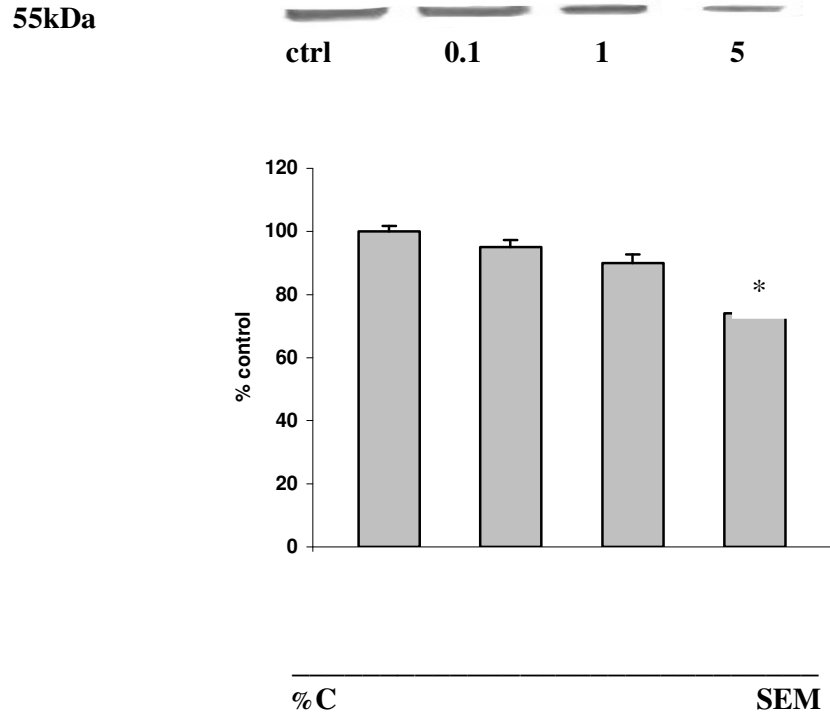


2ME( $\mu$ M)

<b>0</b>	<b>100</b>	<b>2.1</b>
<b>0.1</b>	<b>116</b>	<b>1.2</b>
<b>1</b>	<b>133</b>	<b>2.7</b>
<b>5</b>	<b>128</b>	<b>3.2</b>

Fig. 32. Effect of 2ME on acetylated  $\alpha$ -tubulin expression in db-cAMP differentiated C1300 cells. Representative Western blot band, histogram and values of densitometric analysis of the bands. The %C values (SEM) represent the mean values of four different experiments. Data are expressed as mean  $\pm$ SEM (n=4), \* $P=0.05$ , (Student's *t* test) vs control cells (ctrl).

## Tapsigargin-differentiated C6 cells: tyrosinated $\alpha$ -tubulin - 1:1.000

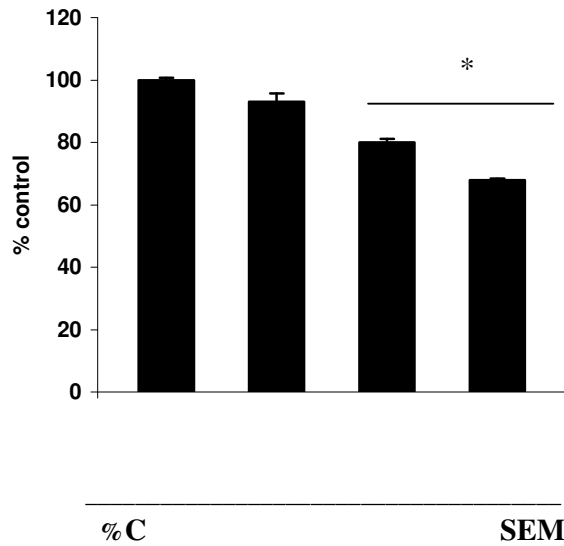


2ME( $\mu$ M)

2ME( $\mu$ M)	%C	SEM
0	100	1.7
0.1	95	2.2
1	90	2.7
5	74	0.9

Fig. 33. Effect of 2ME on tyrosinated  $\alpha$ -tubulin expression in tapsigargin-differentiated C6 cells. Representative Western blot band, histogram and values of densitometric analysis of the bands. The %C values (SEM) represent the mean values of four different experiments. Data are expressed as mean  $\pm$ SEM (n=4), \* $P$ =0.05, (Student's  $t$  test) vs control cells (ctrl).

**db-cAMP-differentiated-C1300 cells:  
tyrosinated  $\alpha$ -tubulin – 1:1.000**



2ME( $\mu$ M)

2ME( $\mu$ M)	%C	SEM
0	100	0.7
0.1	93	2.7
1	80	1.2
5	68	0.5

Fig. 34. Effect of 2ME on tyrosinated  $\alpha$ -tubulin expression in db-cAMP differentiated C1300 cells. Representative Western blot band, histogram and values of densitometric analysis of the bands. The blot is representative from four experiments. The %C values (SEM) represent the mean values of four different experiments. Data are expressed as mean  $\pm$ SEM (n=4), \* $P$ =0.05, (Student's  $t$  test) vs control cells (ctrl).

## ***DISCUSSION***

With the present study we evaluated the 2ME relative effectiveness in undifferentiated C6 & C1300 cells and in taspigargin-differentiated C6 & db-cAMP-differentiated C1300 cells. Our findings present new evidences about 2ME peculiar toxicity on glial and neuronal origin cell lines and contribute to the knowledge of general 2ME mechanisms of action *in vitro*.

2ME cytotoxic and antiproliferative activities both in glial and neuronal origin cell lines were ascertained in agreement with literature reports (Nagakawa-Yagi *et al.*, 1996; Kumar *et al.*, 2003; Lis *et al.*, 2004; Chamaon *et. al.*, 2005 and Braeuninger *et al.*, 2005). However, significant differences in relative the 2ME sensitiveness related to cell phenotype and differentiated or undifferentiated cellular status were ascertained. Indeed,  $IC_{50}^1$  values were  $\alpha$  0.01-0.1 $\mu$ M and  $\alpha$  1-5 $\mu$ M for undifferentiated C1300 and C6 cells respectively, whereas they were  $\pm$ 0.1 and  $\alpha$  0.1-1 $\mu$ M for db-cAMP-differentiated C1300 and taspigargin-differentiated C6 cells in that order. Those results are in good accordance with microscopic examinations, viability tests and proliferation assays.

Secondly, 2ME was confirmed causing alteration of tubulin expression in glial and neuronal cells origin as previously reported by Gokmen-Polar and co-workers (Gokmen-Polar *et al.*, 2005). Modification of total  $\alpha$ -tubulin, acetylated and tyrosinated  $\alpha$ -tubulin expression were related to the cell phenotypes and undifferentiated or differentiated cell status as above assessed. 2ME induced a dose-dependent reduction of tubulin expression both in undifferentiated C6 & C1300 cells.

---

<sup>1</sup>IC<sub>50</sub> is the concentration of 2ME that is necessary to kill 50% of cells *in vitro*.

Indeed, 2ME  $EC_{50/mg \text{ total protein}}$ <sup>2</sup> values of total  $\alpha$ -tubulin, acetylated and tyrosinated  $\alpha$ -tubulin were  $>10\mu\text{M}$ ,  $\geq 10\mu\text{M}$  and  $\alpha$  5-10 $\mu\text{M}$  respectively for undifferentiated C6 cells, whereas  $EC_{50/ mg \text{ total protein}}$  values were  $\alpha$  0.1-1 $\mu\text{M}$ ,  $\geq 5\mu\text{M}$  and  $\pm 1\mu\text{M}$  in that order for undifferentiated C1300 cells. As it is well-known, modification of the tubulin expression and especially the alteration of tyrosinated  $\alpha$ -tubulin<sup>3</sup> supports altered dynamic status of the microtubules. Every perturbation of tubulin dynamics leads to mitosis block and, as consequence, cell death (Brueggemeier *et al.*, 2001). The extreme sensitiveness of undifferentiated C1300 cells to 2ME may be related to the relevant decrease in tubulin expression and marked down-regulation of tyrosinated  $\alpha$ -tubulin.

By contrast, alterations of tubulin expression were almost negligible in taspigargin-differentiated C6 & db-cAMP-differentiated C1300 cells. 2ME determined a slight dose-dependent down-regulation of total  $\alpha$ -tubulin and tyrosinated  $\alpha$ -tubulin (higher in C1300 cells than in C6 cells), whereas 2ME up-regulated acetylated  $\alpha$ -tubulin expression (more markedly in C6 than in C1300 cells). Acetylated  $\alpha$ -tubulin<sup>4</sup> up-regulation and tyrosinated  $\alpha$ -tubulin decrease demonstrate microtubular stabilization since analogous tubulin isoforms expression were ascertained in neurons treated with nocodazole, a potent microtubular stabilizing drug (Popoli *et al.*, 2000).

---

<sup>2</sup> The concentration of 2ME which induces 50% reduction of the total protein amount (express in mg) of tubulin isoforms.

<sup>3</sup> Post-translational modification of  $\alpha$ -tubulin associated with dynamic microtubular structures (Cumming *et al.*, 1984).

<sup>4</sup> Post-translational modification of  $\alpha$ -tubulin associated with stable microtubules (Sasse *et al.*, 1988).

Hence, 2ME-resistance of undifferentiated cells may be due to their microtubular stability. High microtubular stability of taspigargin-differentiated C6 cells may also explain higher 2ME-resistance in comparison with db-cAMP-differentiated C1300 cells. To summarize, our data show that:

- Undifferentiated C6 & C1300 cells are more sensitive to 2ME than taspigargin-differentiated C6 & db-cAMP-differentiated C1300 cells;
- 2ME is more effective in C1300 than in C6 cells independently from the undifferentiated/differentiated status.

The first point agrees with the assumption that 2ME cellular sensitiveness is related to the cell proliferation rate<sup>5</sup> (Lis *et al.*, 2004 and Kamath *et al.*, 2006). 2ME is extremely effective in undifferentiated cells since they have a high proliferation rate. On the other hand, relative 2ME-resistance of differentiated cells is in good accordance with their low proliferation rate<sup>6</sup>. The following mechanisms of action may support this theory:

### **2ME alters tubulin dynamics more intensively in high-proliferating cells than in slow-proliferating cells**

As it is well known 2ME alters tubulin dynamics by its binding

---

<sup>5</sup> The proliferation rate, a measure for the proliferation status of a cell population, is defined as the ratio between the number of cells in mitosis and the total number of cells. The proliferation rate is high in actively dividing cells (i.e. tumoural cells) while it is low in non actively dividing cells (i.e. fibroblasts).

<sup>6</sup> The proliferation rate of undifferentiated C6 & C1300 cells is  $\pm 15$  times higher than the proliferation rate of taspigargin-differentiated C6 cells & db-cAMP-differentiated cells.



ability to colchicine site (RJ D'Amato *et al.*, 1994; Cushman *et al.*, 1995 and Hamel *et al.*, 1996). 2ME modifies microtubular dynamics stopping microtubule growth parameters, increasing the time of steady-state and interfering with chromosome progression or cell division (Seegers *et al.*, 1997; Attalla *et al.*, 1996; Brueggemeier *et al.*, 2001; Tinley *et al.*, 2003 and Kamath *et al.*, 2006). Thus, the intense proliferative and microtubular activity render high-proliferating cells (undifferentiated) much more susceptible than slow-proliferating cells (differentiated) to the alterations of tubulin dynamics. Our results confirm that the marked 2ME-induced alterations of tubulin dynamics are linked to relevant modification of cell physiology and cell morphology.

### **2ME may induce apoptosis in high-proliferating cells**

2ME may induce apoptosis in high-proliferating cells such as tumoral cells (Seegers *et al.*, 1997; Attalla *et al.*, 1998; Huang *et al.*, 2003, Shimada *et al.*, 2003 and Bu *et al.*, 2006). By contrast, 2ME apoptotic activity has not been demonstrated in slow-proliferating cells such as normal cells (Seegers *et al.*, 1997). Several evidences suggest that 2ME can trigger apoptosis by activation of cell surface receptors. 2ME increases the expression of death receptors 5 (DR5) (La Valle *et al.*, 2004), up-regulates p53 (Seegers *et al.*, 1997 and Shimada *et al.*, 2003) or activates various MAP kinases (Attalla *et al.*, 1998, Shimada *et al.*, 2003 and Bu *et al.*, 2006).

2ME may indirectly induce apoptosis through the inhibition of the superoxide dismutases (SODs) as well. Accumulation of cellular

$O_2^-$  causes mitochondrial damages resulting in sequential cascade reactions which initiates apoptosis. Since high-proliferating cells have a more intense  $O_2^-$  production and a weaker SODs activity than slow-proliferating cells, high-proliferating cells are more responsive to any SODs perturbation than slow-proliferating cells (Huang *et al.*, 2003).

The second point apparently disagrees with previous assumptions. Indeed, though C6 cells are more proliferating than C1300<sup>7</sup> cells independently from the undifferentiated/differentiated status, we demonstrated that 2ME was more effective in C1300 cells than in C6 cells. However, the following hypothesis may clarify the apparent contradiction:

**Alteration of microtubule dynamics is more intense in C1300 phenotype than in C6 phenotype**

The marked down-regulation of tubulin isoforms proves higher alteration of microtubule dynamics in C1300 phenotype than in C6 phenotype. We hypothesize that the alteration of microtubule dynamics is more marked in neuronal cells not only because they express a greater pattern of  $\alpha$  and  $\beta$  tubulin isoforms than glial cells, but also because 2ME has more affinity for neuronal  $\alpha$  and  $\beta$  tubulin isoforms (Moura Neto *et al.*, 1983).

**2ME induces metabolic failure and consequent excitotoxicity more intensely in C1300 than in C6 cells**

2ME may induce metabolic failure more intensively in neuronal

---

<sup>7</sup> C6 cells display a proliferation rate  $\pm 6$  times higher than C1300 cells.

than in glial cells resulting in excitotoxicity<sup>8</sup> phenomena. Neuronal and glial sensitiveness to excitotoxicity comes from peculiar neuronal and glial physiological properties.

Neurons, and especially activate neurons, have a higher energy demand than glial cells. Since neurons only produce glutamate<sup>9</sup> and they need higher amounts of glucose and lactate more than glial cells, if glucose and lactate are in short supply, neurons more likely than glial cells starve. Thus, any metabolic failure determines cellular damages greater in neuronal than in glial cells. As pointed out on retinoic acid-differentiated human neuroblastoma cells (Nakagawa-Yagi *et al.*, 1996), we hypothesized that 2ME causes metabolic perturbations resulting in energy depletion higher in C1300 than in C6 cells. Consequence of any energetic depletion is immediate failure of Na<sup>+</sup>/K<sup>+</sup> pumps with depolarization of cellular membranes and immediate breakdown of cellular functions. In neuronal cells depolymerization of membranes arrests the synaptic function and neuronal conductivity inducing the release of disproportionate amounts of glutamate in the synaptic cleft (excitotoxicity). Though glutamate is indispensable for numerous neuronal functions, excessive quantities released in the synaptic cleft could act as neuronal poison. Glutamate activates some specific receptors that are non-selective cation-permeable ion channels. Over-activation of these receptors causes an excessive passive influx of Cl<sup>-</sup> and Na<sup>+</sup> into cells that determines an osmotic failure and

---

<sup>8</sup> *Excitotoxicity*, by definition, is a typical neuronal cytotoxic phenomenon following the over-activation of glutamate receptors determined by the excessive release of glutamate amounts in the synaptic cleft.

<sup>9</sup> The most common excitatory neurotransmitter.

resultant cell death within few minutes. In addition, abnormal glutamate release may also lead to an anomalous  $\text{Ca}^{++10}$  influx into neurons which effect structural damages of neuronal cells after hours or days. Indeed, over-activation of some glutamate receptors that are permeable to  $\text{Ca}^{++}$  causes massive influx of this cation that, by consequence, activates several catabolic enzymes (i.e. proteases, phospholipases and endonucleases) and nitric oxide (NO) syntethase, with following formation of the free radical NO. Free radicals and activated catabolic enzymes destroy structural proteins, membrane lipids, nucleic acids and other cellular contents, causing neuronal necrosis and triggering cellular apoptosis (Dirnagl *et al.*, 1999 and MacDonald *et al.*, 2006).

To summarize, excitotoxicity involves in a lesser extent glial cells because: a) glial cells are less sensitive to any metabolic failure as they have metabolic demands lower than neuronal cells b) glial cells have a lower number of voltage-gated channel than neuronal cells and, by consequence, are not excitable and are not susceptible to any over-activation of glutamate receptors.

Elucidating the differences in sensitiveness between undifferentiated/differentiated C6/C1300 cells is important for understanding mechanisms of 2ME action and to provide information for analogue *in vivo/in vitro* studies.

This study supports the assumption that 2ME toxicity is a phenomenon involving multifactorial mechanisms. We believe

---

<sup>10</sup>  $\alpha$ -amino-3hydroxy-5-methyl-4-isoxazolepropionic receptors (AMPA) and glutamate *N* methyl-D-aspartate receptors (NMDA).

that 2ME cytotoxic action is mainly due to the synergic perturbation of microtubular dynamics and the metabolic patterns rather than the possible indirect induction of apoptosis (SODs inhibition, up-regulation of p53 and activation of various kinases). Our study confirms the pivotal role of cytoskeleton in cytotoxicity 2ME-induced phenomena. We clearly demonstrate that specific cytoskeletal/metabolic patterns are strictly linked with different rate of tubulin dynamics alteration and, as consequence, with relative 2ME effectiveness in cell populations. On the other hand, we believe that a crucial point to better understand 2ME mechanisms of action is the identification of the signaling pathways that link the ability of 2ME to alter tubulin dynamics and to induce apoptosis.

In conclusion, our findings may support further study on *in vitro* glial and neuronal 2ME-exposed cells aimed at determining the correlation between the alteration of tubulin dynamics and the initiation of apoptosis. Comprehension of 2ME mechanisms of action can be crucial for the study of the pathogenesis and the treatment of several neurological disorders.

## ***BIBLIOGRAFY***

Alberts B, Johnson A, Lewis J, Raff M, Roberts K, Walter P. Molecular Biology of Cells. Garland, 4<sup>th</sup> Edition, New York 2002.

Argarana CE, Arce CA, Barra HS, Caputto R. *In vivo* incorporation of [14C] tyrosine into the C-terminal position of the alpha subunit of tubulin. Arch Biochem Biophys. 1977;180(2):264-8.

Argarana CE, Barra HS, Caputto R. Release of [14C]tyrosine from tubulin-[14C]tyrosine by brain extract. Separation of a carboxypeptidase from tubulin-tyrosine ligase. Mol Cell Biochem. 1978;19(1):17-21.

Attalla H, Makela TP, Adlercreutz H, Andersson LC. 2-methoxyestradiol arrests cells in mitosis without depolymerizing tubulin. Biochem Biophys Res Commun. 1996;228(2):467-73.

Attalla H, Westberg JA, Andersson LC, Adlercreutz H, Makela TP. 2-methoxyestradiol-induced phosphorylation of Bcl-2: uncoupling from JNK/SAPK activation. Biochem Biophys Res Commun. 1998;247(3):616-9.

Banerjee A. Coordination of posttranslational modifications of bovine brain alpha-tubulin. Polyglycylation of delta 2 tubulin J Biol Chem. 2002;277(3):46140-44.

Banerjee SN, Sengupta K, Banerjee S, Saxena NK, Banerjee SK. 2-methoxyestradiol exhibits a biphasic effect on VEGF-A in tumor cells and upregulation is mediated through ER-alpha: a possible

signaling pathway associated with the impact of 2-ME2 on proliferative cells. *Neoplasia* 2003;5(5):417-26.

Baulieu EE and Robel P. Neurosteroids: a new brain function? *Journal of Steroid Biochemistry and Molecular Biology* 1990;37:395-403.

Baulieu EE. Neurosteroids: a novel function of the brain *Psychoneuroendocrinology* 1998;23:963-87.

Baulieu EE. Neurosteroids: of the nervous system, by the nervous system, for the nervous system. *Recent Progress in Hormone Research* 1997;52(3):1-33.

Belmont LD and Mitchison TJ. Identification of a protein that interacts with tubulin dimers and increases the catastrophe rate of microtubules. *Cell* 1996;84(4):623-31.

Berg FD, Kuss E. Serum concentration and urinary excretion of "classical" estrogens, catecholestrogens and 2-methoxyestrogens in normal human pregnancy *Arch Gynecol Obstet.* 1992;251(1):17-27.

Beyenburg S, Stoffel-Wagner B, Watzka M, Bluemcke I, Bauer J, Schramm J. Expression of cytochrome P450scc mRNA in the hippocampus of patients with temporal lobe epilepsy. *Neuroreport* 1999;10:3067-70.



Bianchi M, Hagan JJ, Heidebreder CA, Neuronal plasticity, stress and depression: involvement of the cytoskeletal microtubular system? *Curr Drug Targets CNS Neurol Disord.* 2005;(5):597-611.

Bogatcheva NV, Adyshev D, Mambetsariev B, Moldobaeva N, Verin AD. Involvement of microtubules, p38 and Rho kinases pathway in 2-methoxyestradiol-induced lung vascular barrier dysfunction. *Am J Physiol Lung Cell Mol Physiol.* 2007;292(2):487-99.

Boucher D, Larcher JC, Gros F and Denoulet P. Polyglutamylation of tubulin as a progressive regulator of *in vitro* interactions between the microtubule-associated protein Tau and tubulin. *Biochemistry* 1994;33:12471-77.

Braeuninger S, Chamaon K, Kropf S, Mawrin C, Wiedemann FR, Hartig R, Schoeler S, Dietzmann K, Kirches E. Short incubation with 2-methoxyestradiol kills malignant glioma cells independent of death receptor 5 up-regulation. *Clin Neuropathol.* 2005;24(4):175-83.

Brueggemeier RW, Bhat AS, Lovely CJ, Coughenour HD, Joomprabutra S, Weitzel DH, Vandre DD, Yusuf F, Burak WE Jr. 2-Methoxymethylestradiol: a new 2-methoxy estrogen analog that exhibits antiproliferative activity and alters tubulin dynamics. *J Steroid Biochem Mol Biol.* 2001;78(2):145-56.

Brueggemeier RW, Singh U. Inhibition of rat liver microsomal estrogen 2-hydroxylase by 2-methoxyestrogens. *J Steroid Biochem.* 1989;33(4A):589-93.

Bu SZ, Huang Q, Jiang YM, Min HB, Hou Y, Guo ZY, Wei JF, Wang JW, Ni X, Zheng SS. p38 Mitogen-activated protein kinases is required for counteraction of 2-methoxyestradiol to estradiol-stimulated cell proliferation and induction of apoptosis in ovarian carcinoma cells via phosphorylation Bcl-2. *Apoptosis* 2006;11(3):413-25.

Caron JM, Vega LR, Fleming J, Bishop R, Solomon F. Single site alpha-tubulin mutation affects astral microtubules and nuclear positioning during anaphase in *Saccharomyces cerevisiae*: possible role for palmitoylation of alpha-tubulin. *Mol Biol Cell.* 2001;12(9):2672-87.

Caron JM. Posttranslational modification of tubulin by palmitoylation: I. *In vivo* and cell-free studies. *Mol Biol Cell.* 1997;(4):621-36.

Cassimeris L. Regulation of microtubule dynamic instability. *Cell Motil Cytoskeleton* 1993;26(4):275-83.

Caudron N, Arnal I, Buhler E, Job D, Valiron O. Microtubule nucleation from stable tubulin oligomers. *J Boil Chem.* 2002;277(52):50973-79.

Chamaon K, Stojek J, Kanakis D, Braeuninger S, Kirches E, Krause G, Mawrin C, Dietzmann K. Micromolar concentrations of 2-methoxyestradiol kill glioma cells by an apoptotic mechanism, without destroying their microtubule cytoskeleton. *J Neurooncol.* 2005;72(1):11-26.

Chang PA, Wu YJ, Li W, Leng XF. Effect of carbamate esters on neurite outgrowth in differentiating human SK-N-SH neuroblastoma cells. *Chem Biol Interact.* 2006;159:65-72.

Cumming R, Burgoyne RD, Lytton NA. Immunocytochemical demonstration of alpha-tubulin modification during axonal maturation in the cerebellar cortex. *J Cell Biol.* 1984;98(1):347-51.

Cushman M, He HM, Katzenellenbogen JA, Lin CM, Hamel E. Synthesis, antitubulin and antimitotic activity, and cytotoxicity of 2-methoxyestradiol, an endogenous mammalian metabolite of estradiol that inhibits tubulin polymerization by binding to the colchicine binding site. *J Med Chem.* 1995;38(12):2041-9.

D'Amato CM, Lin E, Flynn J, Folkman, Hamel E. 2-methoxyestradiol, an Endogenous Mammalian Metabolite, Inhibits Tubulin Polymerization by Interacting at the Colchicine Site. *Proc Natl Acad Sci.* 1994;91:3964-8.

Dawling S, Roodi N, Mernaugh RL, Wang X, Parl FF. Catechol-O-methyltransferase (COMT)-mediated metabolism of catechol estrogens: comparison of wild-type and variant COMT isoforms. *Cancer Res.* 2001;61(18):6716-22.

Dirnagl U, Iadecola C, Moskowitz MA. Pathobiology of ischaemic stroke: an integrated view. *Trends Neurosci.* 1999;22:391-7.

Eipper BA. Properties of rat brain tubulin. *J Biol Chem.* 1974;249(5):1407-16.

Erck C, Peris L, Andrieux A, Meissirel C, Gruber AD, Vernet M, Schweitzer A, Saoudi Y, Pointu H, Bosc C, Salin PA, Job D, Wehland J. A vital role of tubulin-tyrosine-ligase for neuronal organization. *Proc Natl Acad Sci.* 2005;102(22):7853-78.

Farina V, Zedda M, Bianchi M, Marongiu P, De Riu PL. Tubulin isoforms are differently expressed in developing and mature neurons: a study on the cerebral cortex of newborn and adult rats. *Eur J Histochem.* 1999;43(4):285-91.

Fotsis T, Zhang Y, Pepper MS, Adlercreutz H, Montesano R, Nawroth PP, Schweigerer L. The endogenous oestrogen metabolite 2-methoxyoestradiol inhibits angiogenesis and suppresses tumour growth. *Nature* 1994;368(6468):237-9.

Frye RA. Phylogenetic classification of prokaryotic and eukaryotic Sir2-like proteins. *Biochem Biophys Res Commun.* 2005;273(2):793-8.

Gagnon C, White D, Cosson J, Huitorel P, Edde B, Desbruyeres E, Paturle-Lafanechère L, Multigner L, Job D, Cibert C. The polyglutamylated lateral chain of alpha-tubulin plays a key role in flagellar motility. *J Cell Sci.* 1996;109(6):1545-53.

Gelbke HP, Knuppen R. The excretion of five different 2-hydroxyoestrogen monomethylethers in human pregnancy urine. *J Steroid Biochem.* 1976;7(6-7):457-63.

Gokmen-Polar Y, Escuin D, Walls CD, Soule SE, Wang Y, Sanders KL, La Vallee TM, Wang M, Guenther BD, Giannakakou P, Sledge GW Jr. beta-Tubulin mutations are associated with resistance to 2-methoxyestradiol in MDA-MB-435 cancer cells. *Cancer Res.* 2005;65(20):9406-14.

Gurland G, Gundersen GG. Stable, detyrosinated microtubules function to localize vimentin intermediate filaments in fibroblasts. *J Cell Biol.* 1995;131(5):1275-84.

Hamel E, Lin CM, Flynn E, D'Amato RJ. Interactions of 2-methoxyestradiol, an endogenous mammalian metabolite, with unpolymerized tubulin and with tubulin polymers. *Biochemistry* 1996;35(4):1304-10.

Hampson E. Oestrogen-related variations in human spatial and articulatory motor skills. *Psychoneuroendocrinology* 1990;15:97-111.

Helfand BT, Chang L, Goldman RD. Intermediate filaments are dynamic and motile elements of cellular architecture. *J Cell Sci.* 2004;117(2):133-41.

Huang P, Feng L, Oldham EA, Keating MJ, Plunkett W. Superoxide dismutase as a target for the selective killing of cancer cells. *Nature* 2003;407(6802):309-11.

Hubbert C, Guardiola A, Shao R, Kawaguchi Y, Ito A, Nixon A, Yoshida M, Wang XF, Yao TP. HDAC6 is a microtubule-associated deacetylase. *Nature* 2002;417(6887):455-58.

Kamath K, Okouneva T, Larson G, Panda D, Wilson L, Jordan MA. 2-methoxyestradiol suppresses microtubule dynamics and arrests mitosis without depolymerizing microtubules. *Mol Cancer Ther.* 2006;5(9):2225-33.

Khanna M, Qin K-N, Wang RW & Cheng K-C. Substrate specificity, gene structure, and tissue-specific distribution of multiple human 3 $\alpha$ -hydroxysteroid dehydrogenases. *J Biol Chem.* 1995;270:20162-68.

Kumar AP, Garcia GE, Orsborn J, Levin VA, Slaga TJ. 2-Methoxyestradiol interferes with NF kappa B transcriptional activity in primitive neuroectodermal brain tumors: implications for management. *Carcinogenesis.* 2003;24(2):209-16.

Kuo TC, Lin-Shiau SY. Decrease in Ca<sup>++</sup>-activated K<sup>+</sup> conductance in differentiated C6-glioma cells. *Neurochem Res.* 2004;29(7):1453-9.

LaVallee TM, Zhan XH, Herbstritt CJ, Kough EC, Green SJ, Pribluda VS. 2-Methoxyestradiol inhibits proliferation and induces

apoptosis independently of oestrogen receptors alpha and beta. *Cancer Res.* 2002;62(13):3691-7.

Lee MK, Rebhun LI, Frankfurter A. Posttranslational modification of class III beta-tubulin. *Proc Natl Acad Sci USA.* 1990;7(18):7195-9.

Lis A, Ciesielski MJ, Barone TA, Scott BE, Fenstermaker RA, Plunkett RJ. 2-Methoxyestradiol inhibits proliferation of normal and neoplastic glial cells, and induces cell death, *in vitro*. *Cancer Lett.* 2004;213(1):57-65.

Ludueno RF. Multiple forms of tubulin: different gene products and covalent modifications. *Int Rev Cytol.* 1998;178:207-75.

Mabjeesh NJ, Escuin D, LaVallee TM, Pribluda VS, Swartz GM, Johnson MS, Willard MT, Zhong H, Simons JW, Giannakakou P. 2ME2 inhibits tumor growth and angiogenesis by disrupting microtubules and dysregulating HIF. *Cancer Cell.* 2003;3(4):363-75.

MacDonald JF, Xiong ZG, Jackson MF. Paradox of Ca<sup>2+</sup> signaling, cell death and stroke. *Trends Neurosci.* 2006;29:75-81.)

Magri F, Terenzi F, Ricciardi T, Fioravanti M, Solerte SB, Stabile M *et al.* Association between changes in adrenal secretion and cerebral morphometric correlates in normal aging and senile dementia. *Dem Ger Cogn Dis.* 2000;11:90-99.

Majewska MD. Neurosteroids: endogenous bimodal modulators of the GABAA receptor. Mechanism of action and physiological significance. *Progr Neurobiol.* 1992;38:379-95.

Margolis RL and Wilson P. Microtubule treadmills-possible molecular machinery. *Nature* 1981;293(5835):705-11.

Martel C, Melner MH, Gagne D, Simard J & Labrie F. Widespread tissue distribution of steroid sulfatase, 3 $\beta$ -hydroxysteroid dehydrogenase/D5-D4 isomerase (3 $\alpha$ -H ), 17 $\beta$ -HSD, 5 $\alpha$ -reductase and aromatase activities in the rhesus monkey. *Mol Cell Endocrin.* 1994;104:103-11.

Martucci CP and Fishman J. Impact of continuously administered catechol estrogens on uterine growth and luteinizing hormone secretion. *Endocrinology* 1979;105(6):1288-92.

Mayer F. Cytoskeletal elements in bacteria *Mycoplasma pneumoniae*, *Thermoanaerobacterium* sp., and *Escherichia coli* as revealed by electron microscopy. *J Mol Microbiol Biotechnol.* 2006(3-5): 228-43.

McEwen BS and Alves SE. Estrogen actions in the central nervous system. *Endocrine Reviews* 1999;20:279-307.

McEwen BS, Gould E, Orchinik M, Weiland NG & Wooley CS. Oestrogen and the structural and functional plasticity of neurons: implications for memory, ageing and neurodegenerative processes. *Neurology* 1995;45:52-73.



Mellon S and Deschepper CF. Neurosteroid biosynthesis: genes for adrenal steroidogenic enzymes are expressed in the brain. *Brain Research*. 1993;629:283-29.

Million K, Larcher J, Laoukili J, Bourguignon D, Marano F, Tournier F. Polyglutamylation and polyglycylation of alpha- and beta-tubulins during *in vitro* ciliated cell differentiation of human respiratory epithelial cells. *J Cell Sci*. 1999;112:4357-66.

Miyake S, Shimo Y, Kitamura T. Morphological differentiation *in vitro* of human continuous and functional neuroblastoma cell line, NB-I under treatment of (But) 2cAMP. *Neurosurgery* 1975;3:407-14.

*Molecular Biology of Cells*, 4<sup>th</sup> Edition, Garland, New York 2002.

Moura Neto V, Mallat M, Jeantet C and Prochiantzi A. Microheterogeneity of tubulin proteins in neuronal and glial cells from the mouse brain in culture. *EMBO J*. 1983;8:1243-48.

Nakagawa-Yagi Y, Ogane N, Inoki Y, Kitoh N. The endogenous estrogen metabolite 2-methoxyestradiol induces apoptotic neuronal cell death *in vitro*. *Life Sci*. 1996;58(17):1461-67.

Näsman B, Olsson B, Bäckström T, Eriksson S, Grankvist K, Viitanen M. Serum dehydroepiandrosterone sulfate in Alzheimer's disease and in multi infarct dementia. *Bio. Psychiatry* 1991;30:684-90.

Nogales E. Structural insight into microtubule function. *Annu Rev Biophys Biomol Struct.* 2001;30:397-420.

Paturle-Lafanechère L, Edde B, Denoulet P, Van Dorsselaer A, Mazarguil H, Le Caer JP, Wehland J, Job D. Characterization of a major brain tubulin variant which cannot be tyrosinated. *Biochemistry* 1991;30 (43):10523-8.

Paturle-Lafanechère L, Manier M, Trigault N, Pirollet F, Mazarguil H, Job D. Accumulation of delta 2-tubulin, a major tubulin variant that cannot be tyrosinated, in neuronal tissues and in stable microtubule assemblies. *J Cell Sci.* 1994;107 (6):1529-43.

Peltoketo H, Luu-The V, Simard J, Adamski J. 17 $\beta$ -hydroxysteroid dehydrogenase (HSD)/17-ketosteroid reductase (KSR) family; nomenclature and main characteristics of the 17HSD/KSR enzymes. *J Mol Endocr.* 1999;23:1-11.

Phillips S and Sherwin B. Effects of oestrogen on memory function in surgically menopausal women. *Psychoneuroendocrinology* 1992a;17:485-95.

Phillips S and Sherwin B. Variations in memory function and sex steroid hormones across the menstrual cycle. *Psychoneuroendocrinology.* 1992b;17:497-506.

Pollard T D, Earnshaw W D. *Cell Biology*, Saunders, New York 2004.

Popoli M, Brunello N, Perez J, Racagni G J. Second messenger-regulated protein kinases in the brain: their functional role and the action of antidepressant drugs. *J Neurochem.* 2000;74:21-33.

Redeker V, Levilliers N, Schmitter JM, Le Caer JP, Rossier J, Adoutte A, and Bré MH. Polyglycylation of tubulin: a posttranslational modification in axonemal microtubules. *Science* 1994;266:1688-91.

Redeker V, Rossier J, Frankfurter A. Posttranslational modifications of the C-terminus of alpha-tubulin in adult rat brain: alpha 4 is glutamylated at two residues. *Biochemistry* 1998;37(42):14838-44.

Sasse R Gull K. Tubulin post-translational modifications and the construction of microtubular organelles in *Trypanosoma brucei*. *J Cell Sci.* 1988;90 (4):577-89.

Sattler M, Quinnan LR, Pride YB, Gramlich JL, Chu SC, Even GC, Kraeft SK, Chen LB, Salgia R. 2-methoxyestradiol alters cell motility, migration, and adhesion. *Blood* 2003;102(1):289-96.

Seegers JC, Aveling ML, Van Aswegen CH, Cross M, Koch F, Joubert WS. The cytotoxic effects of estradiol-17 beta, catecholestradiols and methoxyestradiols on dividing MCF-7 and HeLa cells. *J Steroid Biochem.* 1989;32(6):797-809.

Seegers JC, Lottering ML, Grobler CJ, van Papendorp DH, Habbersett RC, Shou Y, Lehnert BE. The mammalian metabolite, 2-

methoxyestradiol, affects P53 levels and apoptosis induction in transformed cells but not in normal cell. *J Steroid Biochem Mol Biol.* 1997;62(4):253-670.

Seyedin SM, Pehrson JR, Cole RD. Loss of chromosomal high mobility group proteins HMG1 and HMG2 when mouse neuroblastoma and Friend erythroleukemia cells become committed to differentiation. *Proc Natl Acad Sci.* 1981;78:5988-92.

Shimada K, Nakamura M, Ishida E, Kishi M, Konishi N. Roles of p38 and c-jun NH2-terminal kinase-mediated pathways in 2-methoxyestradiol-induced p53 induction and apoptosis. *Carcinogenesis* 2003;24(6):1067-75.

Smith DS, Niethammer M, Ayala R, Zhou Y, Gambello MJ, Wynshaw-Boris A, Tsai LH. Regulation of cytoplasmic dynein behaviour and microtubule organization by mammalian Lis1. *Nat Cell Biol.* 2000;2(11):767-75.

Stoffel-Wagner B. Neurosteroid metabolism in the human brain. *Eur. J. Endocrinol.* 2001;145:669-79.

Sutherland TE, Schuliga M, Harris T, Eckhardt BL, Anderson RL, Quan L, Stewart AG. 2-methoxyestradiol is an estrogen receptor agonist that supports tumor growth in murine xenograft models of breast cancer. *Clin Cancer Res.* 2005;11(5):1722-32.

Tinley TL, Leal RM, Randall-Hlubek DA, Cessac JW, Wilkens LR, Rao PN, Mooberry SL. Novel 2-methoxyestradiol analogues with antitumor activity. *Cancer Res.* 2003;63(7):1538-49.

Truss M, and Beato M. Steroid hormone receptors: interaction with deoxyribonucleic acid and transcription factors. *Endocr Rev.* 1988;14:459-79.

Valiron O, Caudron N, Job D. Microtubule dynamics. *Cell Mol Life Sci.* 2001;58(14):2069-84.

Westermann S, Weber K. Post-translational modifications regulate microtubule function. *Nat Rev Mol Cell Biol.* 2003;4(12):938-47.

Wozniak A, Hutchinson RE, Morris CM & Hutchinson JB. Neuroblastoma and Alzheimer's disease brain cells contain aromatase activity. *Steroids* 1998;63:263-67.

Xia L, Hai B, Gao Y, Burnette D, Thazhath R, Duan J, Bre MH, Levilliers N, Gorovsky MA, Gaertig J. Polyglycylation of tubulin is essential and affects cell motility and division in *Tetrahymena thermophila* *J Cell Biol.* 2000;149(5):1097-106.

Zedda M, Lepore G, Gadau S, Manca P, Farina V. Morphological and functional changes induced by the amino acid analogue 3-nitrotyrosine in mouse neuroblastoma and rat glioma cell lines. *Neurosci Lett.* 2004;363(2):190-3.

Zhu BT, Conney AH. Is 2-methoxyestradiol an endogenous estrogen metabolite that inhibits mammary carcinogenesis? *Cancer Res.* 1998;58(11):2269-77.

## ***SITOGRAPHY***

<http://rsb.info.nih.gov/ij>

<http://merckbiosciences.com>

<http://en.wikipedia.org>

[www.ijpb.versailles.inra](http://www.ijpb.versailles.inra)

[www.lbl.gov](http://www.lbl.gov)

[www.ncbi.nlm.nih.gov](http://www.ncbi.nlm.nih.gov)





Grazie Valentina. Non ti ci vedo insalata come Lot, sai. La pioggia ha smesso e io ti auguro tutta la fortuna che meriti. Del resto, *every clouds have a silver lining* as Hal used to said me.

Thank you Dr. Gainer for the scientific and educational experience I had at NIH, thank you for your humanity, your help and for every things I learned there. And thank you Shirley, Ray Chun Mey, of course.

Thank you Todd...*shot the beak* and pay attention to the *Beast*, my friend. Thank you for everything you did for me (your bathroom disappoints).

E infine un Grazie alla mia Famiglia, un Grazie enorme dove c'è davvero tutto.